



Universiteit
Leiden
The Netherlands

Regulation of DNA damage and immune response pathways by post-translational protein modification

Dijk, M.

Citation

Dijk, M. (2020, September 9). *Regulation of DNA damage and immune response pathways by post-translational protein modification*. Retrieved from <https://hdl.handle.net/1887/136522>

Version: Publisher's Version

License: [Licence agreement concerning inclusion of doctoral thesis in the Institutional Repository of the University of Leiden](#)

Downloaded from: <https://hdl.handle.net/1887/136522>

Note: To cite this publication please use the final published version (if applicable).

Cover Page



Universiteit Leiden

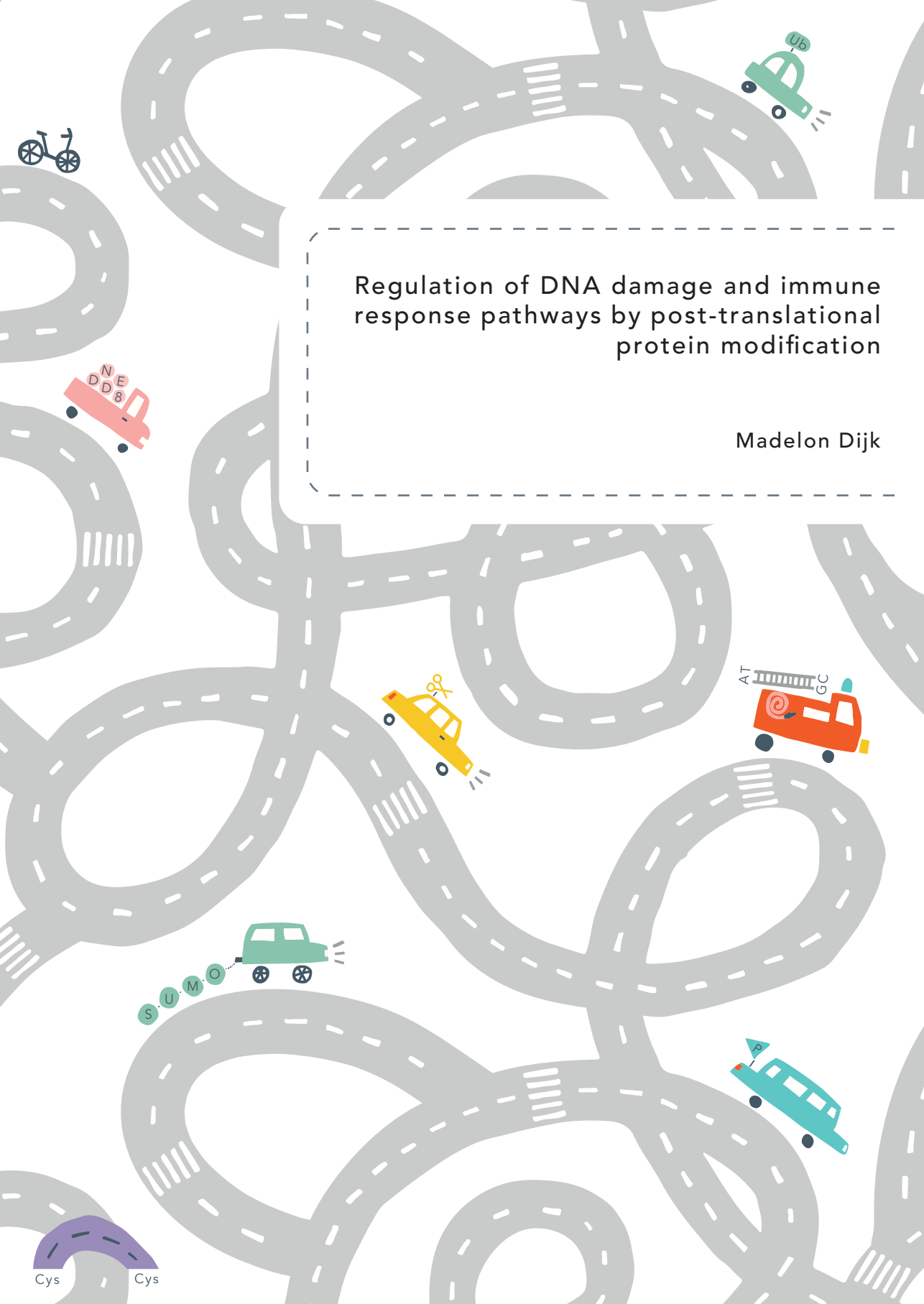


The handle <http://hdl.handle.net/1887/136522> holds various files of this Leiden University dissertation.

Author: Dijk, M.

Title: Regulation of DNA damage and immune response pathways by post-translational protein modification

Issue Date: 2020-09-09



Regulation of DNA damage and immune response pathways by post-translational protein modification

Madelon Dijk

Regulation of DNA damage and immune response pathways by post-translational protein modification

Madelon Dijk

Cover design & layout: Madelon Dijk

Printing: Off Page, www.offpage.nl

ISBN: 978-94-93197-11-4

© Copyright 2020 by Madelon Dijk. All rights reserved

No part of this book may be reprinted, reproduced or transmitted in any form or by any means without the expressed, written consent of the author or, if applicable, of the publisher of the article(s).

Regulation of DNA damage and immune response pathways by post-translational protein modification

Proefschrift

ter verkrijging van
de graad van Doctor aan de Universiteit Leiden,
op gezag van Rector Magnificus prof. mr. C.J.J.M. Stolker,
volgens besluit van het College voor Promoties
te verdedigen op woensdag 9 september 2020
klokke 11.15 uur

door

Madelon Dijk

geboren te Rotterdam
in 1988

Promotor:

Prof. dr. H. van Attikum

Co-promotor:

Prof. dr. S.M. van der Maarel

Leden promotiecommissie:

Prof. dr. A.C.O. Vertegaal

Prof. dr. D.J.M. Peters

Prof. dr. W. Vermeulen

Dr. H. Lans

(Erasmus MC, Rotterdam)

(Erasmus MC, Rotterdam)

Contents

Chapter 1	Introduction	7
Chapter 2	Potential targets of the CSA-based cullin-RING ubiquitin ligase in transcription-coupled DNA repair	33
Chapter 3	TRiC-dependent modulation of the transcription-coupled DNA repair protein CSA	49
Chapter 4	Regulation of the DNA damage response by the SUMO E3 ligase Zimp7	79
Chapter 5	How dextran sulfate affects C1-inhibitor activity: a model for polysaccharide potentiation	101
Chapter 6	Perspectives	115
Appendix	Summary	133
	Samenvatting	136
	Curriculum vitae	139
	Publications	140
	Acknowledgements	141

1

Introduction

Partially adapted from:
Insight in the multilevel regulation of NER
Exp Cell Res 329, 116-23 (2014)

The cellular response to DNA damage

The genetic information that is encoded by DNA harbors all the instructions that are required for proper development and functioning of organisms. Even minor alterations in the genome may disturb normal development and have the potential to drive carcinogenesis, contribute to the progression of ageing-related diseases and underlie hereditary disorders. Conservation of genetic information is thus of upmost importance not only to the life of a single organism, but ultimately also to continuity of species.

The integrity of the vulnerable DNA macromolecule is however continuously threatened by regular endogenous processes that damage the DNA. This damage may result from spontaneous deamination or depurination/depyrimidation or arise from reactions with reactive oxygen species that are produced during normal metabolism¹. On the other hand, DNA lesions are sometimes created by design, as is exemplified by the programmed induction of DNA double-strand breaks during immunoglobulin differentiation and meiotic chromosomal crossover^{2,3}. DNA is furthermore insulted by various exogenous sources, such as ultraviolet (UV) or ionizing (IR) radiation and chemical compounds. If not removed and repaired accurately, replication of DNA damage can result in chromosomal aberrations or mutations that have deleterious effects on cellular functioning and genome stability^{4,5}.

An essential strategy of cells and organisms to counteract genetic alterations encompasses the continuous surveillance of genomes, hence tracing the occurrence of DNA damage and ensuring its removal. Accordingly, cells react to the presence of DNA lesions by activating the DNA damage response (DDR), which constitutes an elaborate network of signaling cascades that concomitantly coordinate gene expression, chromatin structure adjustments, DNA damage repair and cell cycle progression or, if necessary to preserve genome integrity, accommodate apoptosis⁶⁻⁸.

DNA damage repair pathways

Evidently, an important part of the DNA damage response is the employment of suitable repair pathways that can repair the large compilation of structurally different DNA lesions, including base damages, bulky lesions, DNA single- and double-strand breaks and DNA crosslinks.

Base excision repair (BER) is the main pathway for removal of damaged DNA bases that cause only minor distortions of the DNA helix, such as 8-oxoguanine and apurinic/apyrimidinic (AP) sites that result from oxidation or depurination/depyrimidation, respectively, as well as single-strand DNA breaks. Repair of these lesions is initiated by cleavage of the damaged DNA by substrate-specific N-glycosylases and processing by AP endonucleases. Restoration of the DNA is next established via short-patch or long-patch BER, which involves re-synthesis of a single nucleotide or replacement of a stretch of nucleotides, respectively, followed by ligation of the remaining nick^{9,10}.

More bulky DNA damage types are repaired via nucleotide excision repair (NER) – a highly versatile pathway that operates on a broad range of structurally unrelated helix-distorting

lesions. Similarly to BER, NER comprises DNA damage recognition, excision of the lesion, subsequent DNA polymerization to replace the removed stretch of nucleotides, and a ligation reaction¹¹⁻¹³.

The probability of DNA double-strand break formation is highly increased under certain circumstances, which include replication fork stalling or collapse, the presence of multiple adjacent single-strand DNA breaks and exposure to ionizing radiation or chemical compounds. Being active throughout all cell cycle stages, non-homologous end-joining (NHEJ) is the main pathway operating on DNA double-strand breaks in human cells. By rejoining and ligating the broken DNA ends without the use of a homologous DNA sequence, it resolves breaks in a rather straightforward, but often error-prone manner. In contrast, homologous recombination (HR) facilitates error-free repair during the S or G2 phases of the cell cycle. Following resection of the broken ends, a homologous template, generally provided by the sister chromatid, is invaded. This undamaged DNA sequence is then used for DNA re-synthesis, thereby ensuring complete restoration of the original genetic information^{14,15}.

Covalent crosslinks between the 2 DNA strands (that is interstrand crosslinks, ICLs) block DNA replication and transcription by impeding strand separation. The Fanconi anaemia (FA) pathway is activated by replication fork stalling at ICLs. Following detection of the ICL, incisions on both sides of the lesion lead to breakage of the sister chromatid and unhooking of the ICL and the other sister chromatid. Specialized translesion DNA polymerases are able to synthesize DNA across the ICL, thereby generating a template to repair the DSB in the other chromatid via homologous recombination. NER is responsible for the removal of the remaining ICL adduct. In non-replicating cells, a combination of translesion synthesis and NER is applied to resolve ICLs^{16,17}.

In addition to the occurrence of damaged DNA, mutations that arise from faulty nucleotide incorporation during DNA replication pose a serious threat to genome stability. Mismatched base pairs that result from DNA damage-induced or spontaneous nucleotide conversion, such as the formation of uracil by deamination of cytosine, are mostly recognized by DNA glycosylases that trigger repair via BER, whereas mismatch repair (MMR) corrects base substitutions that originate from mistakes made by DNA polymerases. Central to this latter pathway is the introduction of nicks at both sides of the mismatched region, which allows processing by exonucleases to remove a stretch of the newly synthesized DNA, including the mismatched DNA bases, and its replacement via DNA synthesis and ligation¹⁸⁻²⁰.

When encountered during DNA replication, damage that has not accurately been resolved by one of these pathways can initiate post-replication repair (PRR), which comprises different mechanisms to bypass DNA lesions that block progression of the replication machinery. Translesion synthesis (TLS) involves substitution of the replicative DNA polymerase by specialized DNA polymerases that are capable of incorporating bases opposite damaged nucleotides, although at reduced fidelity, for which reason the process is considered to be often error-prone. Conversely, template switching or recombination-dependent events facilitate error-free lesion bypass via pathways that are less well understood²¹.

Nucleotide excision repair

The nucleotide excision repair (NER) pathway, its regulation and associated disorders constitute an important area of the research described in this thesis and are therefore discussed in more detail in the following sections.

NER is capable of removing a wide range of bulky lesions that, despite their structural differences, can be recognized and processed owing to their helix-distorting character. Whereas for instance the specialized BER glycosylases directly recognize particular lesions, the proteins involved in the detection of NER substrates act by sensing destabilized base pairing or arrested transcription²². In this manner, NER operates on lesions ranging from cisplatin-induced intrastrand crosslinks to bulky adducts caused by polycyclic aromatic hydrocarbons. In human cells, the nucleotide excision repair pathway is the only pathway qualified to remove the covalent linkages between adjacent pyrimidines that are inflicted by sunlight, that is 6-4-photoproducts (6-4PPs) and cyclobutane pyrimidine dimers (CPDs). If not accurately and timely removed, these lesions interfere with DNA replication and transcription, perturb cell cycle progression and may promote cancer and accelerated ageing by causing mutations and chromosomal aberrations¹¹.

NER substrates are detected via one of the NER subpathways, referred to as global genome nucleotide excision repair (GG-NER) and transcription-coupled nucleotide excision repair (TC-NER). GG-NER explores disordered base pairing throughout the whole genome, while the specialized TC-NER pathway removes lesions in active genes that hinder progression of the elongating RNA polymerase. After DNA damage recognition, the NER subpathways converge into a common molecular mechanism that involves DNA unwinding and lesion verification, dual incision and elimination of the excised oligonucleotide, and DNA repair synthesis and ligation^{11,13} (Fig. 1).

Importantly, defects in genes that encode proteins involved in NER are associated with a number of disorders (further described in 'Human disorders associated with defects in NER genes'). The nomenclature of many of the core NER proteins, as well as those required for DNA damage recognition via GG-NER or TC-NER, has been derived from the disease that has been linked to mutations in the respective genes. Accordingly, CSA and CSB refer to Cockayne syndrome (CS) complementation groups A and B, respectively, while mutations in the XP proteins XPA through XPG have been found implicated in xeroderma pigmentosum (XP). Defects in UVSSA were shown to cause UV sensitive syndrome (UVsS).

Global genome nucleotide excision repair

By probing the entire genome for disturbed base pairing, the DNA binding protein XPC initiates GG-NER when sensing damage-mediated DNA helix distortion²³⁻²⁶ (Fig. 1). Until its association with unpaired bases opposite the lesion, stabilization of the XPC monomer is ensured by its incorporation into a heterotrimeric complex additionally comprising RAD23B and CEN2 that serve to prevent XPC ubiquitination and degradation²⁷⁻²⁹. DNA damage detection by XPC is assisted by the UV-DDB dimer, which consists of DDB1 and DDB2 (XPE) and is part of a larger CRL^{DDB2} complex (further discussed in 'Regulation of DNA damage repair by post-translational protein modifications'). Substrate specificity of the UV-DDB

complex resides within the DDB2 protein, which accommodates relatively small lesions in its binding pocket. Damage extrusion by DDB2 exposes the opposing single-stranded DNA and facilitates its subsequent recognition by XPC^{11,30-32}.

Binding of XPC to a lesion activates lesion verification and subsequent repair by providing a platform for recruitment of the basal transcription factor TFIIH^{33,34}. The ATPase and helicase activities of its XPB and XPD subunits, respectively, promote DNA strand separation to create an unwound structure around the lesion, which contributes to damage verification and the assembly of a pre-incision complex that additionally consists of XPA, RPA and XPG³⁵⁻³⁸. The roles of XPA include catalyzing the dissociation of the CAK complex from the core TFIIH complex, corroborating the lesion, and recruiting the XPF-ERCC1 heterodimer³⁸⁻⁴¹. RPA, which coats the single-stranded DNA and protects the undamaged strand, assists in damage verification and the positioning of endonucleases XPG and XPF-ERCC1^{42,43}. Subsequent dual incision of the DNA is initiated 5' to the lesion by XPF, after which 3' incision by XPG results in the release of a fragment of 22 to 30 nucleotides⁴⁴. Following incision by XPF-ERCC1, re-synthesis of the excised DNA is executed by DNA polymerase δ , κ or ϵ , and DNA ligase 1 or 3 seals the remaining nick to complete the NER process and restore helix integrity^{11,44} (Fig. 1).

Transcription-coupled nucleotide excision repair

Stalling of elongating RNA polymerase (RNAPII) by DNA lesions in the transcribed strand of active genes initiates fast removal of the road-blocking DNA damage via TC-NER. Accelerated repair as compared to resolution by GG-NER is of prime importance to avoid prolonged transcriptional arrest and consequential cell death⁴⁵⁻⁴⁸. Stabilization of the interaction between the stalled RNAPII and the SWI/SNF2-like ATPase CSB is considered to be the first step in TC-NER and required for the assembly of a TC-NER-specific complex (Fig. 1). The role of CSB may include remodeling of chromatin and/or the RNAPII-DNA interface, which both seem prerequisites for exposure and subsequent repair of the DNA damage. However, these events also rely on the recruitment and activities of other proteins⁴⁹⁻⁵¹. Among these proteins is CSA, which is part of the CRL^{CSA} complex that has common architectural features with the CRL^{DDB2} complex responsible for damage recognition in GG-NER (both further discussed in 'Regulation of DNA damage repair by post-translational modifications')⁵². Its precise role is however yet to be identified. Additionally, a complex comprised of UVSSA and USP7 is recruited specifically to the TC-NER complex, likely to regulate the presence of TC-NER proteins, including CSB, at the site of damage by coordinating their degradations⁵³⁻⁵⁶. Another protein explicitly involved in TC-NER is the pre-mRNA splicing factor XAB2, which may function as a scaffold by binding XPA⁵⁷. Upon the association of the TC-NER-specific proteins with the stalled RNA polymerase, the pre-incision complex is assembled as described for GG-NER, which involves the recruitment of TFIIH, XPA and RPA, as well as the endonucleases XPG and XPF-ERCC1. DNA damage verification, incision and DNA repair synthesis then continue along the further common NER pathway (Fig. 1). Importantly, accurate DNA damage resolution via TC-NER also includes resumption of transcription. Apart from its role in DNA damage repair, CSB plays a crucial role in the transcriptional restart upon lesion removal via yet to be established mechanisms that may

include chromatin remodeling, reconversion of TFIIH to a transcriptionally active complex and/or the generation of hypophosphorylated RNA polymerase⁵⁸⁻⁶⁰.

Displacement of the stalled RNA polymerase

Repair of transcription-blocking CPDs seems to be challenged by the presence of the stalled RNAPII, which covers around 35 nucleotides that are asymmetrically located around the lesion and especially obstructs the 3' XPG cutting site^{61,62}. Several studies have shown that UV irradiation induces degradation of the RNA polymerase in a CSA- and CSB-dependent manner^{53,54,63,64}. UV-irradiated cells lacking one of the CS proteins initiate a signaling cascade prompted by the prolonged stalling of RNAPII that eventually leads to apoptosis^{63,65}.

Despite the general belief that the lesion-shielding RNA polymerase needs to be displaced from the site of damage to increase the accessibility by repair factors and to allow repair, its UV-induced degradation might only be a last resort in case the impaired transcription becomes detrimental to the cell⁶⁶⁻⁶⁸. A mechanism of backtracking of transcribing RNA polymerase, by sliding backward along the DNA, would enable resumption of transcription after repair and hence seems a more efficient process than transcription termination as a prerequisite for NER. Backtracking has been implicated in many processes, including genome stability maintenance and control of transcription elongation/termination, and additionally has been suggested to have a proofreading function^{69,70}. In prokaryotes, it was suggested to be the main mechanism to displace RNA polymerase from the DNA damage during TC-NER and was demonstrated to depend on the helicase UvrD^{71,72}. Accordingly, in vitro studies have demonstrated that the absence of UvrD severely inhibits CPD excision by UvrC when the elongating RNA polymerase complex is located at a position that causes shielding of the lesion. Either the addition of UvrD, or the assembly of RNA polymerase at a position upstream of the CPD were shown to restore CPD excision rates. As opposed to backtracking, the DNA translocase Mfd mediates the forward translocation of RNA polymerase and is thought to promote reactivation of transcription when repair is completed^{73,74}. Whether TC-NER is driven by backtracking in eukaryotes as well remains to be elucidated. However, this may not be unlikely given the evolutionary conservation of TC-NER and the frequent occurrence of backtracking as a regulatory mechanism at natural transcription pausing sites^{69,71}.

NER in a chromatin context

Like other DNA-based processes, NER is to a great extent regulated by chromatin status. Especially during GG-NER, highly compacted heterochromatin poses a challenge to repair, which is manifested by the relatively slow removal of bulky lesions, and most likely necessitates carefully modulated and spatiotemporally precise chromatin remodeling events⁷⁵. Such events usually promote transient chromatin decompaction, thereby facilitating access of the repair machinery. While it has been demonstrated that UV-induced DNA damage per se results in histone eviction, local chromatin decondensation is further mediated by ATP-dependent chromatin remodelers that stimulate nucleosome sliding or disassembly⁷⁶⁻⁷⁸. In addition, ATPases may drive the exchange of histone variants, such as H2A.Z, which contributes to creating an open chromatin structure around sites of DNA damage⁷⁹.

On the other hand, post-translational modification of histones, including ubiquitination, PARylation and acetylation, also modulate the chromatin status to recruit repair proteins and enable DNA damage removal^{77,78,80}. GG-NER damage recognition factor DDB2 was shown to stimulate local chromatin unfolding in several manners. Independently of its association with the CRL E3 ubiquitin ligase complex, it was shown to promote chromatin decompaction and/or histone eviction and thereby the assembly of the NER machinery⁸¹. This notion has been reinforced by studies that demonstrate that DDB2 can promote PARP1-dependent chromatin poly-ADP ribosylation (PARylation, further discussed in 'Regulation of DNA damage repair by post-translational modifications'), which usually leads to a less rigid chromatin environment^{82,83}. In addition, this facilitates the recruitment of the chromatin remodeler ALC1 to further restructure UV damage-containing nucleosomes⁸². Furthermore, UV-DDB has been described to promote chromatin remodeling by associating with the INO80 remodeling complex, and by binding to p300 and the STAGA complex that both stimulate repair by mediating chromatin acetylation⁸⁴⁻⁸⁷. In addition, DDB2 was shown to recruit the histone acetyl transferase HBO1, which most likely contributes to repair in non-replicating cells, not only by facilitating XPC accumulation at damaged DNA, but also by recruiting the ACF1 and SNF2H chromatin remodelers⁸⁸. As a part of CRL^{DDB2}, DDB2 induces the ubiquitination of all core histones, resulting in nucleosome destabilization, H2A-H2B dimer loss and weakened histone-DNA interaction, which are all hallmarks of accessible chromatin⁸⁹⁻⁹¹.

Although transcription-blocking DNA damage is generally encountered in the more relaxed chromatin environment that is required for transcription, repair of these lesions via TC-NER still requires additional chromatin remodeling. For example, a contribution of histone acetylation in human cells was demonstrated by the increased repair of UV-induced lesions via both NER subpathways upon sodium butyrate-induced inhibition of histone deacetylases that mainly affect H4 acetylation⁹². Furthermore, in the mouse CPD removal was delayed upon depletion of HMGN1, which specifically stimulates TC-NER by enhancing H3 acetylation⁹³⁻⁹⁵. As indicated previously, CSB presumably plays an important role in chromatin remodeling by means of its SWI/SNF2-like ATPase activity and by recruiting other chromatin-modifying complexes.

Although an open chromatin conformation is beneficial at the early stages of NER, upon completion of DNA damage repair the chromatin environment needs to be restored to its original state in order to maintain epigenetic marks and transcriptional status⁹⁶. Several studies have underlined that completion of damage repair itself is not sufficient to restart the transcription machinery and that recovery of transcription requires chromatin reorganization to establish pre-damage levels of gene expression. For example, in addition to the contribution of the histone chaperone proteins CAF1 and ASF1, the restart of stalled RNAPII was shown to be promoted by the SPT16 subunit of FACT (facilitates chromatin transcription), which accelerates the damage-induced exchange of H2A and H2B⁹⁶⁻⁹⁸. Moreover, roles in transcriptional restart upon DNA damage repair have been identified for the histone chaperone HIRA and the methyltransferase DOT1L, which act by stimulating H3.3 incorporation and H3K79 dimethylation, respectively⁹⁹⁻¹⁰¹. Thus, next to chromatin relaxation being required for early NER events, specific chromatin remodeling events and histone

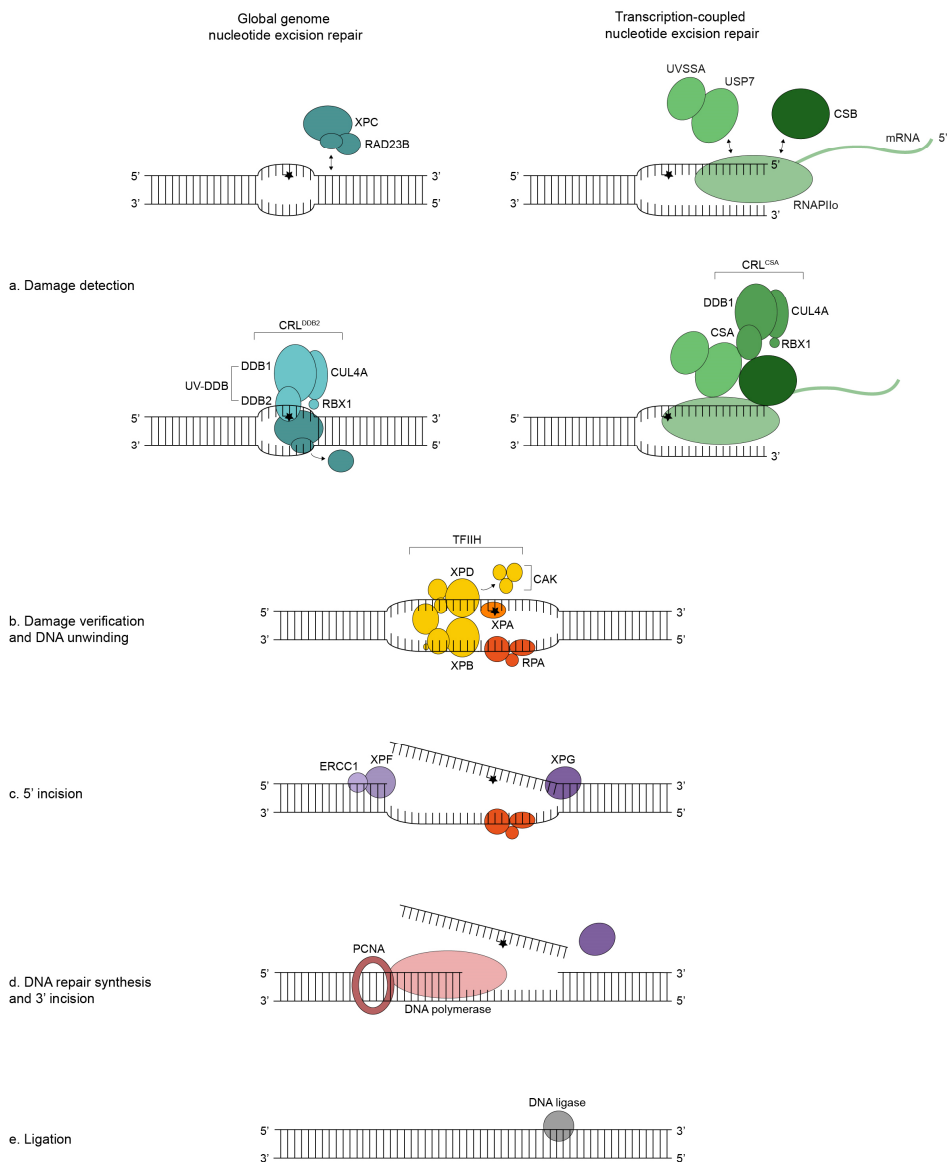


Figure 1. Schematic overview of the nucleotide excision repair pathways

Upon the detection of DNA damage (a) via UV-DDB and XPC (global genome nucleotide excision repair; left panel) or stalling of RNAPII (transcription-coupled nucleotide excision repair; right panel) the subpathways converge into a common molecular mechanism that involves damage verification and DNA unwinding (b), excision of the damaged DNA (c, d), gap filling by DNA synthesis (d) and sealing of the remaining nick (e). A more detailed description of these steps and the involved proteins is given in the main text.

modifications appear to be essential for completion of NER and the continuation of transcription.

Human disorders associated with defects in NER genes

Inherited NER defects are associated with different disorders that display broadly varying symptoms. The (severity of the) clinical outcome is likely explained by a combination of factors, including the subpathway in which the affected protein functions, roles of this protein in other cellular processes and even the specific mutation underlying the manifested disease. Xeroderma pigmentosum (XP) has been linked to defects in seven NER genes (*XPA* through *XPG*) and in a gene encoding DNA polymerase η (XP variant). XP patients are clinically characterized by hypersensitivity to sunlight and predisposition to skin cancer and in a minority of cases (~25%) by severe neurological and developmental problems and ageing. These additional neurodevelopmental abnormalities have been shown to result from mutations in *XPA*, *XPB*, *XPD*, *XPF* or *XPG*¹⁰²⁻¹⁰⁴.

Defects in TC-NER genes *CSA* and *CSB* are among others associated with the severe developmental and neurological disorder Cockayne syndrome (CS). Classic CS is characterized by growth failure, premature ageing and progressive neurological degeneration^{105,106}. Furthermore, mutations in the *CSA* and *CSB* proteins, as well as some of the *XP* genes, have been linked to cerebro-oculo-facio-skeletal (COFS) syndrome – a rare autosomal recessive disease that is classified into the spectrum of CS disorders and outlined by severe developmental delay and facial dysmorphism¹⁰⁵.

Notably, a combined XP/CS phenotype is observed for specific mutations in *XPB*, *XPD*, *XPG* or *XPF*. Other mutations in *XPB* or *XPD* can cause a combination of CS features, though usually not progressively declining, and brittle hair and nails, which is known as trichothiodystrophy (TTD). The explanation for these additional characteristics may be found in the perturbed functioning of TFIIH as a transcription factor that is caused by these particular mutations^{102,107}.

Most cases of UV sensitive syndrome (UVsS), which is a relatively mild condition that is characterized by photosensitivity without cancer predisposition or neurodevelopmental abnormalities, are ascribed to mutations in the gene encoding the TC-NER protein UVSSA. In addition, UVsS patients with a mutated *XPB* or *XPD* gene have been reported¹⁰⁸. Remarkably, in a few cases the disorder has also been linked to a defective CS protein, raising the possibility that the TC-NER impairment that is caused by a defect in either UVSSA, *CSA* or *CSB* only explains the common hypersensitivity to sunlight^{109,110}. Conversely, the neurodevelopmental abnormalities observed for CS patients may arise partly due to defective functioning of *CSA* or *CSB* in other cellular processes, in which a role for UVSSA remains to be established¹¹¹⁻¹¹³. Finally, the ability to remove stalled RNAPII from sites of DNA damage may contribute to the UVsS phenotype (as discussed in Chapter 2), although no evidence is available yet to support this.

Regulation of DNA damage repair by post-translational protein modifications

Fine-tuning of protein activity is a crucial aspect of all processes that underlie correct cellular functioning and accurate organization and protection of organisms. To a great extent, this is established by a large repertoire of chemical protein alterations, collectively referred to as post-translational modifications (PTMs), which in turn modulate the activity, localization and interactions of already available proteins (Fig. 2). The most common PTMs include the formation of disulfide bonds between cysteine residues, proteolytic cleavage of peptide bonds and the removal or introduction of low-molecular-weight groups. In the DDR, important mechanisms of pathway regulation involve the reversible, covalent addition of functional groups, as has been demonstrated frequently by the induction of PTMs such as ubiquitination, SUMOylation, phosphorylation, PARylation and NEDDylation following DNA damage. Accordingly, these modifications significantly contribute to the spatiotemporal coordination of the different steps that constitute the distinct NER pathways, as well as their interplay with signaling cascades that mediate cell cycle progression and gene expression.

The damage recognition step in GG-NER makes a fine example of the significance and function of several PTMs. Given that UV damage recognition appears to be one of the rate-limiting steps in NER, the intricate interplay between the sensor complexes, that is UV-DDB and XPC-RAD23B-CEN2, is paramount¹¹⁴. As a part of the CRL^{DDB2} E3 ubiquitin ligase complex, consisting of DDB2, DDB1, CUL4A/B and RBX1, UV-DDB regulates the retention time of both UV damage recognition complexes¹¹⁵. CRL^{DDB2} promotes the ubiquitination of XPC and itself upon UV irradiation¹¹⁶. Whilst DDB2 poly-ubiquitination leads to its dissociation from the site of damage, as well as its proteasomal degradation, the atypical poly-ubiquitination of XPC increases its stability at the lesion¹¹⁶⁻¹¹⁸. Recruitment and stabilization of XPC is furthermore controlled by a DDB2-independent interaction with PARP1 and was shown to be enhanced by PARP1's PARylating activity¹¹⁹. Notably, the residence time of DDB2 at the damage is regulated by competing post-translational modifications. Poly-APD ribosylation (PARylation) and ubiquitination of DDB2 occur at the same protein region, with the former inhibiting the latter, thereby increasing the half-life of DDB2⁸². The timely removal of DDB2, and later XPC, is controlled by its ubiquitination status and its segregation by VCP/p97, adding an additional regulatory level¹²⁰. Intriguingly, XPC too appears to be tightly regulated by multiple PTMs upon UV irradiation, as it was shown to be ubiquitinated, as well as SUMOylated at several sites^{121,122}. These modifications, in contrast to the competitive character of PARylation and ubiquitination of DDB2, appear to behave cooperatively. More specifically, XPC SUMOylation promotes the accumulation of the SUMO-targeted E3 ubiquitin ligase RNF111, which in turn further decorates XPC with non-proteolytic K63-ubiquitin chains¹¹⁷.

Given that XPC is intrinsically unstable as a monomer, necessitating its association with stabilizing partners RAD23B and CEN2, it is remarkable that RAD23B dissociates upon binding of XPC to damaged DNA^{27,81}. Concomitantly, XPC ubiquitination reaches its peak, raising the possibility that, in addition to potential XPC stabilization by PARP1, the non-canonical XPC ubiquitination might initially be read by downstream effectors in a protective

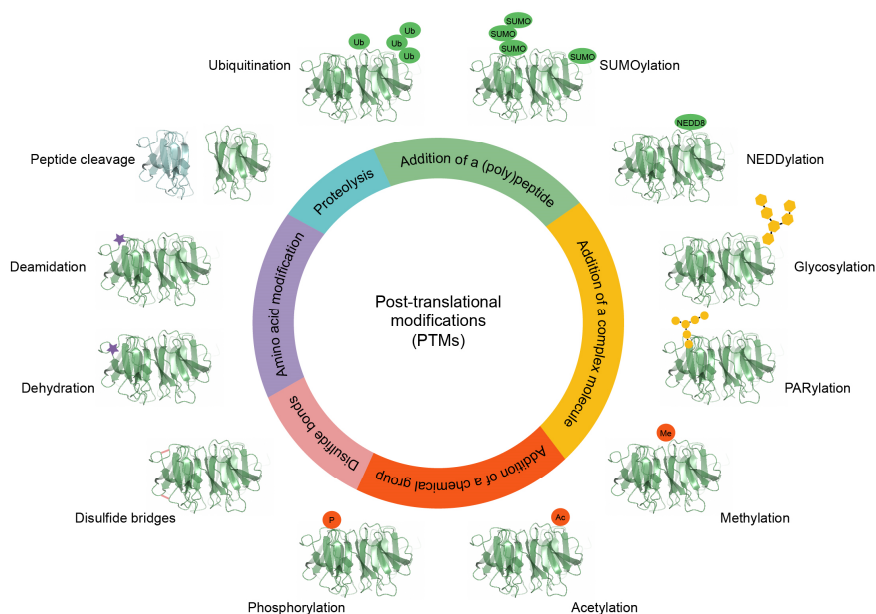


Figure 2. Overview of the most common types of post-translational protein modifications

For each type, examples are shown in a corresponding color.

manner that stabilizes XPC at the damage^{117,119}. Following lesion recognition and verification, ubiquitinated XPC is eventually removed by VCP in order to promote the assembly of the downstream repair complex¹²⁰.

Similarly to DDB2, the TC-NER factor CSA also assembles into a cullin-RING ubiquitin ligase complex (CRL^{CSA}) consisting of CSA, DDB1, CUL4A/B and RBX1⁵². Although proven essential for TC-NER, the exact roles of CRL^{CSA}, apart from recruiting other repair factors, remain largely elusive. CSA has been suggested to contribute to a last resort mechanism that avoids persistently stalled RNAPII_o by promoting its complete dissociation when NER is compromised (further discussed in 'Displacement of the stalled RNA polymerase'). However, as the ubiquitin ligases NEDD4, elongin A/B/C, Von-Hippel Lindau (VHL) and BRCA1 have also been described to promote ubiquitination and subsequent degradation of stalled RNAPII_o, this raises the possibility that CRL^{CSA}'s catalytic activity is not essential¹²³⁻¹²⁸. Another potential CRL^{CSA} target is CSB, which likely dissociates after repair of the damage to enable resumption of transcription¹²⁹. Similar to removal of the GG-NER recognition factors, the eviction of CSB is mediated by VCP, which associates with CRL^{CSA}¹³⁰. Additionally, CSA and CSB could be linked via another CRL^{CSA} target that is being recognized by means of a ubiquitin binding domain in CSB. The retention time of CSB might also be regulated by

UVSSA by virtue of the de-ubiquitinating enzyme USP7, which prevents proteasomal degradation of CSB by removing ubiquitin⁵³. The association of UVSSA with USP7 additionally seems to prevent degradation of UVSSA itself¹³¹. Interestingly, UVSSA-USP7 is potentially recruited via CSA as well^{55,56}. Although this mechanism requires further study, the diminished survival and recovery of RNA synthesis upon UV irradiation displayed by USP7-depleted cells as compared to wildtype cells, again demonstrate that balanced post-translational modifications are crucial for accurate repair and, in this case, resumption of transcription^{53,55}.

The activity of both CRL^{DDB2} and CRL^{CSA}, like that of other cullin-RING ligases, is in turn regulated by NEDDylation¹³². Attachment of NEDD8 to the cullin protein is required for activation of their ligase activities, but counteracted by the COP9 signalosome that mediates deNEDDylation by means of its protease subunit CSN5. While association of COP9 keeps both CRL complexes in an inactive state under unperturbed conditions, DNA damage induction causes the release of COP9 and subsequent NEDDylation and activation of CRL^{DDB2} and CRL^{CSA}, although possibly at a different stages of repair¹¹⁵. Interestingly, NEDDylation in general coordinates the presence of repair factors in the NER complex (described in Chapter 2), recognizing this modification as an additional layer of regulation.

Next to directly influencing the composition and activity of the repair complex, post-translational modifications also contribute significantly to chromatin remodeling (described at 'NER in a chromatin context'). Interestingly, the activities of the chromatin remodelers themselves are often controlled by PTM's as well. For example, the histone acetyl transferase HBO1 is phosphorylated by ATM/ATR upon DNA damage, which likely contributes to TC-NER in non-replicating cells and is required for its CRL^{DDB2}-mediated ubiquitination and dissociation at later stages^{88,133}. Moreover, the ATPase activity of TC-NER factor CSB, which likely contributes to chromatin remodeling, is increased upon its UV-induced dephosphorylation¹³⁴.

The above described examples only provide a glimpse of the mechanisms by which PTMs regulate NER, yet give a good impression of how they affect protein stability, retention time and activity. An extra level of complexity is added when multiple post-translational modifications act to complement each other, as for instance is seen for SUMO-targeted ubiquitin ligases, or in contrast serve to establish opposite effects, as was shown for DDB2 ubiquitination and PARYlation. Not surprisingly, similar mechanisms are employed throughout all processes of the DDR. Pathway regulation by PTMs is excellently illustrated by modification of PCNA, which influences post-replication repair. During unperturbed replication, yeast PCNA is mainly SUMOylated, enhancing its interaction with the anti-recombinogenic helicase Srs2, which avoids unwanted homologous recombination by disrupting RAD51 filaments¹³⁵⁻¹³⁸. In response to replication-stalling damage, PCNA SUMOylation strongly enhances its RAD18-mediated mono-ubiquitination, which can be recognized by TLS polymerases that facilitate (potentially mutagenic) bypass of the lesion¹³⁹⁻¹⁴¹. Interestingly, extension of the ubiquitin chain by UBC13-MMS2 and RAD5 enables an error-free method that involves template switching¹⁴¹⁻¹⁴³. The interaction between PCNA and Srs2 is in turn negatively affected by Srs2 SUMOylation, which is increased upon DNA damage induction and in this manner regulates HR-mediated rescue of stalled

replication forks^{144,145}. Together these mechanisms greatly affect pathway choice during PRR, exemplifying the importance of PTMs in other aspects of the DNA damage response.

Evidently, PTM-mediated regulation of protein activity contributes not merely to an accurate DDR, yet is essential to control all cellular processes. For example, fine-tuning of protein activity is also broadly applied by the immune system, which induces multiple types of PTMs in response to environmental changes¹⁴⁶.

Other methods of pathway regulation: examples from the immune system

As indicated above, apart from the PTMs of proteins that involve the attachment of small chemical moieties or peptides, several other mechanisms exist to influence protein activities (Fig. 2). Indeed the DDR provides excellent examples of protein regulation by the reversible linkage of functional groups, but the variety of mechanisms that are applied to control pathway activation and execution during the immune response, makes this system a fascinating area of research to gain more insight into other PTMs, such as peptide cleavage.

Zymogen activation by proteolytic cleavage

A fundamental aspect of the immune response is the complement system, which is a network of more than 50 membrane-associated proteins, as well as plasma proteins that act in cascades to mediate a wide range of effector functions contributing to pathogen elimination, such as opsonization, chemotaxis and inflammation¹⁴⁷. Activation is established through 3 different processes, referred to as the classical, mannose-binding lectin and alternative pathways. Although triggered by different stimuli and initiated by different proteins, they use comparable signal transduction mechanisms that involve sequential peptide cleavages from inactive proteases (zymogens). This activates their proteolytic functions and in turn catalyzes cleavage of the next enzyme (Fig. 3). In this manner the activation of a small number of plasma proteins upon pathogen detection is quickly amplified and enables rapid coating of the pathogen's surface to accelerate its clearance, which is accompanied by a series of inflammatory responses¹⁴⁸. Evidently, as the activation of only a small number of enzymes can induce a massive response, these processes require tight regulation and inappropriate activation should be avoided. A comparable mechanism is applied by the coagulation system, which encompasses the contact and tissue factor systems and contributes to the innate immune system by increasing vascular permeability and producing agents that assist phagocytic cells. In addition, it serves to induce blood clotting, which is established in a cascade of proteolytic cleavages that eventually lead to the formation of fibrin^{149,150}. Likewise, the breakdown of fibrin by the fibrinolytic system involves the conversion of the zymogen plasminogen to the active protease plasmin¹⁵¹. Regulation of these processes is of great importance not only to ensure the required blood clot stability, but also to warrant its timely removal without dissolving healthy tissue formations.

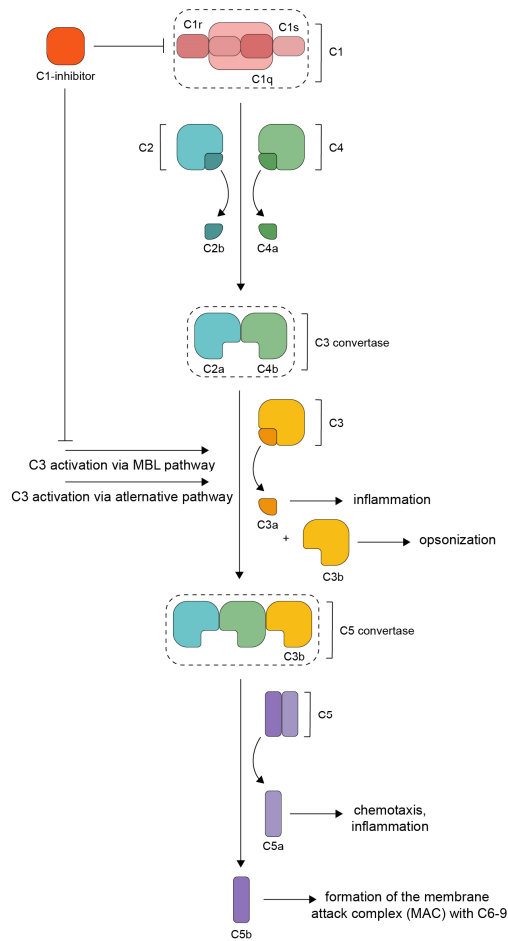


Figure 3. Schematic overview of complement system activation via the classical pathway

Example of a method of pathway regulation and signal amplification that involves sequential proteolytic cleavages. Binding of C1q to an antibody-antigen complex or directly to the pathogen's surface activates C1, which catalyzes cleavage of both C2 and C4 into C2a/b and C4a/b, respectively. C2a and C4b form the C3 convertase that cleaves C3 into C3a/b. While C3a contributes to an inflammatory response, C3b induces opsonization. In addition, C3b together with C2a/C4b forms the C5 convertase that cleaves C5 into C5a/b. C5a stimulates chemotaxis and inflammation, whereas C5b is an essential component of the membrane attack complex (MAC) that is formed on the pathogen's surface to induce its lysis and cell death. The mannose-binding lectin (MBL) and alternative pathways likewise comprise a series of proteolytic cleavages that result in C3 activation. C1-inhibitor avoids inaccurate activation by inhibiting several components of the classical and mannose-binding lectin pathways. A dashed box around a protein complex indicates that it acts as the protease to catalyze the next reaction.

Irreversible protease inactivation by serpins

Essential to the regulation of the above mentioned pathways are the serine protease inhibitors, referred to as serpins, that act as suicide inhibitors on the class of serine proteases of for instance the complement and contact systems¹⁵² (Fig. 3). Well-known examples are antithrombin and α -1-antitrypsin, which both exert their inhibiting actions on multiple proteases. Despite the sometimes poor sequence homology, serpins are characterized by a common structural fold. Fundamental to their inhibitory functions is the presence of the P1-P1' residues, which are presented as a substrate for proteolytic cleavage by the reactive center loop (RCL) that protrudes from the bulk of the protein to be accessible by the protease. Upon cleavage of the P1-P1' bond by the target protease, the insertion of the RCL into the central β -sheet induces a conformational transition, accompanied by the transfer of the protease to the other side of the serpin. The consequential disturbance of the protease's active site makes the hydrolysis of the bond between its serine and the serpin's P1 impossible, resulting in a stable serpin-protease complex that inactivates the protease and is subsequently cleared from circulation and degraded^{153,154}. Thus, the actions of serpins provide excellent examples of irreversible protein inactivation by disruption of the enzyme's active site, as opposed to protein activity modulation by post-translational modifications that can be removed by other specialized proteins.

Fascinatingly, the activities of the inhibitory serpins can in turn be regulated by the binding of small molecules, such as polysaccharides. An interesting serpin in this respect is C1-inhibitor, which is a blood plasma protein that is best-known for its anti-inflammatory activity, yet covers a broad range of biological functions. Being the only inhibitor that acts on the first components of the classical and mannose-binding lectin pathways of the complement system, C1-inhibitor plays a crucial role in regulating these cascades by preventing their spontaneous activations. Next to inactivating C1s and C1r (classical complement pathway) and MASP-1 and -2 (mannose-binding lectin pathway), C1-inhibitor downregulates the levels of active kallikrein and factor XII (coagulation/contact system), plasmin and tissue plasminogen activator (fibrinolytic system) and factor XIa and thrombin (coagulation system)¹⁵⁵. Importantly, deficiency of functional C1-inhibitor underlies hereditary angioedema (HAE), which is characterized by recurrent attacks of potentially life-threatening swelling in various subcutaneous and submucosal tissues due to inadequate activation of the contact system^{156,157}. As observed for other serpins, C1-inhibitor activity is enhanced by glycosaminoglycans (GAGs), of which the naturally occurring penta-saccharide heparin and synthetic dextran sulfate have been the most studied in the context of C1-inhibitor potentiation¹⁵⁸⁻¹⁶¹. Intriguingly, the effect of GAGs on C1-inhibitor activity appears to be different towards the different target proteases¹⁶¹. For example, GAG binding to C1-inhibitor only minimally affects kallikrein inactivation, while it can greatly enhance inhibition of C1s. Gaining more insight into the underlying mechanisms not only offers possibilities for HAE treatment optimization by selective protease inhibition, but also extends our knowledge on protein activity regulation¹⁶².

Although the above described methods of protease (in)activation and modulation of their inhibitors only give a glance at pathway regulation during the immune response, they

elegantly illustrate how every cellular process is tightly controlled by protein fine-tuning and emphasize once more the importance of pathway regulation in the prevention of disease.

Aims and outline

Genetic information has to be protected to ensure correct transmission to the next generation as well as proper functioning on the cellular and organismal level. Upon detection of DNA damage, elaborate response networks are activated that cooperatively protect genome stability by organizing lesion removal and adjusting cell cycle progression. Insight in the regulation of repair and signaling cascades that maintain genome integrity, may improve our understanding of their spatiotemporal coordination and the consequences of inaccurate activation, execution or completion.

The first chapters of this thesis address the regulation of DNA damage response processes, with a focus on the (transcription-coupled) nucleotide excision repair pathway that is crucial for the repair of transcription-blocking DNA lesions such as UV-induced photolesions. As outlined above, defects in NER genes have been associated with multiple disorders, displaying symptoms that vary from mild photosensitivity to severe neurodevelopmental defects. In the last decades, most of the core NER machinery has been described, shifting attention to the molecular mechanisms that either facilitate NER in the context of chromatin or promote the timely and accurate interplay between NER factors and post-translational modifications.

Chapter 2 studies the role of the cullin-RING ubiquitin ligase CRL^{CSA} during TC-NER by inhibiting its NEDDylation-induced activation. It demonstrates the significance of both NEDDylation in general, as well as the presence of CSA for the UV-dependent degradation of RNAPII α that presumably prevents cell death when NER is compromised. Furthermore, it describes how NEDDylation modulates the interaction between CRL^{CSA} and RNAPII α .

Whereas this research reveals a potential mechanism to coordinate the presence and activity of CRL^{CSA} at DNA damage, Chapter 3 evaluates how the stability of CSA and assembly of the CRL^{CSA} complex are guaranteed. Mass spectrometry-based approaches to further elucidate the role of CSA uncover the TRiC complex as a stable CSA-interacting factor. Additional functional assays reveal a crucial role for this chaperonin in the stabilization and localization of (CRL)^{CSA}.

Chapter 4 describes the discovery and characterization of a new SUMO E3 ligase, Zimp7, that is recruited to laser-inflicted DNA damage. The findings covered by this chapter include a solid interaction with PCNA and convincingly argue for further investigation of the roles of Zimp7 in both the DNA damage response and DNA replication.

In addition to DNA damage that may result from metabolic processes or be caused by exogenous sources, potential infection by for instance bacteria or viruses can pose a serious threat to life. Host defense against invasive pathogens is established via several immune responses, which display distinct methods of protein and pathway regulation as compared to the DDR. Chapter 5 briefly digresses from DNA damage repair, to explain and investigate the potentiation of C1-inhibitor – a protein that modulates multiple immune response

pathways – by the binding of glycosaminoglycans. The herein presented models shed light on how binding of dextran sulfate to C1-inhibitor affects the serpin's activity towards its target proteases to different extents.

Finally, Chapter 6 not only discusses the contribution of the described observations to our understanding of cell-protecting mechanisms and the (clinical) implications of loss of pathway regulation, but also makes recommendations for follow-up studies.

References

1. Lindahl, T. Instability and decay of the primary structure of DNA. *Nature* 362, 709-15 (1993).
2. Lam, I. & Keeney, S. Mechanism and regulation of meiotic recombination initiation. *Cold Spring Harb Perspect Biol* 7, a016634 (2014).
3. Nicolas, L., Cols, M., Choi, J.E., Chaudhuri, J. & Vuong, B. Generating and repairing genetically programmed DNA breaks during immunoglobulin class switch recombination. *F1000Res* 7, 458 (2018).
4. Hoeijmakers, J.H. DNA damage, aging, and cancer. *N Engl J Med* 361, 1475-85 (2009).
5. Bartek, J., Bartkova, J. & Lukas, J. DNA damage signalling guards against activated oncogenes and tumour progression. *Oncogene* 26, 7773-9 (2007).
6. Roos, W.P. & Kaina, B. DNA damage-induced cell death: from specific DNA lesions to the DNA damage response and apoptosis. *Cancer Lett* 332, 237-48 (2013).
7. Hanawalt, P.C. Historical perspective on the DNA damage response. *DNA Repair (Amst)* 36, 2-7 (2015).
8. Ciccia, A. & Elledge, S.J. The DNA damage response: making it safe to play with knives. *Mol Cell* 40, 179-204 (2010).
9. Robertson, A.B., Klungland, A., Rognes, T. & Leiros, I. DNA repair in mammalian cells: Base excision repair: the long and short of it. *Cell Mol Life Sci* 66, 981-93 (2009).
10. Parsons, J.L. & Dianov, G.L. Co-ordination of base excision repair and genome stability. *DNA Repair (Amst)* 12, 326-33 (2013).
11. Marteijn, J.A., Lans, H., Vermeulen, W. & Hoeijmakers, J.H. Understanding nucleotide excision repair and its roles in cancer and ageing. *Nat Rev Mol Cell Biol* 15, 465-81 (2014).
12. Nospikel, T. DNA repair in mammalian cells : Nucleotide excision repair: variations on versatility. *Cell Mol Life Sci* 66, 994-1009 (2009).
13. Shuck, S.C., Short, E.A. & Turchi, J.J. Eukaryotic nucleotide excision repair: from understanding mechanisms to influencing biology. *Cell Res* 18, 64-72 (2008).
14. Pardo, B., Gomez-Gonzalez, B. & Aguilera, A. DNA repair in mammalian cells: DNA double-strand break repair: how to fix a broken relationship. *Cell Mol Life Sci* 66, 1039-56 (2009).
15. Chapman, J.R., Taylor, M.R. & Boulton, S.J. Playing the end game: DNA double-strand break repair pathway choice. *Mol Cell* 47, 497-510 (2012).
16. Chatterjee, N. & Walker, G.C. Mechanisms of DNA damage, repair, and mutagenesis. *Environ Mol Mutagen* 58, 235-263 (2017).
17. Deans, A.J. & West, S.C. DNA interstrand crosslink repair and cancer. *Nat Rev Cancer* 11, 467-80 (2011).
18. Hsieh, P. & Yamane, K. DNA mismatch repair: molecular mechanism, cancer, and ageing. *Mech Ageing Dev* 129, 391-407 (2008).
19. Li, G.M. Mechanisms and functions of DNA mismatch repair. *Cell Res* 18, 85-98 (2008).
20. Reyes, G.X., Schmidt, T.T., Kolodner, R.D. & Hombauer, H. New insights into the mechanism of DNA mismatch repair. *Chromosoma* 124, 443-62 (2015).
21. Gao, Y., Mutter-Rottmayer, E., Zlatanou, A., Vaziri, C. & Yang, Y. Mechanisms of Post-Replication DNA Repair. *Genes (Basel)* 8(2017).
22. Yang, W. Structure and mechanism for DNA lesion recognition. *Cell Res* 18, 184-97 (2008).
23. Krasikova, Y.S. et al. Influence of centrin 2 on the interaction of nucleotide excision repair factors with damaged DNA. *Biochemistry (Mosc)* 77, 346-53 (2012).
24. Masutani, C. et al. Purification and cloning of a nucleotide excision repair complex involving the xeroderma pigmentosum group C protein and a human homologue of yeast RAD23. *EMBO J* 13, 1831-43 (1994).
25. Nishi, R. et al. Centrin 2 stimulates nucleotide excision repair by interacting with xeroderma pigmentosum group C protein. *Mol Cell Biol* 25, 5664-74 (2005).
26. Sugawara, K. et al. Xeroderma pigmentosum group C protein complex is the initiator of global genome nucleotide excision repair. *Mol Cell* 2, 223-32 (1998).
27. Ng, J.M. et al. A novel regulation mechanism of DNA repair by damage-induced and RAD23-dependent stabilization of xeroderma pigmentosum group C protein. *Genes Dev* 17, 1630-45 (2003).

28. Sugasawa, K. & Hanaoka, F. Sensing of DNA damage by XPC/Rad4: one protein for many lesions. *Nat Struct Mol Biol* 14, 887-8 (2007).
29. Xie, Z., Liu, S., Zhang, Y. & Wang, Z. Roles of Rad23 protein in yeast nucleotide excision repair. *Nucleic Acids Res* 32, 5981-90 (2004).
30. Ruthemann, P., Balbo Pogliano, C. & Naegeli, H. Global-genome Nucleotide Excision Repair Controlled by Ubiquitin/Sumo Modifiers. *Front Genet* 7, 68 (2016).
31. Sugasawa, K. et al. A multistep damage recognition mechanism for global genomic nucleotide excision repair. *Genes Dev* 15, 507-21 (2001).
32. Scrima, A. et al. Structural basis of UV DNA-damage recognition by the DDB1-DDB2 complex. *Cell* 135, 1213-23 (2008).
33. Yokoi, M. et al. The xeroderma pigmentosum group C protein complex XPC-HR23B plays an important role in the recruitment of transcription factor IIH to damaged DNA. *J Biol Chem* 275, 9870-5 (2000).
34. Volker, M. et al. Sequential assembly of the nucleotide excision repair factors in vivo. *Mol Cell* 8, 213-24 (2001).
35. Coin, F., Oksenysh, V. & Egly, J.M. Distinct roles for the XPB/p52 and XPD/p44 subcomplexes of TFIIH in damaged DNA opening during nucleotide excision repair. *Mol Cell* 26, 245-56 (2007).
36. Oksenysh, V. & Coin, F. The long unwinding road: XPB and XPD helicases in damaged DNA opening. *Cell Cycle* 9, 90-6 (2010).
37. Zotter, A. et al. Recruitment of the nucleotide excision repair endonuclease XPG to sites of UV-induced dna damage depends on functional TFIIH. *Mol Cell Biol* 26, 8868-79 (2006).
38. Li, C.L. et al. Tripartite DNA Lesion Recognition and Verification by XPC, TFIIH, and XPA in Nucleotide Excision Repair. *Mol Cell* 59, 1025-34 (2015).
39. Coin, F. et al. Nucleotide excision repair driven by the dissociation of CAK from TFIIH. *Mol Cell* 31, 9-20 (2008).
40. Camenisch, U., Dip, R., Schumacher, S.B., Schuler, B. & Naegeli, H. Recognition of helical kinks by xeroderma pigmentosum group A protein triggers DNA excision repair. *Nat Struct Mol Biol* 13, 278-84 (2006).
41. Tsodikov, O.V. et al. Structural basis for the recruitment of ERCC1-XPF to nucleotide excision repair complexes by XPA. *EMBO J* 26, 4768-76 (2007).
42. de Laat, W.L. et al. DNA-binding polarity of human replication protein A positions nucleases in nucleotide excision repair. *Genes Dev* 12, 2598-609 (1998).
43. Hermanson-Miller, I.L. & Turchi, J.J. Strand-specific binding of RPA and XPA to damaged duplex DNA. *Biochemistry* 41, 2402-8 (2002).
44. Staresincic, L. et al. Coordination of dual incision and repair synthesis in human nucleotide excision repair. *EMBO J* 28, 1111-20 (2009).
45. Mellon, I., Bohr, V.A., Smith, C.A. & Hanawalt, P.C. Preferential DNA repair of an active gene in human cells. *Proc Natl Acad Sci U S A* 83, 8878-82 (1986).
46. Bohr, V.A., Smith, C.A., Okumoto, D.S. & Hanawalt, P.C. DNA repair in an active gene: removal of pyrimidine dimers from the DHFR gene of CHO cells is much more efficient than in the genome overall. *Cell* 40, 359-69 (1985).
47. Barrett, S.F., Robbins, J.H., Tarone, R.E. & Kraemer, K.H. Evidence for defective repair of cyclobutane pyrimidine dimers with normal repair of other DNA photoproducts in a transcriptionally active gene transfected into Cockayne syndrome cells. *Mutat Res* 255, 281-91 (1991).
48. Ljungman, M. & Zhang, F. Blockage of RNA polymerase as a possible trigger for u.v. light-induced apoptosis. *Oncogene* 13, 823-31 (1996).
49. Citterio, E. et al. ATP-dependent chromatin remodeling by the Cockayne syndrome B DNA repair-transcription-coupling factor. *Mol Cell Biol* 20, 7643-53 (2000).
50. Cho, I., Tsai, P.F., Lake, R.J., Basheer, A. & Fan, H.Y. ATP-dependent chromatin remodeling by Cockayne syndrome protein B and NAP1-like histone chaperones is required for efficient transcription-coupled DNA repair. *PLoS Genet* 9, e1003407 (2013).
51. Lake, R.J. & Fan, H.Y. Structure, function and regulation of CSB: a multi-talented gymnast. *Mech Ageing Dev* 134, 202-11 (2013).

52. Fischer, E.S. et al. The Molecular Basis of CRL4(DDB2/CSA) Ubiquitin Ligase Architecture, Targeting, and Activation. *Cell* 147, 1024-1039 (2011).
53. Schwertman, P. et al. UV-sensitive syndrome protein UVSSA recruits USP7 to regulate transcription-coupled repair. *Nat Genet* 44, 598-602 (2012).
54. Nakazawa, Y. et al. Mutations in UVSSA cause UV-sensitive syndrome and impair RNA polymerase II processing in transcription-coupled nucleotide-excision repair. *Nat Genet* 44, 586-92 (2012).
55. Zhang, X. et al. Mutations in UVSSA cause UV-sensitive syndrome and destabilize ERCC6 in transcription-coupled DNA repair. *Nat Genet* 44, 593-7 (2012).
56. Fei, J. & Chen, J. KIAA1530 protein is recruited by Cockayne syndrome complementation group protein A (CSA) to participate in transcription-coupled repair (TCR). *J Biol Chem* 287, 35118-26 (2012).
57. Nakatsu, Y. et al. XAB2, a novel tetratricopeptide repeat protein involved in transcription-coupled DNA repair and transcription. *J Biol Chem* 275, 34931-7 (2000).
58. van Oosterwijk, M.F., Versteeg, A., Filon, R., van Zeeland, A.A. & Mullenders, L.H. The sensitivity of Cockayne's syndrome cells to DNA-damaging agents is not due to defective transcription-coupled repair of active genes. *Mol Cell Biol* 16, 4436-44 (1996).
59. Rockx, D.A. et al. UV-induced inhibition of transcription involves repression of transcription initiation and phosphorylation of RNA polymerase II. *Proc Natl Acad Sci U S A* 97, 10503-8 (2000).
60. Proietti-De-Santis, L., Drane, P. & Egly, J.M. Cockayne syndrome B protein regulates the transcriptional program after UV irradiation. *EMBO J* 25, 1915-23 (2006).
61. Tornaletti, S., Reines, D. & Hanawalt, P.C. Structural characterization of RNA polymerase II complexes arrested by a cyclobutane pyrimidine dimer in the transcribed strand of template DNA. *J Biol Chem* 274, 24124-30 (1999).
62. Sarker, A.H. et al. Recognition of RNA polymerase II and transcription bubbles by XPG, CSB, and TFIIH: insights for transcription-coupled repair and Cockayne Syndrome. *Mol Cell* 20, 187-98 (2005).
63. McKay, B.C. et al. UV light-induced degradation of RNA polymerase II is dependent on the Cockayne's syndrome A and B proteins but not p53 or MLH1. *Mutat Res* 485, 93-105 (2001).
64. Bregman, D.B. et al. UV-induced ubiquitination of RNA polymerase II: a novel modification deficient in Cockayne syndrome cells. *Proc Natl Acad Sci U S A* 93, 11586-90 (1996).
65. Vrouwe, M.G., Pines, A., Overmeer, R.M., Hanada, K. & Mullenders, L.H. UV-induced photolesions elicit ATR-kinase-dependent signaling in non-cycling cells through nucleotide excision repair-dependent and -independent pathways. *J Cell Sci* 124, 435-46 (2011).
66. Woudstra, E.C. et al. A Rad26-Def1 complex coordinates repair and RNA pol II proteolysis in response to DNA damage. *Nature* 415, 929-33 (2002).
67. Wilson, M.D., Harreman, M. & Svejstrup, J.Q. Ubiquitylation and degradation of elongating RNA polymerase II: the last resort. *Biochim Biophys Acta* 1829, 151-7 (2013).
68. Lommel, L., Bucheli, M.E. & Sweder, K.S. Transcription-coupled repair in yeast is independent from ubiquitylation of RNA pol II: implications for Cockayne's syndrome. *Proc Natl Acad Sci U S A* 97, 9088-92 (2000).
69. Sahoo, M. & Klumpp, S. Backtracking dynamics of RNA polymerase: pausing and error correction. *J Phys Condens Matter* 25, 374104 (2013).
70. Nudler, E. RNA polymerase backtracking in gene regulation and genome instability. *Cell* 149, 1438-45 (2012).
71. Epshtein, V. et al. UvrD facilitates DNA repair by pulling RNA polymerase backwards. *Nature* 505, 372-7 (2014).
72. Epshtein, V. UvrD helicase: an old dog with a new trick: how one step backward leads to many steps forward. *Bioessays* 37, 12-9 (2015).
73. Park, J.S., Marr, M.T. & Roberts, J.W. E. coli Transcription repair coupling factor (Mfd protein) rescues arrested complexes by promoting forward translocation. *Cell* 109, 757-67 (2002).
74. Ganesan, A., Spivak, G. & Hanawalt, P.C. Transcription-coupled DNA repair in prokaryotes. *Prog Mol Biol Transl Sci* 110, 25-40 (2012).
75. van Hoffen, A., Balajee, A.S., van Zeeland, A.A. & Mullenders, L.H. Nucleotide excision repair and its interplay with transcription. *Toxicology* 193, 79-90 (2003).

76. Duan, M.R. & Smerdon, M.J. UV damage in DNA promotes nucleosome unwrapping. *J Biol Chem* 285, 26295-303 (2010).
77. Dinant, C., Houtsmuller, A.B. & Vermeulen, W. Chromatin structure and DNA damage repair. *Epigenetics Chromatin* 1, 9 (2008).
78. Nag, R. & Smerdon, M.J. Altering the chromatin landscape for nucleotide excision repair. *Mutat Res* 682, 13-20 (2009).
79. Xu, Y. et al. Histone H2A.Z controls a critical chromatin remodeling step required for DNA double-strand break repair. *Mol Cell* 48, 723-33 (2012).
80. Li, S. Implication of posttranslational histone modifications in nucleotide excision repair. *Int J Mol Sci* 13, 12461-86 (2012).
81. Luijsterburg, M.S. et al. DDB2 promotes chromatin decondensation at UV-induced DNA damage. *J Cell Biol* 197, 267-81 (2012).
82. Pines, A. et al. PARP1 promotes nucleotide excision repair through DDB2 stabilization and recruitment of ALC1. *J Cell Biol* 199, 235-49 (2012).
83. Robu, M. et al. Role of poly(ADP-ribose) polymerase-1 in the removal of UV-induced DNA lesions by nucleotide excision repair. *Proc Natl Acad Sci U S A* 110, 1658-63 (2013).
84. Jiang, Y. et al. INO80 chromatin remodeling complex promotes the removal of UV lesions by the nucleotide excision repair pathway. *Proc Natl Acad Sci U S A* 107, 17274-9 (2010).
85. Datta, A. et al. The p48 subunit of the damaged-DNA binding protein DDB associates with the CBP/p300 family of histone acetyltransferase. *Mutat Res* 486, 89-97 (2001).
86. Martinez, E. et al. Human STAGA complex is a chromatin-acetylating transcription coactivator that interacts with pre-mRNA splicing and DNA damage-binding factors in vivo. *Mol Cell Biol* 21, 6782-95 (2001).
87. Guo, R., Chen, J., Mitchell, D.L. & Johnson, D.G. GCN5 and E2F1 stimulate nucleotide excision repair by promoting H3K9 acetylation at sites of damage. *Nucleic Acids Res* 39, 1390-7 (2011).
88. Niida, H. et al. Phosphorylated HBO1 at UV irradiated sites is essential for nucleotide excision repair. *Nat Commun* 8, 16102 (2017).
89. Guerrero-Santorio, J. et al. The cullin 4B-based UV-damaged DNA-binding protein ligase binds to UV-damaged chromatin and ubiquitinates histone H2A. *Cancer Res* 68, 5014-22 (2008).
90. Wang, H. et al. Histone H3 and H4 ubiquitylation by the CUL4-DDB-ROC1 ubiquitin ligase facilitates cellular response to DNA damage. *Mol Cell* 22, 383-94 (2006).
91. Kapetanaki, M.G. et al. The DDB1-CUL4ADDB2 ubiquitin ligase is deficient in xeroderma pigmentosum group E and targets histone H2A at UV-damaged DNA sites. *Proc Natl Acad Sci U S A* 103, 2588-93 (2006).
92. Smerdon, M.J., Lan, S.Y., Calza, R.E. & Reeves, R. Sodium butyrate stimulates DNA repair in UV-irradiated normal and xeroderma pigmentosum human fibroblasts. *J Biol Chem* 257, 13441-7 (1982).
93. Lim, J.H. et al. Chromosomal protein HMGN1 modulates histone H3 phosphorylation. *Mol Cell* 15, 573-84 (2004).
94. Birger, Y. et al. Chromosomal protein HMGN1 enhances the rate of DNA repair in chromatin. *EMBO J* 22, 1665-75 (2003).
95. Trieschmann, L., Martin, B. & Bustin, M. The chromatin unfolding domain of chromosomal protein HMG-14 targets the N-terminal tail of histone H3 in nucleosomes. *Proc Natl Acad Sci U S A* 95, 5468-73 (1998).
96. Green, C.M. & Almouzni, G. Local action of the chromatin assembly factor CAF-1 at sites of nucleotide excision repair in vivo. *EMBO J* 22, 5163-74 (2003).
97. Dinant, C. et al. Enhanced chromatin dynamics by FACT promotes transcriptional restart after UV-induced DNA damage. *Mol Cell* 51, 469-79 (2013).
98. Polo, S.E., Roche, D. & Almouzni, G. New histone incorporation marks sites of UV repair in human cells. *Cell* 127, 481-93 (2006).
99. Oksenyich, V. et al. Histone methyltransferase DOT1L drives recovery of gene expression after a genotoxic attack. *PLoS Genet* 9, e1003611 (2013).
100. Mandemaker, I.K., Vermeulen, W. & Marteijn, J.A. Gearing up chromatin: A role for chromatin remodeling during the transcriptional restart upon DNA damage. *Nucleus* 5, 203-10 (2014).

101. Adam, S., Polo, S.E. & Almouzni, G. Transcription recovery after DNA damage requires chromatin priming by the H3.3 histone chaperone HIRA. *Cell* 155, 94-106 (2013).
102. DiGiovanna, J.J. & Kraemer, K.H. Shining a light on xeroderma pigmentosum. *J Invest Dermatol* 132, 785-96 (2012).
103. Bradford, P.T. et al. Cancer and neurologic degeneration in xeroderma pigmentosum: long term follow-up characterises the role of DNA repair. *J Med Genet* 48, 168-76 (2011).
104. Barnes, D.E. & Lindahl, T. Repair and genetic consequences of endogenous DNA base damage in mammalian cells. *Annu Rev Genet* 38, 445-76 (2004).
105. Laugel, V. Cockayne syndrome: the expanding clinical and mutational spectrum. *Mech Ageing Dev* 134, 161-70 (2013).
106. Laugel, V. et al. Mutation update for the CSB/ERCC6 and CSA/ERCC8 genes involved in Cockayne syndrome. *Hum Mutat* 31, 113-26 (2010).
107. Kraemer, K.H. et al. Xeroderma pigmentosum, trichothiodystrophy and Cockayne syndrome: a complex genotype-phenotype relationship. *Neuroscience* 145, 1388-96 (2007).
108. Calmels, N. et al. Uncommon nucleotide excision repair phenotypes revealed by targeted high-throughput sequencing. *Orphanet J Rare Dis* 11, 26 (2016).
109. Nardo, T. et al. A UV-sensitive syndrome patient with a specific CSA mutation reveals separable roles for CSA in response to UV and oxidative DNA damage. *Proc Natl Acad Sci U S A* 106, 6209-14 (2009).
110. Horibata, K. et al. Complete absence of Cockayne syndrome group B gene product gives rise to UV-sensitive syndrome but not Cockayne syndrome. *Proc Natl Acad Sci U S A* 101, 15410-5 (2004).
111. Cleaver, J.E. Photosensitivity syndrome brings to light a new transcription-coupled DNA repair cofactor. *Nat Genet* 44, 477-8 (2012).
112. Brooks, P.J. Blinded by the UV light: how the focus on transcription-coupled NER has distracted from understanding the mechanisms of Cockayne syndrome neurologic disease. *DNA Repair (Amst)* 12, 656-71 (2013).
113. Schwertman, P., Vermeulen, W. & Marteijn, J.A. UVSSA and USP7, a new couple in transcription-coupled DNA repair. *Chromosoma* 122, 275-84 (2013).
114. Luijsterburg, M.S. et al. Stochastic and reversible assembly of a multiprotein DNA repair complex ensures accurate target site recognition and efficient repair. *J Cell Biol* 189, 445-63 (2010).
115. Groisman, R. et al. The ubiquitin ligase activity in the DDB2 and CSA complexes is differentially regulated by the COP9 signalosome in response to DNA damage. *Cell* 113, 357-67 (2003).
116. Sugawara, K. et al. UV-induced ubiquitylation of XPC protein mediated by UV-DDB-ubiquitin ligase complex. *Cell* 121, 387-400 (2005).
117. Poulsen, S.L. et al. RNF111/Arkadia is a SUMO-targeted ubiquitin ligase that facilitates the DNA damage response. *J Cell Biol* 201, 797-807 (2013).
118. Rápic-Otrin, V., McLenigan, M.P., Bisi, D.C., Gonzalez, M. & Levine, A.S. Sequential binding of UV DNA damage binding factor and degradation of the p48 subunit as early events after UV irradiation. *Nucleic Acids Res* 30, 2588-98 (2002).
119. Robu, M. et al. Poly(ADP-ribose) polymerase 1 escorts XPC to UV-induced DNA lesions during nucleotide excision repair. *Proc Natl Acad Sci U S A* 114, E6847-E6856 (2017).
120. Puumalainen, M.R. et al. Chromatin retention of DNA damage sensors DDB2 and XPC through loss of p97 segregase causes genotoxicity. *Nat Commun* 5, 3695 (2014).
121. Povlsen, L.K. et al. Systems-wide analysis of ubiquitylation dynamics reveals a key role for PAF15 ubiquitylation in DNA-damage bypass. *Nat Cell Biol* 14, 1089-98 (2012).
122. Wang, Q.E. et al. DNA repair factor XPC is modified by SUMO-1 and ubiquitin following UV irradiation. *Nucleic Acids Res* 33, 4023-34 (2005).
123. Anindya, R., Aygun, O. & Svejstrup, J.Q. Damage-induced ubiquitylation of human RNA polymerase II by the ubiquitin ligase Nedd4, but not Cockayne syndrome proteins or BRCA1. *Mol Cell* 28, 386-97 (2007).
124. Yasukawa, T. et al. Mammalian Elongin A complex mediates DNA-damage-induced ubiquitylation and degradation of Rpb1. *EMBO J* 27, 3256-66 (2008).

125. Aune, G.J. et al. Von Hippel-Lindau-coupled and transcription-coupled nucleotide excision repair-dependent degradation of RNA polymerase II in response to trabectedin. *Clin Cancer Res* 14, 6449-55 (2008).
126. Kleiman, F.E. et al. BRCA1/BARD1 inhibition of mRNA 3' processing involves targeted degradation of RNA polymerase II. *Genes Dev* 19, 1227-37 (2005).
127. Starita, L.M. et al. BRCA1/BARD1 ubiquitinate phosphorylated RNA polymerase II. *J Biol Chem* 280, 24498-505 (2005).
128. Harreman, M. et al. Distinct ubiquitin ligases act sequentially for RNA polymerase II polyubiquitylation. *Proc Natl Acad Sci U S A* 106, 20705-10 (2009).
129. Groisman, R. et al. CSA-dependent degradation of CSB by the ubiquitin-proteasome pathway establishes a link between complementation factors of the Cockayne syndrome. *Genes Dev* 20, 1429-34 (2006).
130. He, J., Zhu, Q., Wani, G., Sharma, N. & Wani, A.A. Valosin-containing Protein (VCP)/p97 Segregase Mediates Proteolytic Processing of Cockayne Syndrome Group B (CSB) in Damaged Chromatin. *J Biol Chem* 291, 7396-408 (2016).
131. Higa, M., Tanaka, K. & Saijo, M. Inhibition of UVSSA ubiquitination suppresses transcription-coupled nucleotide excision repair deficiency caused by dissociation from USP7. *FEBS J* 285, 965-976 (2018).
132. Enchev, R.I., Schulman, B.A. & Peter, M. Protein neddylation: beyond cullin-RING ligases. *Nat Rev Mol Cell Biol* 16, 30-44 (2015).
133. Matsunuma, R. et al. UV Damage-Induced Phosphorylation of HBO1 Triggers CRL4DDB2-Mediated Degradation To Regulate Cell Proliferation. *Mol Cell Biol* 36, 394-406 (2016).
134. Christiansen, M. et al. Functional consequences of mutations in the conserved SF2 motifs and post-translational phosphorylation of the CSB protein. *Nucleic Acids Res* 31, 963-73 (2003).
135. Watts, F.Z. Sumoylation of PCNA: Wrestling with recombination at stalled replication forks. *DNA Repair (Amst)* 5, 399-403 (2006).
136. Pfander, B., Moldovan, G.L., Sacher, M., Hoege, C. & Jentsch, S. SUMO-modified PCNA recruits Srs2 to prevent recombination during S phase. *Nature* 436, 428-33 (2005).
137. Krejci, L. et al. DNA helicase Srs2 disrupts the Rad51 presynaptic filament. *Nature* 423, 305-9 (2003).
138. Veaute, X. et al. The Srs2 helicase prevents recombination by disrupting Rad51 nucleoprotein filaments. *Nature* 423, 309-12 (2003).
139. Parker, J.L. & Ulrich, H.D. A SUMO-interacting motif activates budding yeast ubiquitin ligase Rad18 towards SUMO-modified PCNA. *Nucleic Acids Res* 40, 11380-8 (2012).
140. Kannouche, P.L., Wing, J. & Lehmann, A.R. Interaction of human DNA polymerase eta with monoubiquitinated PCNA: a possible mechanism for the polymerase switch in response to DNA damage. *Mol Cell* 14, 491-500 (2004).
141. Garcia-Rodriguez, N., Wong, R.P. & Ulrich, H.D. Functions of Ubiquitin and SUMO in DNA Replication and Replication Stress. *Front Genet* 7, 87 (2016).
142. Hoege, C., Pfander, B., Moldovan, G.L., Pyrowolakis, G. & Jentsch, S. RAD6-dependent DNA repair is linked to modification of PCNA by ubiquitin and SUMO. *Nature* 419, 135-41 (2002).
143. Stelter, P. & Ulrich, H.D. Control of spontaneous and damage-induced mutagenesis by SUMO and ubiquitin conjugation. *Nature* 425, 188-91 (2003).
144. Kolesar, P., Sarangi, P., Altmannova, V., Zhao, X. & Krejci, L. Dual roles of the SUMO-interacting motif in the regulation of Srs2 sumoylation. *Nucleic Acids Res* 40, 7831-43 (2012).
145. Urulangodi, M. et al. Local regulation of the Srs2 helicase by the SUMO-like domain protein Esc2 promotes recombination at sites of stalled replication. *Genes Dev* 29, 2067-80 (2015).
146. Ribet, D. & Cossart, P. Post-translational modifications in host cells during bacterial infection. *FEBS Lett* 584, 2748-58 (2010).
147. Giang, J. et al. Complement Activation in Inflammatory Skin Diseases. *Front Immunol* 9, 639 (2018).
148. Du Clos, T.W. & Mold, C. Complement and complement deficiencies. in *Clinical Immunology: Principles and Practice* 305-325 (Mosby, 2008).
149. Cole, L. & Kramer, P.R. Chapter 3.3 - The Circulation. in *Human Physiology, Biochemistry and Basic Medicine* 85-91 (Academic Press, Boston, 2016).

150. Parvizi, J. & Kim, G.K. Chapter 17 - Anticoagulation. in *High Yield Orthopaedics* 34-36 (W.B. Saunders, Philadelphia, 2010).
151. Gabriela, C.M. & A., H.K. Molecular mechanisms of fibrinolysis. *British Journal of Haematology* 129, 307-321 (2005).
152. Huntington, J.A. Serpin structure, function and dysfunction. *J. Thromb. Haemost* 9 Suppl 1, 26-34 (2011).
153. Huntington, J.A., Read, R.J. & Carrell, R.W. Structure of a serpin-protease complex shows inhibition by deformation. *Nature* 407, 923 (2000).
154. Gettins, P.G. & Olson, S.T. Inhibitory serpins. New insights into their folding, polymerization, regulation and clearance. *Biochem J* 473, 2273-93 (2016).
155. Davis, A.E., 3rd, Lu, F. & Mejia, P. C1 inhibitor, a multi-functional serine protease inhibitor. *Thromb Haemost* 104, 886-93 (2010).
156. Cugno, M., Zanichelli, A., Foieni, F., Caccia, S. & Cicardi, M. C1-inhibitor deficiency and angioedema: molecular mechanisms and clinical progress. *Trends Mol. Med* 15, 69-78 (2009).
157. Carugati, A., Pappalardo, E., Zingale, L.C. & Cicardi, M. C1-inhibitor deficiency and angioedema. *Mol. Immunol* 38, 161-173 (2001).
158. Zhou, Z.H., Rajabi, M., Chen, T., Karnaukhova, E. & Kozlowski, S. Oversulfated chondroitin sulfate inhibits the complement classical pathway by potentiating C1 inhibitor. *PLoS. One* 7, e47296 (2012).
159. Rajabi, M., Struble, E., Zhou, Z. & Karnaukhova, E. Potentiation of C1-esterase inhibitor by heparin and interactions with C1s protease as assessed by surface plasmon resonance. *Biochim. Biophys. Acta* 1820, 56-63 (2012).
160. Caldwell, E.E. et al. Heparin binding and augmentation of C1 inhibitor activity. *Arch. Biochem. Biophys* 361, 215-222 (1999).
161. Wuillemin, W.A. et al. Potentiation of C1 inhibitor by glycosaminoglycans: dextran sulfate species are effective inhibitors of in vitro complement activation in plasma. *J. Immunol* 159, 1953-1960 (1997).
162. Karnaukhova, E. C1-Esterase inhibitor: biological activities and therapeutic applications. *J Hematol Thromb Dis* 1(2013).

2

Potential targets of the CSA-based cullin-RING ubiquitin ligase in transcription-coupled DNA repair

Madelon Dijk, Mischa G. Vrouwe and Leon H. Mullenders

Abstract

Transcription-coupled nucleotide excision repair (TC-NER) is responsible for the fast removal of helix-distorting DNA lesions that interfere with elongating RNA polymerase II (RNAPII_o). Stalling of RNAPII_o at sites of DNA damage triggers the assembly of a repair complex, which is initiated by the recruitment of key TC-NER factors CSA and CSB. CSA is part of a larger complex, consisting of CSA, DDB1, CUL4A/B and RBX1, which together form the culling-RING ubiquitin ligase CRL^{CSA}. Although CSA is essential for repair of UV-induced damage and subsequent resumption of transcription, the precise role of CRL^{CSA} during NER remains largely elusive. Here we show that NEDDylation, which is required for the activation of cullin-RING ligases, modulates the presence of CRL^{CSA} at the repair complex, as well as the CSA-dependent degradation of the phosphorylated RNAPII subunit RPB1 after high doses of UV. Together our data uncover both CSA and RPB1 as potential CRL^{CSA} ubiquitination targets, showing that CRL^{CSA} may contribute not only to repair, but also to the avoidance of persistently stalled RNAPII_o when TC-NER cannot be properly executed.

Introduction

2

The nucleotide excision repair (NER) pathway removes a wide variety of helix-distorting lesions, including the mutagenic and toxic cyclobutane pyrimidine dimers (CPDs) and pyrimidine(6-4)pyrimidone photoproducts (6-4 PPs) that are caused by UV irradiation¹. These photolesions are repaired via either the global genome repair (GG-NER) or transcription-coupled repair (TC-NER) subpathway. The damage recognition complexes XPC-RAD23B and UV-DDB are designed to continuously probe the whole genome for damage, initiating GG-NER when needed². TC-NER is triggered by the encounter of lesions by elongating RNA polymerase II (RNAPII) and thus is responsible for the repair of transcription-blocking lesions in transcriptionally active DNA³. The recruitment of the SWI/SNF2 ATPase CSB and the CSA protein to the stalled RNA polymerase is essential for repair of UV-induced damage and ultimately, for resumption of transcription⁴⁻⁷. Furthermore, UVSSA and its associated factor USP7 specifically contribute to transcription-coupled repair, possibly by regulating the presence of CSB⁸. Upon lesion detection, the formation of a pre-incision complex that facilitates damage verification is common to both pathways. In this complex, TFIIH exploits the ATPase and helicase activities of its XPB and XPD subunits, respectively, to unwind the DNA. In this way it cooperates with XPA to verify the damage. Next to directly recognizing structurally altered ssDNA, XPA is thought to play a central role in NER as it interacts with a large range of NER proteins⁹. Subsequent incision on both sides of the lesion by XPF-ERCC1 (5') and XPG (3') removes a DNA stretch containing the damage². Using the undamaged strand as a template, a DNA polymerase fills the gap, after which NER is completed by DNA ligase-dependent sealing of the final nick⁹.

Defects in NER genes underlie several disorders that display broadly varying symptoms. While classic Cockayne syndrome, resulting from mutations in CSA or CSB, is characterized by severe neurological and developmental abnormalities, the defects in the gene encoding UVSSA detected to date only lead to the mild photo-sensitivity observed in UV sensitivity syndrome (UVsS) patients^{7,10,11}. Defective XP proteins mainly give rise to xeroderma pigmentosum (XP), which is marked by sensitivity to sun light and a strong cancer predisposition, although certain mutations in XPB, XPD, XPF or XPG can cause a combined CS/XP patient phenotype¹²⁻¹⁶. Furthermore, mutations in TFIIH subunits can lead to trichothiodystrophy (TTD) – a disorder characterized by brittle hair and nails and intellectual impairment¹⁷.

The variety in NER-associated disorders underscores the importance of correct execution of each step of the pathway. Several post-translational modifications have been shown to contribute to NER regulation, of which ubiquitination has been mostly studied¹⁸⁻²⁰. Notably, both the GG-NER factor DDB2, as well as the TC-NER protein CSA assemble into a larger complex with DDB1, CUL4A/B and RBX1, forming the cullin-RING ubiquitin ligases CRL^{DDB2} and CRL^{CSA}, respectively²¹. The activation of cullin-RING ligases typically requires NEDDylation of the cullin protein²². In unperturbed conditions, this is counteracted by the COP9 signalosome that keeps CRL^{DDB2} and CRL^{CSA} in an inactive state by removing NEDD8 from CUL4A/B. Upon UV irradiation the dissociation of COP9 is thought to enable activation of both ligases, although possibly at different stages²³. Whereas the ubiquitination targets of

CRL^{DDB2} have been extensively studied and were shown to include XPC, histones and DDB2 itself, the role of CRL^{CSA} during NER is less well described^{24,25,26}. Possibly CRL^{CSA} employs auto-ubiquitination of CSA or ubiquitinates CSB to regulate repair^{21,27}. Furthermore, a last resort mechanism that degrades RNA polymerase II subunit RPB1 when repair is compromised has been shown to depend on CSA²⁸⁻³⁰.

Here we investigate CSA and RPB1 as potential CRL^{CSA} targets. By using a NEDDylation inhibitor, we show that NEDDylation modulates the amount of CRL^{CSA} that interacts with RNAPII upon UV irradiation. Possibly this reflects CRL^{CSA} auto-ubiquitination as a mechanism to control CRL^{CSA} levels at sites of DNA damage. In addition, we reveal a NEDDylation-dependent reduction in the total cellular levels of the RPB1 subunit of elongating RNAPII after UV irradiation. Interestingly, this UV-induced degradation of RPB1 appears to also depend on CSB and CSA, but not on XPA or UVSSA. Although further research is required to fully uncover the role of CRL^{CSA} during NER, these findings propose a contribution of CRL^{CSA} to the regulation of TC-NER under normal conditions, as well as to an alternative solution that removes the stalled RNA polymerase when TC-NER fails.

Results

NEDDylation modulates the presence of CRL^{CSA} at the TC-NER complex

Given that CRL^{DDB2} ubiquitinates itself during GG-NER to coordinate its removal from the repair complex, we hypothesized that the structurally comparable CRL^{CSA} could control its own dissociation from the TC-NER complex in a similar manner³¹. To investigate this possibility, the composition of the TC-NER complex was studied 1 hour after UV irradiation by immunoprecipitation of the RPB1 subunit of active RNA polymerase II complexes, which are characterized by RPB1's heavily phosphorylated C-terminal domain (CTD). Either serine 5-phosphorylated RPB1 (p-S5-RPB1; Fig. 1), which is usually detected during early transcription, or serine 2-phosphorylated RPB1 (p-S2-RPB1; Supplementary Fig. 1), which is associated with the positioning of elongating RNAPII (RNAPII_o) further along the gene, was precipitated. As expected, both p-S5-RPB1 and p-S2-RPB1 showed a UV-specific increase in the interaction with core TC-NER factor CSB. Furthermore, the build-up of the TC-NER complex was reflected by UV-induced interactions between p-S5-RPB1 or p-S2-RPB1 and members of CRL^{CSA} (DDB1, CUL4A, CSA). Interestingly, when the activation of E3 ubiquitin ligases was inhibited by the NEDDylation inhibitor MLN4924 (NEDDi), we observed increased levels of the CRL^{CSA} components associated with p-S5-RPB1 or p-S2-RPB1 after UV irradiation (Fig. 1b). In contrast, although CSB has been suggested to be a CRL^{CSA} target as well, the amount of CSB interacting with p-S5-RPB1 or p-S2-RPB1 appeared to be unaffected by the inhibition of culling-RING ubiquitin ligases²⁷. Although the use of a general NEDDylation inhibitor constrains any conclusions related to the involved ubiquitin ligase, these observations are supportive of considering CRL^{CSA} itself as a putative ubiquitination target of CRL^{CSA} during TC-NER. In agreement with this, *in vitro* studies have shown that CRL^{CSA} is capable of auto-ubiquitination²¹.

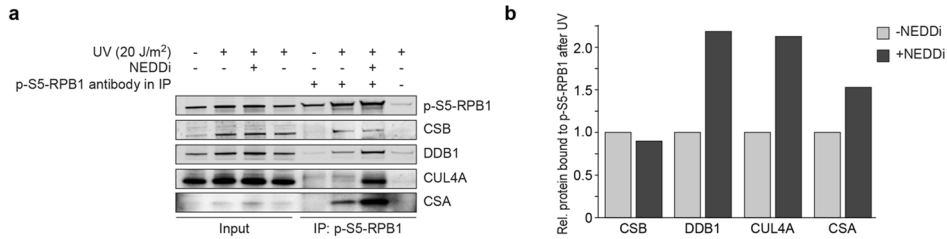


Figure 1. NEDDylation modulates the presence of CRL^{CSA} at the TC-NER complex

(a) Immunoprecipitation of the serine 5-phosphorylated RNAPII subunit RPB1 (p-S5-RPB1) from VH10-hTert cells 1 hour after mock treatment or UV-C irradiation (20 J/m²). Where indicated, global NEDDylation had been inhibited prior to UV-C irradiation by treatment with the NEDDylation inhibitor MLN4924. A similar experiment, in which p-S2-RPB1 was precipitated, is shown in Supplementary Fig. 1. (b) Relative amounts of CSB, DDB1, CUL4A and CSA that coprecipitated with p-S5-RPB1 1 hour after UV-C irradiation (20 J/m²).

Inhibition of CRL activation prevents UV-induced degradation of phosphorylated RPB1

Next to CRL^{CSA} itself, we envisaged RPB1 a possible target for CRL^{CSA}-mediated ubiquitination. RPB1 has been described to undergo CSA- and CSB-dependent ubiquitination upon induction of transcription-stalling DNA damage^{28,29}. Its subsequent eviction from the site of damage is considered to be a last resort mechanism when repair cannot be properly executed^{3,30,32,33}. To investigate the effect of NEDDylation on RPB1 degradation, total levels of p-S5-RPB1 were studied in non-irradiated or UV-irradiated non-dividing fibroblasts that were mock treated or treated with NEDDi (Fig. 2). Under unperturbed conditions, we observed a considerable decrease in total p-S5-RPB1 levels 6 hours after damage induction. In contrast, following treatment with NEDDi p-S5-RPB1 levels did not decrease and rather appeared to be substantially increased. Interestingly, a similar rise in total p-S5-RPB1 levels after UV has been shown for CSB- or CSA-deficient cells without inhibition of NEDDylation²⁹. Together these results indicate that p-S5-RPB1 is indeed subjected to NEDDylation-dependent degradation after UV, and open up the possibility of CRL^{CSA}-mediated ubiquitination of RPB1.

UV-induced degradation of phosphorylated RPB1 is dependent on CSA and CSB

To further study a potential role for CRL^{CSA} in RPB1 ubiquitination, the effect of UV damage on total p-S5-RPB1 levels was examined in different human cell lines. In accordance with our previous observations (Fig. 2), p-S5-RPB1 levels were reduced after UV in wildtype VH10-hTert cells (Fig. 3). A distinct degradation of p-S5-RPB1 was also observed in UV sensitive syndrome (UVsS) patient-derived UVSSA-deficient cells. In contrast, CSA-deficient cells derived from a Cockayne syndrome (CS) patient displayed no reduction in total p-S5-RPB1 levels after UV, but rather showed an increase in the p-RPB1 levels. The effect of CSA deficiency on p-S5-RPB1 stability mimicked the effect of inactivation of CRL^{CSA} and other cullin-RING E3 ligases by NEDDi treatment (Fig. 2). Similarly, in the absence of CSB, which is

essential for the recruitment of CRL^{CSA} to the TC-NER complex, no reduction in p-S5-RPB1 levels upon UV irradiation could be detected³⁴. Moreover, CS-B cells, similarly to CS-A cells, also displayed an increase of p-S5-RPB1 after UV. Together these observations hint towards CSA-dependent degradation of p-S5-RPB1 upon UV-induced transcription stalling. However, further research should elucidate whether the E3 ligase activity of CRL^{CSA} itself, or another ubiquitin ligase that is dependent on CSA is responsible for p-S5-RPB1 degradation.

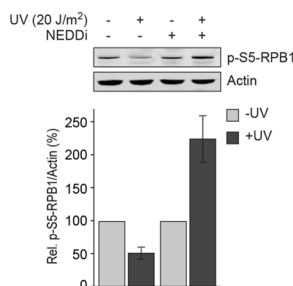


Figure 2. Inhibition of CRL activation prevents UV-induced degradation of p-RPB1

Total levels of serine 5-phosphorylated RPB1 (p-S5-RPB1) in VH10-hTert cells 6 hours after mock treatment or UV-C irradiation (20 J/m²). Where indicated, NEDDylation had been inhibited prior to UV irradiation. Bar graphs show p-S5-RPB1 levels relative to those in non-irradiated cells and represent the average \pm SEM of 2 independent experiments.

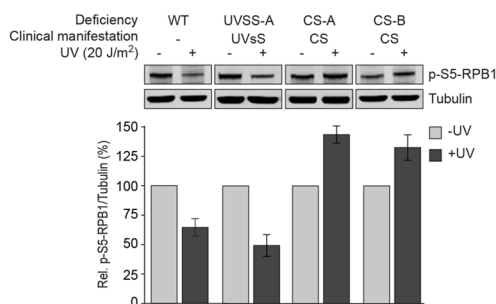


Figure 3. UV-induced degradation of p-RPB1 is dependent on CSA

Total levels of serine 5-phosphorylated RPB1 (p-S5-RPB1) in VH10-hTert (WT), KPS3-hTert (UVSS-A), CS3BE-hTert (CS-A) and CS1AN-hTert (CS-B) cells 6 hours after mock treatment or UV-C irradiation (20 J/m²). Bar graphs show p-S5-RPB1 levels relative to those in non-irradiated cells and represent the average \pm SEM of 2 independent experiments.

UV-induced degradation of p-RPB1 is similar in XP and combined XP/CS patient cell lines

UV-irradiated cells from UV sensitive syndrome patients and Cockayne syndrome patients display defective TC-NER and UV hypersensitivity, yet differ in the ability to degrade p-S5-RPB1 (Fig. 3). Displacement of abortive TC-NER complexes trapped at UV-inflicted photolesions has been suggested as one of the mechanisms to enable DNA damage repair via alternative pathways². Furthermore, avoidance of persistently stalled RNAPII is crucial in the prevention of accelerated cell death via p53-mediated apoptosis^{35,36}. Therefore, we hypothesized that the inability to remove stalled RNAPII from damaged DNA could cause, or contribute to the development of the more severe neurodevelopmental phenotype of Cockayne syndrome patients. To investigate this possibility, we first studied p-S5-RPB1 degradation in cells derived from a xeroderma pigmentosum (XP) patient harboring a mutation in the *XPB* gene. In agreement with our hypothesis, p-S5-RPB1 was efficiently degraded upon UV irradiation of these cells (Fig. 4). Accordingly, a distinct level of UV-induced p-S5-RPB1 degradation could also be detected in cells obtained from an XP patient with a mutation in the *XPB* gene. However, we observed a similar extent of UV-induced degradation in cells from a patient that suffered from combined XP/CS, caused by a mutation in the *XPB* gene that differs from the *XPB* mutations underlying classic xeroderma pigmentosum. Notably, XP and XP/CS cell lines harboring mutations in the *XPB* gene degraded RPB1 upon UV to an extent that was comparable to that in WT cells, as well as in the investigated *XPB*-deficient cell lines (data not shown). Together, our observations in UVsS, CS, XP, and XP/CS patient cell lines indicate that the ability to remove stalled RNAPII and/or repair complexes may contribute, but is likely not sufficient to prevent the development of the CS phenotype. Other mechanisms may play a role as well, such as the participation of CS proteins in mitochondrial repair and base excision repair³⁷⁻³⁹. Further research should elucidate the exact significance of RNAPII degradation and additional factors in determining the clinical outcome of genetic NER defects.

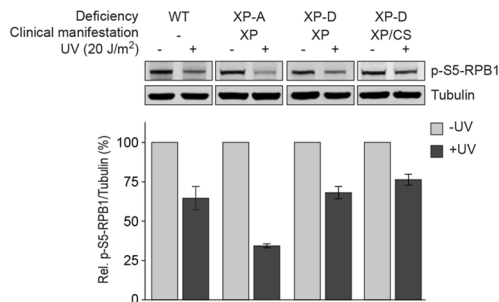


Figure 4. UV-induced degradation of p-RPB1 is similar in XP and combined XP/CS patient cell lines

Total levels of serine 5-phosphorylated RPB1 (p-S5-RPB1) in Vh10-hTert (WT), XP25RO-hTert (XP-A), XP1DU-hTert (XP-D) and XP8BR-hTert (XP-D/CS) cells 6 hours after mock treatment or UV-C irradiation (20 J/m²). Bar graphs show p-S5-RPB1 levels relative to those in non-irradiated cells and represent the average \pm SEM of 2 independent experiments.

Discussion

Tight regulation of each step of NER is essential for its proper activation, as well as for faithful repair of the damage and restoration of the cellular state prior to DNA damage occurrence. Post-translational modifications are a powerful tool to control repair proteins by affecting their localization, function and stability, in addition to regulating their crosstalk with proteins involved in other processes. For example, ubiquitination has been described to contribute to the regulation of NER in various manners¹⁸⁻²⁰. The significance of this modification and its different biological applications is illustrated by the E3 ubiquitin ligase CRL^{DDB2}, which is important for GG-NER². CRL^{DDB2} ubiquitinates both DDB2 and XPC, thereby altering the faith of these proteins in different ways. Whereas auto-ubiquitination induces proteasomal degradation of DDB2, ubiquitinated XPC shows increased affinity for damaged DNA³¹. Moreover, CRL^{DDB2} ubiquitinates core histones and DDB2 associates with PARP1 to stimulate chromatin remodeling^{25,26,40,41}.

In contrast to the extensively studied CRL^{DDB2} complex, the exact function of the structurally similar CRL^{CSA}, which is crucial for TC-NER, remains largely elusive. Notably, CRL^{CSA} has been described to function differently in terms of activation of its ligase activity. The COP9 signalosome, which keeps cullin-RING ligases in an inactive state by preventing NEDDylation of the cullin, has been shown to dissociate from CRL^{DDB2} directly after damage induction. In contrast, COP9 dissociation from CRL^{CSA} was suggested to occur at later times, when repair has already been completed²³. Alternatively, *in vitro* studies suggest that CSA might replace the COP9 signalosome, enabling CRL^{CSA} to become activated by NEDD8²¹. In support of this, we clearly observed a UV-induced interaction between RNAPII α and CSA, but have never been able to detect the COP9 signalosome in the TC-NER complex (unpublished data, Fig. 1, Supplementary Fig. 1).

To investigate to which extent the function of CRL^{CSA} during TC-NER resembles that of CRL^{DDB2} during GG-NER, we have studied the composition of the TC-NER complex under conditions of unperturbed NEDDylation or after inhibiting NEDD8 E1 activating enzyme (NAE) by MLN4924. The increased association of CRL^{CSA} factors with p-S5-RPB1 and p-S2-RPB1 after UV and NEDDi treatment shows that NEDDylation regulates the stoichiometry of the TC-NER complex. Possibly this implies that CRL^{CSA}, comparably to CRL^{DDB2}, in conditions that allow normal activation of cullin-RING ligases (partly) dissociates from the repair complex. Interestingly, the association of DDB1, CUL4A and CSA with p-S5-RPB1 or p-S2-RPB1 increased to approximately the same extent, showing that the protein stoichiometry within CRL^{CSA} is maintained.

Another explanation for the increased levels of CRL^{CSA} proteins that coprecipitated with p-S2-RPB1 after NEDDylation inhibition would be that only non-ubiquitinated or non-NEDDylated CRL^{CSA} is able to become part of the TC-NER complex. In this case, the elevated amounts of CRL^{CSA} in this repair complex after NEDDi would result from the increased availability of unmodified CRL^{CSA}. However, CRL^{CSA} levels in chromatin (Fig. 1, input) appeared to be unaffected by NEDDylation, which suggest that ubiquitination of CRL^{CSA} might occur after its recruitment to the TC-NER complex. Moreover, under conditions of unperturbed NEDDylation we observed preferential binding of modified CUL4A to p-S5-

RPB1 (Fig. 1) or p-S2-RPB1 (Supplementary Fig. 1). Although probing with NEDD8-specific antibodies is required to confirm the modification, this most likely represents the NEDDylated form of CUL4A, which would also further support the presence of activated CRL^{CSA} in the TC-NER complex. Since NEDDylation is a general mechanism of cullin-RING ligase activation, we cannot ascribe the observed effects to the activity of CRL^{CSA}²². However, given the structural similarities to CRL^{DDB2} and the ability of CRL^{CSA} to ubiquitinate itself in vitro, coordination of CRL^{CSA} dissociation from the TC-NER complex by auto-ubiquitination seems a plausible method to regulate repair²¹.

CRL^{CSA} has also been proposed to ubiquitinate CSB²⁷. Interestingly, we did not observe increased levels of CSB in the TC-NER complex upon inhibiting NEDDylation. Nevertheless, these results do not completely exclude CSB as a possible CRL^{CSA} ubiquitination target. CSB has been shown to be deubiquitinated by USP7, which is recruited via UVSSA in a CSA-dependent manner^{11,42}. In this way, the eviction of CSB from the complex can be tightly regulated by the balanced actions of a ubiquitin ligase and a deubiquitinating enzyme. Thus, ubiquitination of CSB by CRL^{CSA} might have been counteracted by USP7. Alternatively, the effect of CRL^{CSA} ubiquitination might have gone unnoticed in these experiments if ubiquitination of CSB affects the protein in a way other than guiding its proteasomal degradation, as described for XPC ubiquitination by CRL^{DDB2}.

The actual dissociation of CSB has been suggested to occur at a later stage, after repair of the damage, enabling resumption of transcription²⁷. Remarkably, inhibition of the VCP/p97 segregase that mediates its dissociation was shown to enhance the recovery of RNA synthesis after UV⁴³. Importantly, VCP/p97 associates with CRL^{CSA} and interacts with both unmodified and ubiquitinated CSB⁴³. In this way, catalytically inactive CRL^{CSA} may still contribute to the degradation of CSB.

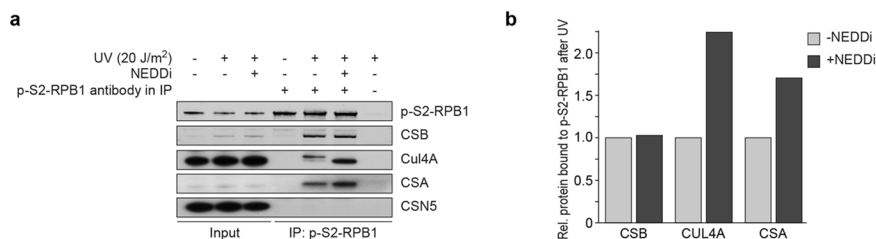
Apart from controlling the presence of (TC-NER) factors to regulate repair under normal circumstances, CRL^{CSA} may also assist in the removal of stalled RNAPII_o when the TC-NER pathway for some reason cannot be properly and timely executed. Despite this removal is considered a last resort response to transcription-stalling damage, it is crucial in the prevention of persistently stalled RNAPII_o that activates a signaling cascade eventually leading to p53-dependent cell death^{3,30,32,33,35,36}. As described previously, we observed CSA-dependent degradation of p-S5-RPB1 upon high doses of UV, although we cannot conclude whether the ligase activity of CRL^{CSA} itself contributes to this effect^{7,28,29}. Next to CRL^{CSA}, NEDD4, elongin A/B/C, Von-Hippel Lindau and BRCA1 have all been described to promote ubiquitination and subsequent degradation of stalled RNAPII_o⁴⁴⁻⁴⁸. Possibly, depending on for instance cell cycle stage, time after UV exposure and tissue type, multiple mechanisms are employed. The eventual degradation of RPB1 might result from the interplay between different ubiquitinating and deubiquitinating enzymes, ensuring that RNAPII_o is only degraded if other solutions fail. In agreement with this concept, NEDD4, its associated ubiquitin protease UBP2 and the elongin A/B/C complex have been shown to act sequentially in the step-wise poly-ubiquitination of RPB1⁴⁹. Furthermore, degradation is likely stimulated by proteins that contribute to the disassembly of RNAPII_o. Accordingly, VCP/p97 has also been shown to remove RPB1 from the elongation complex and to directly channel it into the 26S proteasome⁵⁰.

Future studies should reveal whether CSA itself, CSB and/or RPB1 are true CRL^{CSA} ubiquitination targets and potentially identify additional substrates. Ideally, experiments should be done after specific inhibition of CRL^{CSA}. That is, its ligase activity should be inactivated without compromising its incorporation into the TC-NER complex and its ability to recruit other factors. However, given the numerous compositions of cullin-RING ligases and their implications in even more cellular processes, general CUL4A/B inactivating mutations are not suitable to study CRL^{CSA}-specific responses, as is also the case for NEDDylation inhibitors^{51,52}. Alternatively, interfering with the interaction between CSA and the other CRL factors, with the aim to recruit solely CSA to the TC-NER complex, is equally complicated, as CSA stability and localization greatly depend on the establishment of the CRL^{CSA} complex⁵³. CRL^{CSA} ubiquitination targets may therefore be more straightforwardly identified by employing mass spectrometry-based approaches, uncovering differentially ubiquitinated proteins in WT and CSA-deficient cells.

Given the versatile roles of CRL^{DDB2} in the regulation of repair(-facilitating) factors during GG-NER, it is unlikely that the function of CRL^{CSA} is restricted to the ubiquitination of a single target. Almost certainly, uncovering CRL^{CSA}'s ubiquitination targets and revealing new interaction partners will expand our understanding of TC-NER regulation by CRL^{CSA} and show that CSA contributes to the UV response in a broader manner than previously anticipated.

Supplementary information

Supplementary figures



Supplementary Figure 1. NEDDylation modulates the presence of CRL^{CSA} at the TC-NER complex

Immunoprecipitation of the serine 2-phosphorylated RNAPII subunit RPB1 (p-S2-RPB1) from VH10-hTert cells 1 hour after mock treatment or UV-C irradiation (20 J/m²). Where indicated, global NEDDylation had been inhibited prior to UV-C irradiation by treatment with the NEDDylation inhibitor MLN4924. A similar experiment, in which p-S5-RPB1 was precipitated, is shown in Fig. 1. (b) Relative amounts of CSB, DDB1, CUL4A and CSA that coprecipitated with p-S2-RPB1 1 hour after UV-C irradiation (20 J/m²).

Methods

Cell culture

VH10-hTert (WT), CS1AN-hTert (CS-B), CS3BE-hTert (CS-A), KPS3-hTert (UVSS-A), XP1DU-hTert (XP-D; XP phenotype), XP8BR-hTert (XP-D; XP/CS phenotype) and XP25RO-hTert (XP-A) cells were cultured in DMEM (Invitrogen) supplemented with 10% fetal bovine serum (FBS; Bodinco BV) and penicillin/streptomycin (Sigma).

UV-C irradiation

UV damage was induced using a 254 nanometer TUV PL-S 9W lamp (Philips).

Inhibition of NEDDylation

NEDDylation was inhibited by the addition of 1 μ M MLN4924 (BostonBiochem) to the culturing medium. The inhibitor was added 3 to 4 hours before UV irradiation and kept in the medium during recovery.

Western blotting

Proteins were separated in 4-12% Bis-Tris NuPAGE® gels (Invitrogen) or hand casted 6% acrylamide gels in MOPS (Life Technologies). Separated proteins were blotted onto PVDF membranes (Millipore), which were incubated with the following primary antibodies: rabbit α -p-S2-RPB1 (CTD YSPTSPS repeat phospho S2, Abcam, ab5095); mouse α -p-S5-RPB1 (CTD YSPTSPS repeat phospho S5, Abcam, ab5408); rabbit α -CSB (Santa Cruz Biotechnology, sc-25370); goat α -DDB1 (Abcam, ab9194); rabbit α -CUL4A (Bethyl Laboratories, A300-739A); rabbit α -CSA (Abcam, ab137033); rabbit α -H2B (Millipore, 07-371), rabbit α -actin (Sigma, A2066), mouse α -tubulin (Sigma, T6199). Protein bands were visualized using the Odyssey® Imaging System (LI-COR) after incubation with CFTM dye-labelled secondary antibodies (Sigma), or detected by the ECLTM Prime Western blotting system (GE Healthcare) following incubation with horseradish peroxidase-conjugated secondary antibodies (Dako). Protein band intensities were quantified in ImageJ (<https://imagej.nih.gov/ij/>) or using the Odyssey® Imaging System software (LI-COR).

Immunoprecipitations

Cells were lysed in IP buffer (30 mM HEPES pH 7.5, 130 mM NaCl, 2 mM MgCl₂, 0.5 % Triton X-100, protease inhibitor cocktail (Roche)) during 1.5 hours at 4 °C. The pellet obtained by centrifugation was resuspended in IP buffer supplemented with 300 U/mL benzonase® nuclease (Novagen) and 1.5 µl mouse α-p-S5-RPB1 antibody (Abcam; ab5408) or rabbit α-p-S2-RPB1 antibody (Abcam, ab5095) and incubated during 3 hours at 4 °C. After another round of centrifugation, protein complexes were pulled down from the supernatant (solubilized chromatin) during 2 hours of incubation with Protein A Agarose beads (Millipore).

Determination of total p-S5-RPB1 levels

Cells were mock treated or UV irradiated at 20 J/m² and allowed to recover in medium supplemented with 25 µg/mL cycloheximide (Sigma) during 6 hours. Subsequently, cells were pelleted and lysed in 30 mM HEPES pH 7.5, 130 mM NaCl, 2 mM MgCl₂, 0.5% Triton X-100, protease inhibitor cocktail (Roche) and 125 U/mL benzonase® nuclease during 45 minutes at room temperature. Laemmli-SDS sample buffer was added 1:1 to the supernatant obtained after centrifugation (soluble fraction plus solubilized chromatin) and samples were heated at 95 °C for 10 minutes prior to Western blot analysis.

References

1. Svejstrup, J.Q. Mechanisms of transcription-coupled DNA repair. *Nat Rev Mol Cell Biol* 3, 21-9 (2002).
2. Marteijn, J.A., Lans, H., Vermeulen, W. & Hoeijmakers, J.H. Understanding nucleotide excision repair and its roles in cancer and ageing. *Nat Rev Mol Cell Biol* 15, 465-81 (2014).
3. Dijk, M., Typas, D., Mullenders, L. & Pines, A. Insight in the multilevel regulation of NER. *Exp Cell Res* 329, 116-23 (2014).
4. van Hoffen, A. et al. Deficient repair of the transcribed strand of active genes in Cockayne's syndrome cells. *Nucleic Acids Res* 21, 5890-5 (1993).
5. Venema, J., Mullenders, L.H., Natarajan, A.T., van Zeeland, A.A. & Mayne, L.V. The genetic defect in Cockayne syndrome is associated with a defect in repair of UV-induced DNA damage in transcriptionally active DNA. *Proc Natl Acad Sci U S A* 87, 4707-11 (1990).
6. Mayne, L.V. & Lehmann, A.R. Failure of RNA synthesis to recover after UV irradiation: an early defect in cells from individuals with Cockayne's syndrome and xeroderma pigmentosum. *Cancer Res* 42, 1473-8 (1982).
7. Nakazawa, Y. et al. Mutations in UVSSA cause UV-sensitive syndrome and impair RNA polymerase II processing in transcription-coupled nucleotide-excision repair. *Nat Genet* 44, 586-92 (2012).
8. Schwertman, P., Vermeulen, W. & Marteijn, J.A. UVSSA and USP7, a new couple in transcription-coupled DNA repair. *Chromosoma* 122, 275-84 (2013).
9. Scharer, O.D. Nucleotide excision repair in eukaryotes. *Cold Spring Harb Perspect Biol* 5, a012609 (2013).
10. Laugel, V. et al. Mutation update for the CSB/ERCC6 and CSA/ERCC8 genes involved in Cockayne syndrome. *Hum Mutat* 31, 113-26 (2010).
11. Zhang, X. et al. Mutations in UVSSA cause UV-sensitive syndrome and destabilize ERCC6 in transcription-coupled DNA repair. *Nat Genet* 44, 593-7 (2012).
12. Oh, K.S. et al. Phenotypic heterogeneity in the XPB DNA helicase gene (ERCC3): xeroderma pigmentosum without and with Cockayne syndrome. *Hum Mutat* 27, 1092-103 (2006).
13. Andressoo, J.O. et al. An Xpd mouse model for the combined xeroderma pigmentosum/Cockayne syndrome exhibiting both cancer predisposition and segmental progeria. *Cancer Cell* 10, 121-32 (2006).
14. Ito, S. et al. XPG stabilizes TFIIH, allowing transactivation of nuclear receptors: implications for Cockayne syndrome in XP-G/CS patients. *Mol Cell* 26, 231-43 (2007).
15. Lehmann, A.R. DNA repair-deficient diseases, xeroderma pigmentosum, Cockayne syndrome and trichothiodystrophy. *Biochimie* 85, 1101-11 (2003).

16. Kashiyama, K. et al. Malfunction of nuclease ERCC1-XPF results in diverse clinical manifestations and causes Cockayne syndrome, xeroderma pigmentosum, and Fanconi anemia. *Am J Hum Genet* 92, 807-19 (2013).
17. Giglia-Mari, G. et al. A new, tenth subunit of TFIIH is responsible for the DNA repair syndrome trichothiodystrophy group A. *Nat Genet* 36, 714-9 (2004).
18. Li, J., Bhat, A. & Xiao, W. Regulation of nucleotide excision repair through ubiquitination. *Acta Biochim Biophys Sin (Shanghai)* 43, 919-29 (2011).
19. Nospikel, T. Multiple roles of ubiquitination in the control of nucleotide excision repair. *Mech Ageing Dev* 132, 355-65 (2011).
20. van Cuijk, L., Vermeulen, W. & Marteijn, J.A. Ubiquitin at work: the ubiquitous regulation of the damage recognition step of NER. *Exp Cell Res* 329, 101-9 (2014).
21. Fischer, E.S. et al. The Molecular Basis of CRL4(DDB2/CSA) Ubiquitin Ligase Architecture, Targeting, and Activation. *Cell* 147, 1024-1039 (2011).
22. Enchev, R.I., Schulman, B.A. & Peter, M. Protein neddylation: beyond cullin-RING ligases. *Nat Rev Mol Cell Biol* 16, 30-44 (2015).
23. Groisman, R. et al. The ubiquitin ligase activity in the DDB2 and CSA complexes is differentially regulated by the COP9 signalosome in response to DNA damage. *Cell* 113, 357-67 (2003).
24. Sugawara, K. UV-induced ubiquitylation of XPC complex, the UV-DDB-ubiquitin ligase complex, and DNA repair. *J Mol Biol* 37, 189-202 (2006).
25. Guerrero-Santoro, J. et al. The cullin 4B-based UV-damaged DNA-binding protein ligase binds to UV-damaged chromatin and ubiquitinates histone H2A. *Cancer Res* 68, 5014-22 (2008).
26. Wang, H. et al. Histone H3 and H4 ubiquitylation by the CUL4-DDB-ROC1 ubiquitin ligase facilitates cellular response to DNA damage. *Mol Cell* 22, 383-94 (2006).
27. Groisman, R. et al. CSA-dependent degradation of CSB by the ubiquitin-proteasome pathway establishes a link between complementation factors of the Cockayne syndrome. *Genes Dev* 20, 1429-34 (2006).
28. Bregman, D.B. et al. UV-induced ubiquitination of RNA polymerase II: a novel modification deficient in Cockayne syndrome cells. *Proc Natl Acad Sci U S A* 93, 11586-90 (1996).
29. McKay, B.C. et al. UV light-induced degradation of RNA polymerase II is dependent on the Cockayne's syndrome A and B proteins but not p53 or MLH1. *Mutat Res* 485, 93-105 (2001).
30. Wilson, M.D., Harreman, M. & Svejstrup, J.Q. Ubiquitylation and degradation of elongating RNA polymerase II: the last resort. *Biochim Biophys Acta* 1829, 151-7 (2013).
31. Sugawara, K. et al. UV-induced ubiquitylation of XPC protein mediated by UV-DDB-ubiquitin ligase complex. *Cell* 121, 387-400 (2005).
32. Lommel, L., Bucheli, M.E. & Sweder, K.S. Transcription-coupled repair in yeast is independent from ubiquitylation of RNA pol II: implications for Cockayne's syndrome. *Proc Natl Acad Sci U S A* 97, 9088-92 (2000).
33. Woudstra, E.C. et al. A Rad26-Def1 complex coordinates repair and RNA pol II proteolysis in response to DNA damage. *Nature* 415, 929-33 (2002).
34. Saijo, M. The role of Cockayne syndrome group A (CSA) protein in transcription-coupled nucleotide excision repair. *Mech Ageing Dev* 134, 196-201 (2013).
35. Lagerwerf, S., Vrouwe, M.G., Overmeer, R.M., Fousteri, M.I. & Mullenders, L.H. DNA damage response and transcription. *DNA Repair (Amst)* 10, 743-50 (2011).
36. Ljungman, M. & Zhang, F. Blockage of RNA polymerase as a possible trigger for u.v. light-induced apoptosis. *Oncogene* 13, 823-31 (1996).
37. Aamann, M.D. et al. Cockayne syndrome group B protein promotes mitochondrial DNA stability by supporting the DNA repair association with the mitochondrial membrane. *FASEB J* 24, 2334-46 (2010).
38. Menoni, H., Hoeijmakers, J.H. & Vermeulen, W. Nucleotide excision repair-initiating proteins bind to oxidative DNA lesions in vivo. *J Cell Biol* 199, 1037-46 (2012).
39. Scheibye-Knudsen, M., Croteau, D.L. & Bohr, V.A. Mitochondrial deficiency in Cockayne syndrome. *Mech Ageing Dev* 134, 275-83 (2013).
40. Luijsterburg, M.S. et al. DDB2 promotes chromatin decondensation at UV-induced DNA damage. *J Cell Biol* 197, 267-81 (2012).

41. Pines, A. et al. PARP1 promotes nucleotide excision repair through DDB2 stabilization and recruitment of ALC1. *J Cell Biol* 199, 235-49 (2012).
42. Fei, J. & Chen, J. KIAA1530 protein is recruited by Cockayne syndrome complementation group protein A (CSA) to participate in transcription-coupled repair (TCR). *J Biol Chem* 287, 35118-26 (2012).
43. He, J., Zhu, Q., Wani, G., Sharma, N. & Wani, A.A. Valosin-containing Protein (VCP)/p97 Segregase Mediates Proteolytic Processing of Cockayne Syndrome Group B (CSB) in Damaged Chromatin. *J Biol Chem* 291, 7396-408 (2016).
44. Anindya, R., Aygun, O. & Svejstrup, J.Q. Damage-induced ubiquitylation of human RNA polymerase II by the ubiquitin ligase Nedd4, but not Cockayne syndrome proteins or BRCA1. *Mol Cell* 28, 386-97 (2007).
45. Yasukawa, T. et al. Mammalian Elongin A complex mediates DNA-damage-induced ubiquitylation and degradation of Rpb1. *EMBO J* 27, 3256-66 (2008).
46. Aune, G.J. et al. Von Hippel-Lindau-coupled and transcription-coupled nucleotide excision repair-dependent degradation of RNA polymerase II in response to trabectedin. *Clin Cancer Res* 14, 6449-55 (2008).
47. Kleiman, F.E. et al. BRCA1/BARD1 inhibition of mRNA 3' processing involves targeted degradation of RNA polymerase II. *Genes Dev* 19, 1227-37 (2005).
48. Starita, L.M. et al. BRCA1/BARD1 ubiquitinate phosphorylated RNA polymerase II. *J Biol Chem* 280, 24498-505 (2005).
49. Harreman, M. et al. Distinct ubiquitin ligases act sequentially for RNA polymerase II polyubiquitylation. *Proc Natl Acad Sci U S A* 106, 20705-10 (2009).
50. He, J., Zhu, Q., Wani, G. & Wani, A.A. UV-induced proteolysis of RNA polymerase II is mediated by VCP/p97 segregase and timely orchestration by Cockayne syndrome B protein. *Oncotarget* (2016).
51. Petroski, M.D. & Deshaies, R.J. Function and regulation of cullin-RING ubiquitin ligases. *Nat Rev Mol Cell Biol* 6, 9-20 (2005).
52. Jackson, S. & Xiong, Y. CRL4s: the CUL4-RING E3 ubiquitin ligases. *Trends Biochem Sci* 34, 562-70 (2009).
53. Pines, A. et al. TRiC controls transcription resumption after UV damage by regulating Cockayne syndrome protein A. *Nat Commun* 9, 1040 (2018).

TRiC-dependent modulation of the transcription-coupled DNA repair protein CSA

Madelon Dijk*, Alex Pines*, Matthew Makowski, Elisabeth M. Meulenbroek, Mischa G. Vrouwe, Yana van der Weegen, Marijke Baltissen, Pim J. French, Martin E. van Royen, Martijn S. Luijsterburg, Leon H. Mullenders, Michiel Vermeulen, Wim Vermeulen⁺, Navraj S. Pannu⁺ and Haico van Attikum⁺

** co-first authors, ⁺ co-corresponding authors*

Published as:

TRiC controls transcription resumption after UV damage by regulating Cockayne syndrome protein A
Nat Commun 9, 1040 (2018)

Abstract

Transcription-blocking DNA lesions are removed by transcription-coupled nucleotide excision repair (TC-NER) to preserve cell viability. TC-NER is triggered by the stalling of RNA polymerase II at DNA lesions, leading to the recruitment of TC-NER-specific factors such as the CSA-DDB1-CUL4A-RBX1 cullin-RING ubiquitin ligase complex (CRL^{CSA}). Despite its vital role in TC-NER, little is known about the regulation of the CRL^{CSA} complex during TC-NER. Using conventional and crosslinking immunoprecipitations coupled to mass spectrometry, we uncover a stable interaction between CSA and the TRiC chaperonin. TRiC's binding to CSA ensures its stability and DDB1-dependent assembly into the CRL^{CSA} complex. Consequently, loss of TRiC leads to mislocalization and depletion of CSA, as well as impaired transcription recovery following UV damage, suggesting defects in TC-NER. Furthermore, mutations in CSA that cause Cockayne syndrome (CS) lead to increased TRiC binding and a failure to compose the CRL^{CSA} complex. Thus, we uncover CSA as a TRiC substrate and reveal that TRiC regulates CSA-dependent TC-NER and the development of CS.

Introduction

Environmental pollutants, radiation and cellular metabolites have the propensity to damage DNA and promote genome instability and ageing-related diseases¹. The versatile nucleotide excision repair (NER) pathway is an important defense mechanism, which removes a remarkably wide spectrum of DNA-helix destabilizing lesions, including those induced by UV irradiation, via 2 distinct damage-recognizing subpathways: global genome NER (GG-NER) and transcription-coupled NER (TC-NER). While GG-NER removes DNA damage from the entire genome, TC-NER specifically targets transcription-blocking DNA lesions, thereby preserving transcription programs^{2,3}. TC-NER is initiated by the stalling of RNA polymerase II at DNA lesions. This triggers the recruitment of the SNF2/SWI2 ATPase CSB and the CSA protein, which promote the assembly of a large repair complex that unwinds the damaged DNA, excises a single-stranded DNA region containing the lesion, and promotes DNA synthesis and ligation to seal the gap^{4,5}.

CSA comprises a 7-bladed WD40 propeller that, through interactions with DDB1, assembles into a cullin-RING ubiquitin ligase (CRL) complex with CUL4A/B and RBX1 (CRL^{CSA})⁶. CRL^{CSA} binds the COP9 signalosome (CSN) complex, which renders CUL4A inactive through deNEDDylation⁷. Following UV damage, COP9 is likely displaced by CSB when CSA becomes incorporated into the TC-NER complex, triggering CUL4A activation by NEDDylation⁶. This process is thought to lead to poly-ubiquitination and subsequent proteasome-dependent degradation of CSB^{6,8}. UVSSA on the other hand stabilizes CSB by counteracting its CSA-dependent ubiquitination by recruiting the broad-spectrum deubiquitinating enzyme USP7⁹⁻¹¹. In this way, CRL^{CSA} and UVSSA-USP7 act antagonistically to coordinate the timely removal of CSB from transcription-blocking lesions, allowing efficient restart of transcription following TC-NER.

Genetic defects in CSA and CSB mostly give rise to Cockayne syndrome – a multisystem disorder characterized by premature aging, progressive mental and sensorial retardation, microcephaly, severe growth failure and cutaneous photosensitivity¹². Despite the important role of CSA in controlling TC-NER and preventing adverse effects on health, remarkably little is known about the regulation of CSA in the context of the CRL^{CSA} complex.

Here we used conventional and crosslinking immunoprecipitations coupled to mass spectrometry to uncover proteins that bind and regulate the function of CSA. Using this approach, we identified several new CSA-interacting proteins, including all subunits of the TRiC complex. TRiC is a eukaryotic chaperonin that has evolved to ensure proteome integrity of essential and topologically complex proteins, including cell-cycle regulators, signaling proteins, and cytoskeletal components^{13,14}. We found that TRiC's binding to CSA ensures its proper folding and DDB1-dependent assembly into the CRL^{CSA} complex. Consequently, loss of functional TRiC affects CSA's localization and stability, and impaired transcription recovery after DNA damage induction. These findings show that CSA is a TRiC substrate and reveal a role for the TRiC chaperonin in regulating CSA-dependent TC-NER.

Results

CSA interacts with chaperonin TRiC

To identify CSA-regulating proteins we stably expressed FLAG-tagged CSA in CSA-deficient patient cells (CS3BE-SV40), and performed a pulldown of CSA-FLAG followed by mass spectrometry (MS). Among the top hits were known interactors of CSA, such as the members of the COP9 signalosome (for instance COPS2 and COPS3) and the CRL^{CSA} complex (including DDB1 and CUL4A), as well as the TC-NER proteins CSB and UVSSA^{2,6,7,15} (Supplementary Data 1). Unexpectedly, our approach also identified all eight subunits of the TRiC chaperonin complex as CSA-interacting factors (Fig. 1a and Supplementary Data 1). A FLAG pulldown from cells expressing CSA-FLAG followed by Western blot analysis confirmed the interaction between CSA and the TRiC subunit TCP1 (Fig. 1b). Moreover, immunoprecipitation of CSA from human fibroblasts followed by Western blot analysis confirmed a UV-independent interaction between CSA and TCP1 at the endogenous level, as well as the known UV-dependent interaction with the elongating form of RNAPII (RNAPIIo)¹⁶ (Fig. 1c). Finally, pulldown of CSA-GFP from CSA-deficient patient cells confirmed interactions between CSA and the TRiC subunits CCT4 and CCT5 (Fig. 1d, e). These results demonstrate that CSA interacts with the TRiC complex.

We then addressed if the CSA-TRiC complex is distinct from the CRL^{CSA} complex that is important for TC-NER by performing a tandem pulldown of CSA-FLAG and DDB1-GFP from U2OS cells that co-expressed these fusion proteins. Pulldown of CSA-FLAG confirmed interactions with both GFP-DDB1 and CUL4A, as well as TRiC components CCT4 and CCT7 (Fig. 1e). Importantly, subsequent specific enrichment of CRL^{CSA} by pulldown of GFP-DDB1 revealed an interaction with CUL4, but not with CCT4 or CCT7 (Fig. 1e). We therefore conclude that TRiC preferentially interacts with CRL-free CSA.

CSA binds the inner pocket of TRiC

TRiC/CCT (TCP1 ring complex/chaperonin containing TCP1) is an ATP-dependent complex composed of two stacked octameric rings. Each ring consists of 8 different but related subunits, which are present once per ring¹⁷. Moreover, each ring creates an inner pocket where substrate proteins interact to become properly folded^{18,19}. To gain more insight into the interaction between CSA and TRiC, we stably expressed CSA-GFP in CSA-deficient patient cells, and identified CSA interacting proteins using a label free quantification (LFQ), GFP-Trap affinity purification (AP)-MS/MS approach (Fig. 2a). Even after stringent washing at 1M NaCl and 1% NP-40, the interaction between CSA and DDB1, CUL4A, RBX1, and members of the COP9 signalosome was preserved. Importantly, the LFQ analysis also detected all subunits of the TRiC complex, indicating that the CSA-TRiC interaction is highly stable. Moreover, the use of ethidium bromide excludes the possibility that these interactions are mediated by DNA, which is in agreement with our observation that most CSA-TRiC complexes are found in the soluble fraction of the cell (Fig. 1b,c). Finally, we used an iBAQ based method to estimate the relative stoichiometries of the various proteins immunoprecipitated by CSA²⁰. This revealed an interaction stoichiometry of approximately 1 TRiC subunit per 3 CSA proteins (Fig. 2b).

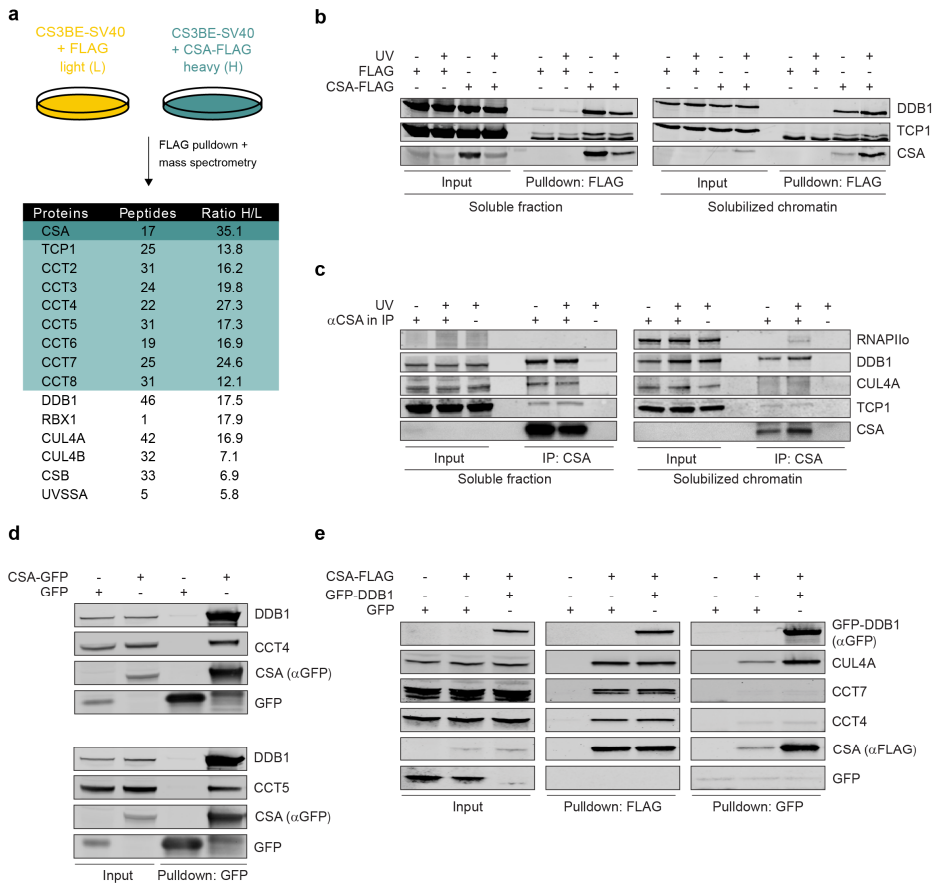


Figure 1. CSA interacts with chaperonin TRiC

(a) A SILAC-mass spectrometry approach identified all TRiC subunits as CSA-interacting proteins. CSA-deficient CS3BE-SV40 cells expressing FLAG or CSA-FLAG were cultured in medium containing light or heavy lysine and arginine isotopes, respectively. FLAG- and CSA-FLAG-interacting proteins were pulled down and samples were processed and analyzed by mass spectrometry. The table shows the number of unique peptides found for the top ranked interactors, as well as the ratio of the interactors in the CSA-FLAG pulldown to that in the control FLAG pulldown (ratio H/L). (b) FLAG pulldowns confirm the UV-independent interaction between CSA-FLAG and TCP1. CS3BE-SV40 cells expressing FLAG or CSA-FLAG were mock treated or UV-C-irradiated (20 J/m²). After 1 hour of recovery cells were lysed and chromatin was fractionated into soluble or solubilized chromatin. FLAG pulldowns using both fractions were followed by Western blot analysis. (c) CSA co-immunoprecipitation confirms the interaction between endogenous CSA and TCP1. As in b, except that V10-hTert cells were used and that endogenous CSA was immunoprecipitated. (d) GFP pulldowns confirm the interaction between CSA and TRiC subunits CCT4 and CCT5. GFP or CSA-GFP was pulled down from CS3BE-SV40 cells. (e) Tandem FLAG and GFP pulldowns show preferential binding of TRiC to DDB1-CUL4A-RBX1-free CSA. CSA-FLAG, GFP and GFP-DDB1 were expressed in U2OS cells as indicated. Enrichment of CSA-interacting proteins by means of FLAG pulldowns confirmed interactions between CSA and DDB1 and CUL4A, as well as the TRiC subunits CCT4 and CCT7. Subsequently, eluted protein complexes were subjected to pulldown of GFP-DDB1, revealing an interaction with CUL4A, but not CCT4 and CCT7.

To examine whether the strong nature of the CSA-TRiC interaction is mediated by other proteins or can be ascribed to direct binding of CSA to TRiC, we applied xIP-MS²¹. Immunoprecipitation of CSA-GFP by GFP-TRAP was followed by on-bead crosslinking and tryptic digestion of the bound proteins into covalently crosslinked peptides. Identification of crosslinked peptides was performed using pLink after analysis by mass spectrometry, which revealed residues in close spatial proximity²². We identified 149 unique, high confidence residue crosslinks in total (Fig. 2c and Supplementary Data 2). Of these, 62 linkages were intra- or inter-linkages mapping to subunits of the TRiC complex (Supplementary Fig. 1a). All of these TRiC crosslinks were consistent with a crosslinker spacer length of 34 Å, confirming the structural validity of our data (Supplementary Fig. 1b). Importantly, we observed 11 crosslinks between CSA and TRiC subunits CCT3, CCT4, and CCT6 involving CSA residues Lys34, Lys85, Lys167, and Lys212 (Fig. 2c). Although this does not provide any information about specific residues that mediate the interaction, the location of these lysine residues in the outer regions of the β -propeller blades made up by the WD40 domain of CSA suggests that these regions are important for the interaction with TRiC (Supplementary Fig. 4a). Given these inter-protein linkages as distance restraints, we used DisVis to identify the accessible interaction space for CSA on the TRiC surface²³ (Fig. 2d). Our data indicate that the only available interaction space for CSA that is consistent with our crosslinking data is within TRiC's inner pocket.

Loss of TRiC components reduces CSA stability

TRiC has been described to be involved in the folding or stabilization of approximately 10% of all newly synthesized proteins²⁴. Among the known TRiC substrates are many WD40 repeat-containing proteins. Given that CSA contains 7 of such repeats and considering our observation that TRiC directly interacts with CSA, we hypothesized that TRiC could be important for proper folding of CSA and consequently for its stability. To assess this, we depleted TCP1 using siRNAs and examined CSA levels in whole cell extracts by Western blot analysis at different times after siRNA transfection (Fig. 3a,b and Supplementary Fig. 3a,b). TCP1 knockdown resulted in a marked decrease in the overall amount of CSA when compared to control cells treated with siRNAs against luciferase, whereas the levels of DDB1 remained unaffected. The reduction in CSA levels correlated with the knockdown efficiency of TCP1.

Knockdown of a single TRiC component has been shown to negatively impact the stability of other subunits in the complex, thereby lowering the availability of functional TRiC complexes in the cell²⁵. To confirm that our observations are not specific for TCP1 knockdown, but are the consequence of the loss of TRiC complexes, we also examined the effect of CCT4, CCT5 and CCT7 depletion on CSA protein abundance. Knockdown of these TRiC subunits using different siRNAs also caused a reduction in the CSA levels (Fig. 3c and Supplementary Fig. 3c). Similarly, treatment with a TRiC inhibitor (TRiCi), which has been shown to inhibit archaeal TCP1 activity *in vitro*, led to a substantial decrease in CSA levels while not affecting TCP1 levels itself²⁶ (Fig. 3d).

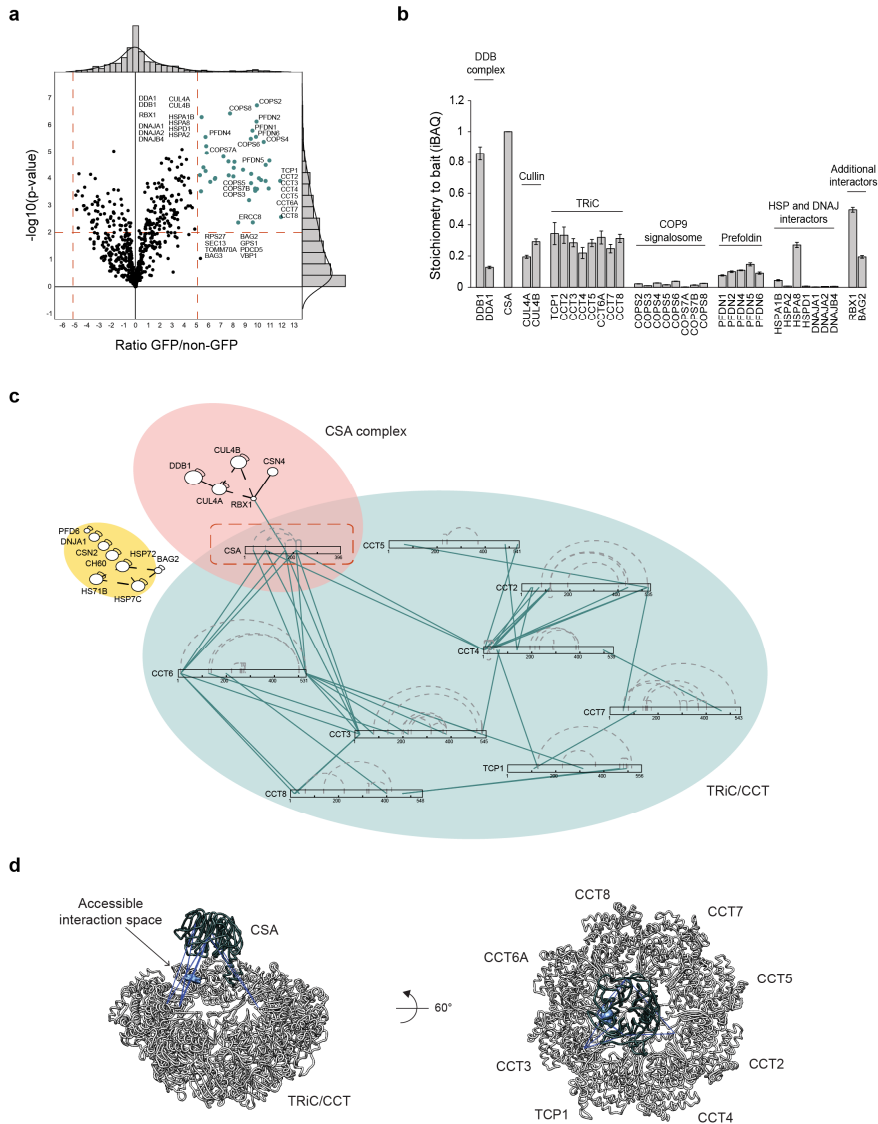
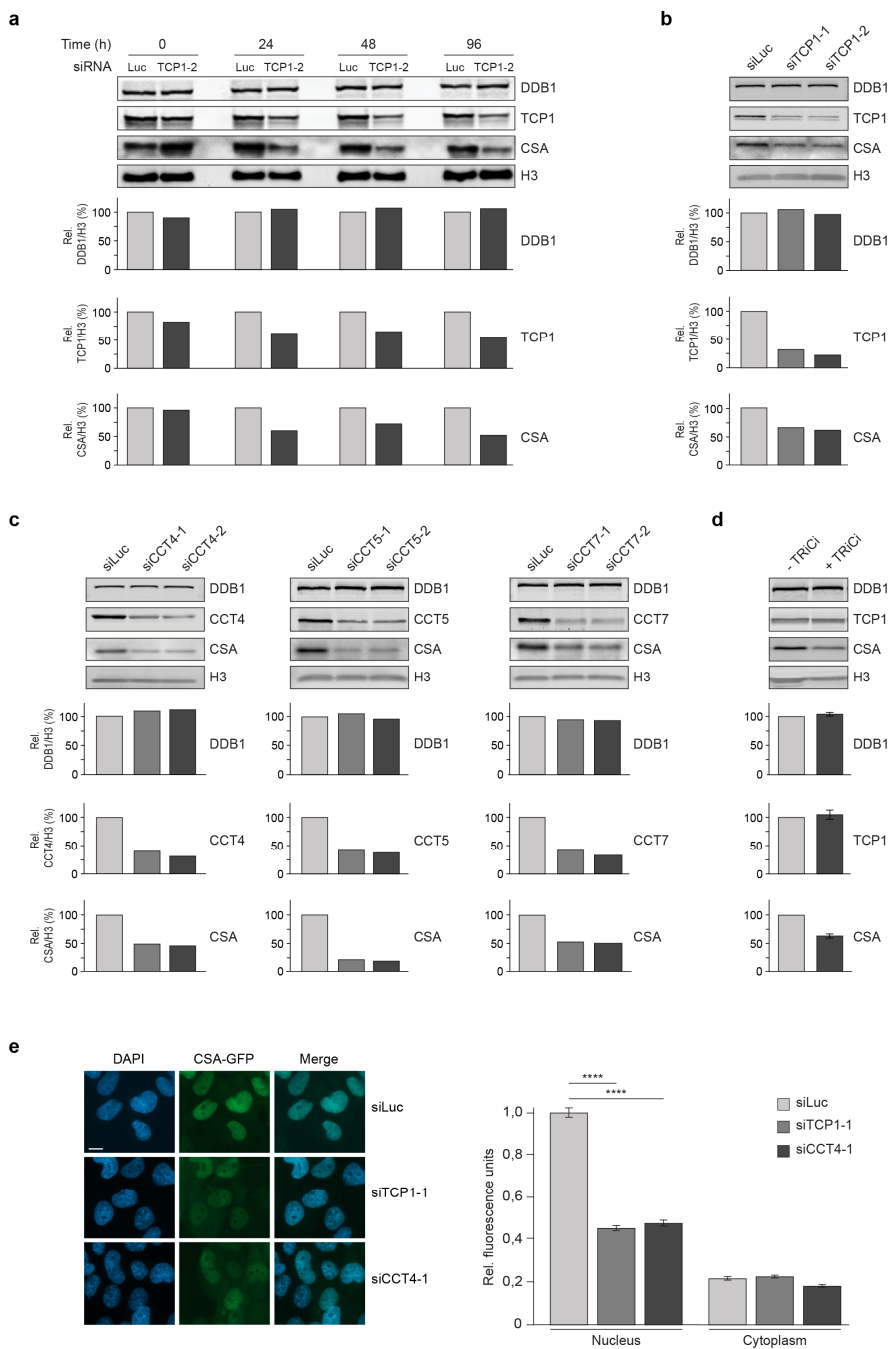


Figure 2. xIP-MS reveals that CSA interacts with TRiC's inner pocket

(a) LFQ analysis after CSA-GFP pulldown indicates that all TrIC subunits interact with CSA even after stringent washing. Ratio of protein signal in GFP versus non-GFP pulldowns is plotted on the x-axis, and the significance of the difference, $-\log_{10}(\text{p-value})$, is plotted on the y-axis. Cutoffs are selected such that no protein significantly interacted with the non-GFP control beads. (b) iBAQ-based stoichiometry of selected interactors relative to the bait protein (CSA), which was set to 1. (c) Crosslinking map of all identified residue linkages: TrIC subunits in linear form, inter- and intra-links in dark green and dashed grey, resp. (d) CSA inter-protein linkages with the TrIC octamer indicate that CSA binds TrIC's inner pocket. Inter-protein crosslinks in blue. CSA was positioned manually to give a visual interpretation to possible CSA-TrIC interactions. The accessible CSA interaction space satisfying 10/11 inter-protein crosslinks is shown as a blue cloud.



legend on next page

Figure 3. Loss of TRiC components reduces CSA stability

(a) Depletion of TCP1 decreases CSA protein abundance. VH10-hTert cells were transfected with the indicated siRNAs and total cell extracts were prepared at the indicated time points after siRNA transfection. Protein levels were determined by Western blot analysis of the indicated proteins. H3 is a loading control. Graphs represent the ratio of protein signal intensities over H3 control signal intensities for siTCP1-treated cells relative to that for siLuc-treated control cells, which was set to 100%, at each time point. A repeat of the experiment is shown in Supplementary Fig. 3a. (b) Depletion of TCP1 decreases CSA protein abundance. As in a, except that two different siRNAs against TCP1 were used and that protein levels were determined 72 hours after siRNA transfection. A repeat of the experiment is shown in Supplementary Fig. 3b. (c) Depletion of CCT4, CCT5 or CCT7 decreases CSA protein abundance. As in a, except that CCT4, CCT5 or CCT7 siRNAs were used and that protein levels were determined 72 hours after siRNA transfection. A repeat of the experiment is shown in Supplementary Fig. 3c. (d) TRiC inhibition decreases CSA protein abundance. VH10-hTert cells were treated with DMSO or an inhibitor against the TRiC subunit TCP1 (TRiCi). Protein levels were determined after 72 hours of treatment. (e) TCP1 or CCT4 loss decreases CSA-GFP protein abundance in the nucleus. TCP1 or CCT4 was depleted from CSA-GFP expressing CS3BE-SV40 cells using the indicated siRNAs. Nuclear and cytoplasmic CSA-GFP levels were analyzed and quantified by fluorescence microscopy and ImageJ. GFP signal intensities were normalized to the average nuclear signal in siLuc-treated cells. Data represent mean \pm SEM of 190 cells quantified in 2 independent experiments. p-Values were derived from an unpaired t-test.

This shows that CSA stability is not only negatively affected by the loss of TRiC protein, but also by inhibition of its chaperonin activity. To validate these findings, we expressed CSA-GFP in CSA-deficient patient cells and examined the effect of TCP1 and CCT4 knockdown on CSA-GFP expression by fluorescence microscopy analysis. Similar to endogenous CSA, we found that CSA-GFP is primarily expressed in the nucleus. Depletion of either TCP1 or CCT4 significantly reduced the levels of CSA-GFP in the nucleus (Fig. 3e). This reduction in CSA-GFP protein levels is consistent with the effect on endogenous CSA as observed by Western blot analysis (Fig. 3a-c and Supplementary Fig. 3). Taken together, these findings indicate that the TRiC complex is involved in regulating CSA stability, likely by affecting proper folding of CSA.

TRiC is involved in the formation of the CSA-DDB1-CUL4A-RBX1 complex

CSA is a stable component of the DDB1- and RBX1-containing CRL^{CSA} complex. In this complex, it directly associates with DDB1 and likely functions as the substrate receptor⁶. Considering that TRiC is required for CSA stability, we wondered whether DDB1 acts as an acceptor of TRiC-bound CSA in the CRL^{CSA} complex. To test this, we first pulled down CSA-GFP from CSA-deficient patient cells that were treated with siRNAs against DDB1. Knockdown of DDB1 not only led to a decrease in the association of CSA with DDB1 and CUL4A, but also negatively affected the binding to CSB (Fig. 4a). Strikingly, however, the efficiency by which CSA binds to the TRiC subunit TCP1 appeared to be substantially increased, suggesting that DDB1 may serve as an acceptor of CSA. Secondly, we created a mutant, CSA Δ N, that lacks the first 21 amino acids required for DDB1 binding (Fig. 4b), which was stably expressed in CRISPR/Cas9-mediated CSA knockout U2OS cells⁶ (Fig. 4c).

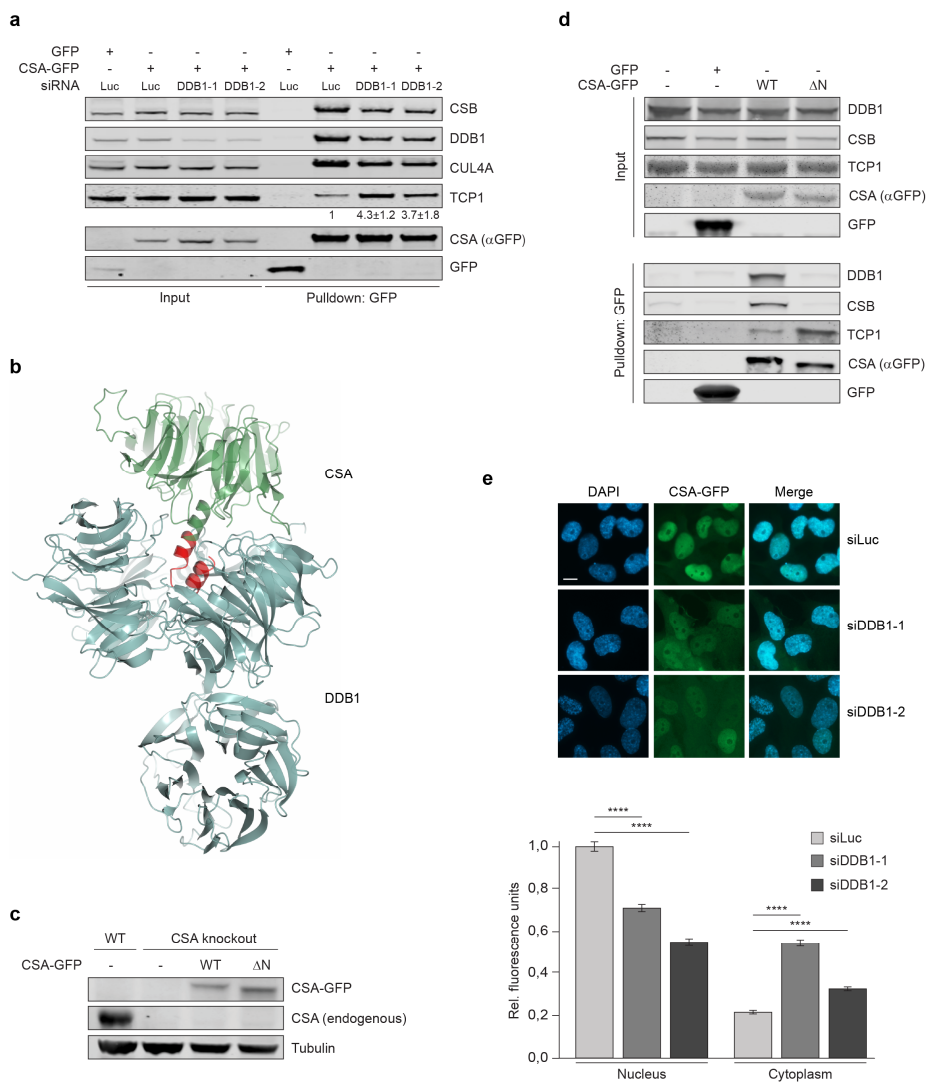


Figure 4. TriC is involved in the formation of the CSA-DDB1-CUL4A-RBX1 complex

(a) DDB1 loss enhances the interaction between TCP1 and CSA. CSA-GFP was pulled down from CS3BE-SV40 cells treated with the indicated siRNAs. Protein levels were determined by Western blot analysis. The ratio of TCP1 signal intensities over CSA for siDDB1-treated cells relative to that for siLuc-treated control cells (set to 1) is shown as the mean \pm SEM of 3 independent experiments. (b) Overall structure of CSA (green) bound to DDB1 (blue), showing that CSA's N-terminus is directly involved in DDB1 binding. CSA Δ N lacks amino acids 1-21 (red). Visualization was done in ccp4mg using structure 4a11 from the PDB. (c) Stable expression of CSA-GFP WT or CSA-GFP Δ N in CSA knockout U2OS. Protein levels were determined by Western blot analysis. Tubulin is a loading control. (d) Deletion of CSA's DDB1-interacting domain leads to increased TriC binding. Stably expressed GFP-NLS, CSA-GFP WT and CSA-GFP Δ N were pulled down from CSA knockout U2OS cells as indicated.

legend continues on next page

(e) DDB1 decreases CSA-GFP protein abundance in the nucleus concomitantly with an increase in cytoplasmic localization. DDB1 was depleted from CSA-GFP expressing CS3BE-SV40 cells using the indicated siRNAs. Nuclear and cytoplasmic CSA-GFP levels were analyzed and quantified by fluorescence microscopy and ImageJ. GFP signal intensities were normalized to the average nuclear signal in siLuc-treated cells. Data represent mean \pm SEM of 190 cells quantified in 2 independent experiments. p-Values were derived from an unpaired t-test.

Pulldown of GFP-tagged CSA Δ N from these cells not only showed the expected decrease in DDB1 binding as compared to CSA WT, but also abolished the interaction with CSB (Fig. 4d). Importantly, the interaction between CSA Δ N and TCP1 was substantially increased as compared to full length CSA (Fig. 4d). These results show that interfering with the CSA-DDB1 interaction, either by depletion of DDB1 or deletion of the DDB1-interacting domain in CSA, strongly enhances the interaction between CSA and TRiC. This suggests that in the absence of DDB1, CSA remains tightly bound to the TRiC complex and that DDB1 serves as an acceptor of TRiC-bound CSA in the CRL^{CSA} complex. Next, we studied the effect of DDB1 loss on the expression and localization of CSA-GFP following its expression in CSA-deficient patient cells by fluorescence microscopy analysis. DDB1 knockdown led to a significant decrease in nuclear CSA-GFP levels, while CSA-GFP levels in the cytoplasm increased (Fig. 4e), likely due to persistent binding of CSA-GFP to TRiC (Fig. 4a). The latter is consistent with the fact that TRiC is a chaperonin that primarily localizes to and functions in the cytoplasm. Together our findings suggest a hand-over mechanism in which cytoplasmic TRiC provides properly folded CSA to DDB1, thereby facilitating its assembly into CRL^{CSA} complexes that translocate into the nucleus. Hand-over of CSA might occur directly after its release by TRiC in the cytoplasm, as we detected TRiC-bound as well as DDB1-bound cytoplasmic CSA (Supplementary Fig. 2).

A CSA mutant of the top platform shows increased TRiC interaction

The 4 residues in CSA that were revealed by xIP-MS to be in proximity of the CSA-TRiC binding interface surround a platform at the top of CSA that is formed by the β -propeller blades⁶ (Supplementary Fig. 4a and Supplementary Data 2). In order to further assess the functional relevance of the CSA-TRiC interaction, we created 8 different CSA mutants in which one of the residues Glu103, Phe120, Lys122, Arg164, Lys247, Lys292, Lys293 or Arg354 in this platform was substituted by alanine (Supplementary Fig. 4a). Immunoprecipitation of these mutants from CSA-deficient patient cells did not reveal any major difference in their interaction with TCP1, or the CRL^{CSA} complex members DDB1 and CUL4A, as compared to wildtype CSA (Supplementary Fig. 4b). Accordingly, expression of each mutant could also rescue the UV sensitivity of the CSA-deficient patient cells (Supplementary Fig. 4c). Aiming to induce a greater effect on CSA, we next generated a CSA mutant (CSA 8M) that contains all the 8 afore-studied mutations in the top platform. Since according to the 3D structure of CSA-DDB1 this platform of CSA is not directly involved in DDB1 binding (Fig. 4b and 5a), we expected that the combined 8 mutations would leave the CRL^{CSA} complex intact⁶ (Fig. 5a,b). Surprisingly, however, pulldown of GFP-tagged CSA WT and CSA 8M from CSA-deficient patient cells showed decreased binding of CSA 8M to CSB, DDB1 and CUL4A when compared to CSA WT (Fig. 5c). This indicated that the mutations impacted CSA's interactions in a manner similarly to DDB1 depletion or deletion of the DDB1-interacting domain in CSA (Fig. 4a,d).

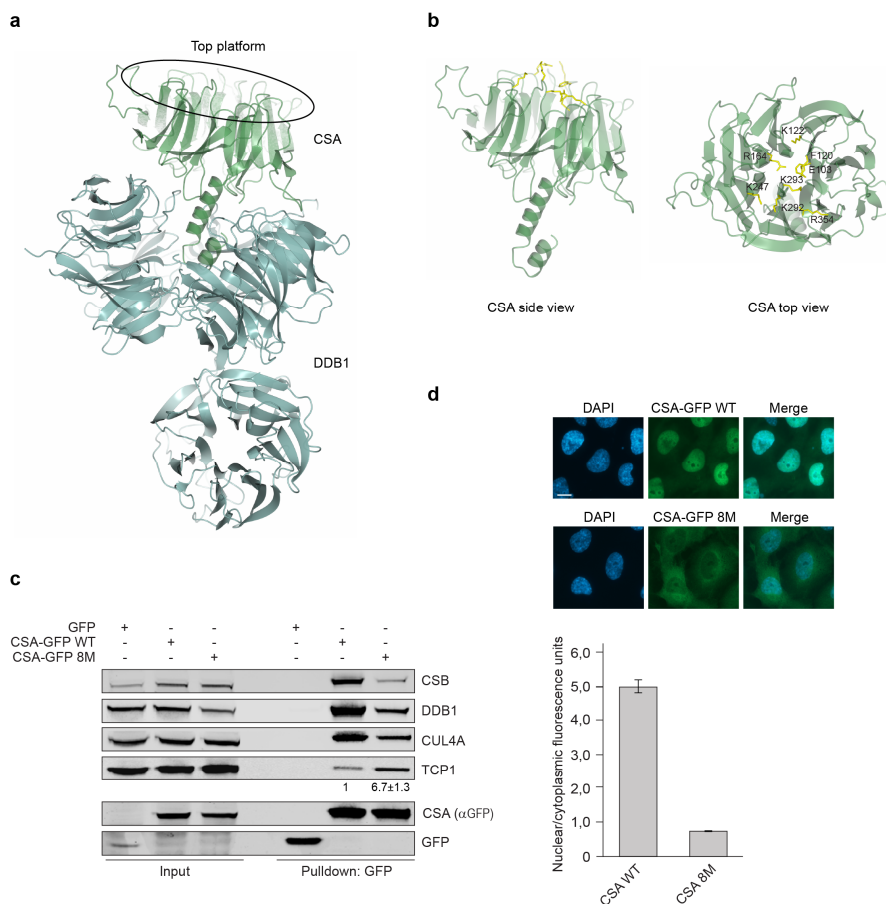


Figure 5. A CSA mutant of the top platform shows increased TRiC interaction

(a) Overall structure of CSA (green) bound to DDB1 (blue), showing that not CSA's top platform, but its N-terminus is directly involved in DDB1 binding. Visualization was done in ccp4mg using structure 4a11 from the PDB. (b) Side and top view of CSA. The amino acids Glu103, Phe120, Lys122, Arg164, Lys247, Lys292, Lys293 and Arg354 in CSA's top platform that were mutated to alanines in the CSA 8M mutant are shown in yellow. (c) The CSA 8M mutant shows decreased incorporation into the CRLCSA complex, but increased TCP1 binding. CSA-GFP WT and CSA-GFP 8M were pulled down from CS3BE-SV40 cells. Protein levels were determined by Western blot analysis of the indicated proteins. The ratio of TCP1 signal intensity over CSA-GFP 8M relative to that of TCP1 over CSA-GFP WT, which was set to 1, is shown as the mean \pm SEM of 2 independent experiments. (d) CSA-GFP 8M shows reduced protein abundance in the nucleus concomitantly with an increase in cytoplasmic localization. Mean nuclear and cytoplasmic GFP levels were analyzed and quantified by fluorescence microscopy and ImageJ. For each cell the nuclear/cytoplasmic ratio was calculated. Data represent mean \pm SEM of 160 cells quantified in 2 independent experiments.

We therefore wondered whether the altered interactions observed for CSA 8M could be explained by, or lead to a change in TRiC binding. Indeed, CSA 8M showed greatly increased binding to TCP1 when compared to CSA WT (Fig. 5c). Given that the mutated residues do not directly bind to DDB1, we consider it most plausible that the mutations negatively affect the release of CSA by TRiC. This is strengthened by fluorescence microscopy-based analysis of CSA 8M expression, which revealed that this mutant largely fails to localize to the nucleus and remains mainly cytoplasmic (Fig. 5d) – a phenotype reminiscent of that observed after DDB1 knockdown (Fig. 4e). This corroborates our conclusion that cytoplasmic TRiC provides properly folded CSA to DDB1 for incorporation into CRL^{CSA} complexes and subsequent translocation into the nucleus.

Loss of TRiC components reduces RNA synthesis recovery and protection against UV damage

The CRL^{CSA} complex is a nuclear core component of the TC-NER machinery. Since TRiC is critical for regulating CSA stability and formation of the CRL^{CSA} complex, we asked whether the TRiC-dependent regulation of CSA is a prerequisite for functional TC-NER. Indeed, we found that the recovery of RNA synthesis (RRS) after global UV irradiation, which is an established measure for TC-NER, was impaired in TCP1-depleted cells when compared to control cells (Fig. 6a), while basal transcription levels remained unaffected by TCP1 knockdown (Supplementary Fig. 5a). A similar effect on RRS could be observed after knockdown of CCT4, CCT5 or CCT7 (Supplementary Fig. 5b). In contrast, depletion of several individual TRiC subunits did not affect GG-NER, as determined by measuring DNA repair synthesis (Supplementary Fig. 5c,d). Furthermore, we found that in CSA-deficient patient cells expressing CSA 8M RRS was reduced when compared to that in cells expressing CSA WT (Fig. 6b), showing that not only CSA instability, but also persistent binding of CSA to TRiC negatively impacts TC-NER. In agreement with a defect in TC-NER, we also observed that TCP1-depleted cells, as well as cells depleted of several other individual TRiC subunits, were markedly more sensitive to UV when compared to control cells as measured in alamarBlue-based viability assays (Fig. 6c and Supplementary Fig. 6a). Notably, overexpression of CSA partially alleviated the UV sensitivity of TCP1-depleted cells, suggesting that this phenotype is largely due to loss of CSA stability and not that of another TRiC substrate (Supplementary Fig. 6b). Moreover, expression of mutant CSA 8M in patient cells failed to complement the relatively high UV sensitivity caused by CSA deficiency, whereas expression of CSA WT could do so, as determined in clonogenic survival assays (Fig. 6d, Supplementary Fig. 6c). Finally, expression of CSA Δ N in CSA knockout U2OS cells could not rescue the extreme sensitivity of these cells to illudin S, which is an agent that induces transcription-blocking DNA lesions that are repaired by TC-NER, whereas expression of CSA WT fully rescued this phenotype²⁷ (figure 6e). Together these data show that TRiC, by regulating CSA stability and incorporation into the CRL^{CSA} complex, promotes TC-NER and protects cells against UV-induced damage.

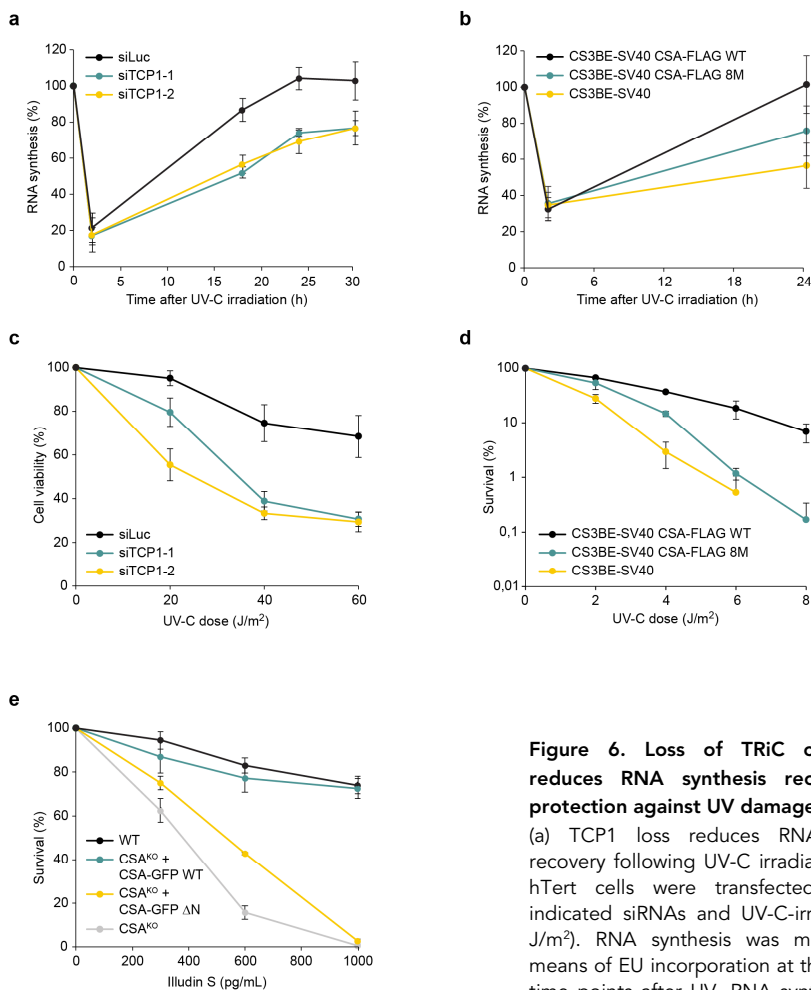


Figure 6. Loss of TRiC components reduces RNA synthesis recovery and protection against UV damage

(a) TCP1 loss reduces RNA synthesis recovery following UV-C irradiation. VH10-hTert cells were transfected with the indicated siRNAs and UV-C-irradiated (10 J/m²). RNA synthesis was measured by means of EU incorporation at the indicated time points after UV. RNA synthesis levels were normalized to those in non-irradiated cells, which were set to 100%. Data

represent the mean \pm SEM of 4 independent experiments. (b) Expression of CSA-FLAG 8M shows reduced RNA synthesis recovery as compared to expression of CSA-FLAG WT. As in a, except that CS3BE-SV40 cells expressing CSA-FLAG WT or CSA-FLAG 8M were used. Data represent the mean \pm SEM of 4 independent experiments. (c) TCP1 loss renders cells hypersensitive to UV damage. VH10-hTert cells were transfected with the indicated siRNAs, UV-C-irradiated at the indicated doses and 72 hours later assayed for viability using alamarBlue®. Data represent mean \pm SEM of 4 independent experiments. (d) Expression of CSA-FLAG 8M in CS3BE-SV40 cells fails to rescue UV-sensitivity. CS3BE-SV40 cells stably expressing CSA-FLAG WT or CSA-FLAG 8M were UV-C-irradiated and clonogenic survival was measured. Data represent mean \pm SEM of 3 independent experiments. (e) CSA WT, but not CSA Δ N, complements the illudin S sensitivity of CSA knockout (KO) U2OS cells. The indicated cells were treated with different concentrations of illudin S and clonogenic survival was determined. Data represent mean \pm SEM of 3 independent experiments.

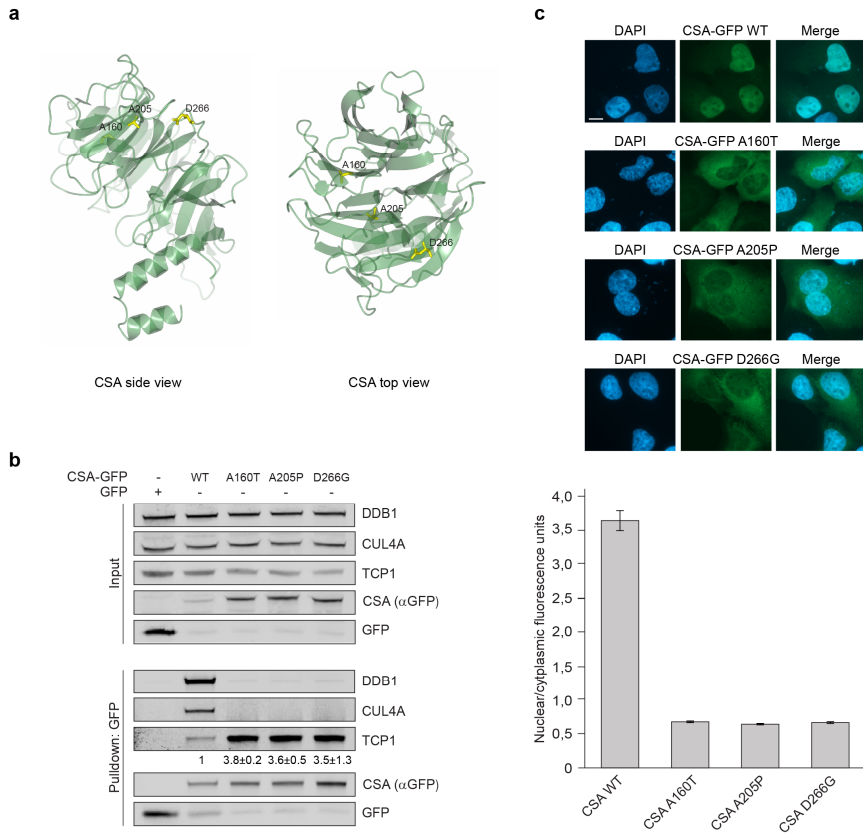


Figure 7. Patient mutations in CSA cause increased TrIC binding and cellular mislocalization

(a) Side and top view of CSA. Residues Ala160, Ala205 and Asp266 that have been found mutated in Cockayne syndrome patients are shown in yellow. Visualization was done in ccp4mg using structure 4a11 from the PDB. (b) CSA harboring patient mutation A160T, A205P or D266G shows increased binding to TrIC and failure to be incorporated into the CRLCSA complex. CSA-GFP WT and CSA-GFP containing the indicated mutations were pulled down from U2OS cells. Protein levels were determined by Western blot analysis. The signal intensity ratio of TCP1 over the CSA-GFP mutant relative to that of TCP1 over CSA-GFP WT, which was set to 1, is shown as the mean \pm SEM of 2 independent experiments. (c) CSA harboring mutation A160T, A205P or D266G shows predominant cytoplasmic localization. CSA-GFP WT and CSA-GFP containing the indicated mutations were expressed in U2OS. Mean nuclear and cytoplasmic GFP intensities were analyzed and quantified by fluorescence microscopy and ImageJ. For each cell the nuclear/cytoplasmic ratio was calculated. Data represent mean \pm SEM of 100 cells quantified in 2 independent experiments.

Patient mutations in CSA cause increased TRiC binding and cellular mislocalization

Mutations in the *CSA* gene have been found to underlie the multisystem disorder Cockayne syndrome (CS). CS patients suffer from cutaneous photosensitivity and severe neurological and developmental defects¹². Although part of the cases can be explained by mutations that lead to a non-functional and/or truncated CSA protein, it remains to be established how a group of single missense mutations can give rise to CS. Importantly, the majority of these mutations are present in the WD40 repeats of CSA that we discovered to be important for the interaction with TRiC (and Supplementary Fig. 4a). To unravel the effect of such disease-causing point mutations on the CSA protein, we created GFP-tagged CSA constructs harboring patient mutations A160T, A205P or D266G, which are found in WD40 repeats 3, 4 and 5, respectively²⁸ (Fig. 7a). A160T and A205 have been predicted to interfere with the integrity of the overall fold, whereas D266G is expected to have mostly local effects⁶. Interestingly, pulldown of these mutants from U2OS cells revealed substantially increased TRiC binding as compared to wildtype CSA, suggesting misfolding of the mutated CSA proteins (Fig. 7b). Moreover, none of the 3 mutants appeared to adopt a conformation suitable for incorporation into the CRL^{CSA} complex, as reflected by the lack of DDB1 and CUL4A binding. Fluorescence microscopy further illustrated that whereas wildtype CSA was translocated into the nucleus, all 3 mutants were predominantly present in the cytoplasm (Fig. 7c), indicating that these patient mutations lead to a CSA protein that fails to localize to the nucleus. Thus, we provide evidence that disease-associated missense mutations in CSA can lead to enhanced interaction with TRiC and cause cellular mislocalization. This underscores the importance of the TRiC chaperonin in CSA folding/stabilization and assembly of the CRL^{CSA} complex, as well as in the development of CS.

Discussion

A network of chaperones and protein degradation machineries, called the proteostasis network (PN), is required to maintain protein homeostasis²⁹. By regulating protein stability and degradation in cells, the PN drives vital processes³⁰. Although several components of the PN have been found implicated in the DNA damage response, mechanistic insight into how this network affects these processes has remained largely elusive³¹⁻³⁴. Here we demonstrate that one of the components of the PN, the chaperonin TRiC, stably interacts with the core TC-NER protein CSA. By encapsulating CSA in its inner pocket, TRiC ensures its stability and mediates the incorporation of CSA into the CRL^{CSA} complex. Our findings suggest a hand-over mechanism in which TRiC provides properly folded CSA to DDB1, which is crucial to enable the formation of the CRL^{CSA} complex and its nuclear localization. Interfering with the TRiC/CSA interaction, either by disturbing or strengthening it, lowers the levels of functional CSA in the nuclear CRL^{CSA} complex and results in impaired recovery of RNA synthesis and decreased cell viability upon UV-C-induced DNA damage. Thus, we uncover CSA as a TRiC substrate and reveal a role for the TRiC chaperonin in regulating CSA-dependent TC-NER. CSA has been shown to stably interact with DDB1⁶. However, our iBAQ analysis suggests that approximately 15% of the CSA protein pool is not bound by DDB1 (Fig. 2b). This fraction

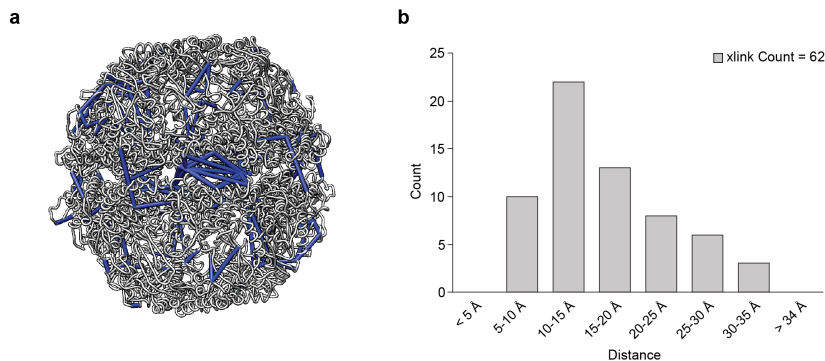
of CSA is likely unstable and/or improperly folded and therefore bound by TRiC. Consistently, pulldowns of CRL^{CSA} revealed that TRiC preferentially binds CSA that is not associated with the CRL complex (Fig. 1e). From our iBAQ analysis, a (DDB1-free) CSA to TRiC subunit ratio of approximately 1:2 can be inferred. As every TRiC complex contains two copies of each of the 8 subunits, this stoichiometry may suggest a model in which 1 CSA protein is encapsulated per TRiC complex. Interestingly, this model differs from the proposed encapsulation mode for the TRiC substrate tubulin, for which 2 molecules were shown to bind the complex simultaneously³⁵. This suggests that TRiC employs different methods of substrate binding and folding. To fully understand the constitution and conformation of TRiC in complex with CSA, a more detailed structural analysis would be required.

Our results suggest that TRiC interacts with CSA through its WD40 domain, thereby regulating CSA stability. Interestingly, TRiC has been described to regulate the folding and stability of several other WD40 domain-containing proteins^{25,36-42}. For instance, TRiC is required to maintain functional TCAB1, a cofactor of telomerase. Loss of TRiC leads to mislocalization of telomerase and a failure to elongate telomeres²⁵. Importantly, TCAB1 mutations found in patients with dyskeratosis congenita (DC) – a stem cell disease caused by defects in telomere maintenance – were shown to disrupt TRiC-mediated TCAB1 folding, providing clinical relevance to TRiC's role in stabilizing this protein⁴³. Mutations in CSA have been mostly linked to CS¹². All types of mutations (missense, nonsense, frameshift, splicing mutations, as well as large deletions) have been detected in CS patients⁴⁴. With the exception of the missense mutations, most mutations likely lead to the production of a truncated and/or non-functional CSA protein, providing a plausible explanation for the cause of CS. Interestingly, the majority of the missense mutations were found in the 7 WD motifs that form the WD40 domain^{16,44}. Here we show that 3 of these patient mutations lead to protein instability, resulting in increased TRiC binding and consequently a loss of functional CRL^{CSA}-bound CSA in the nucleus. Whether the other reported disease-causing missense mutations similarly impact TRiC-mediated folding and stabilization of CSA remains to be established.

DNA repair defects are a major source of genomic instability. Given that TRiC by affecting CSA stability contributes to TC-NER, it may play an important role in preserving genome stability following UV damage. Whether TRiC generally preserves genome stability by affecting DNA damage repair pathways other than TC-NER is not clear and may require the identification of additional, yet to be identified substrates. However, in support of such a scenario, it was shown that TRiC regulates the stability of the p53 tumor suppressor protein that is involved in genome stability maintenance⁴⁵. In addition, TRiC was found to regulate the folding and stability of the WD40 domain-containing CDC20 protein, which is a member of the anaphase promoting complex^{36,46} (APC). CDC20 controls cell division and genome integrity and has been implicated in cancer⁴⁷. Thus, TRiC likely affects genome stability maintenance by facilitating the folding of proteins other than CSA. Future endeavors may shed light on how misregulation of TRiC generally affects genome instability and contributes to diseases such as cancer⁴⁸. Such work may also provide potential targets for diagnostics and therapeutics for pathological conditions associated with genome instability, such as cancer and ageing-related diseases.

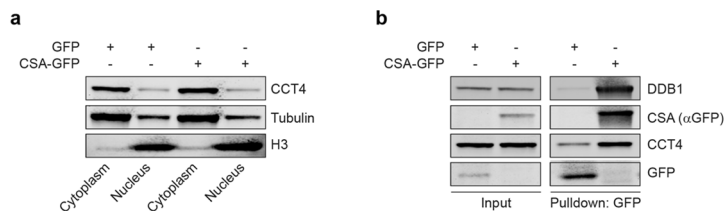
Supplementary information

Supplementary Figures



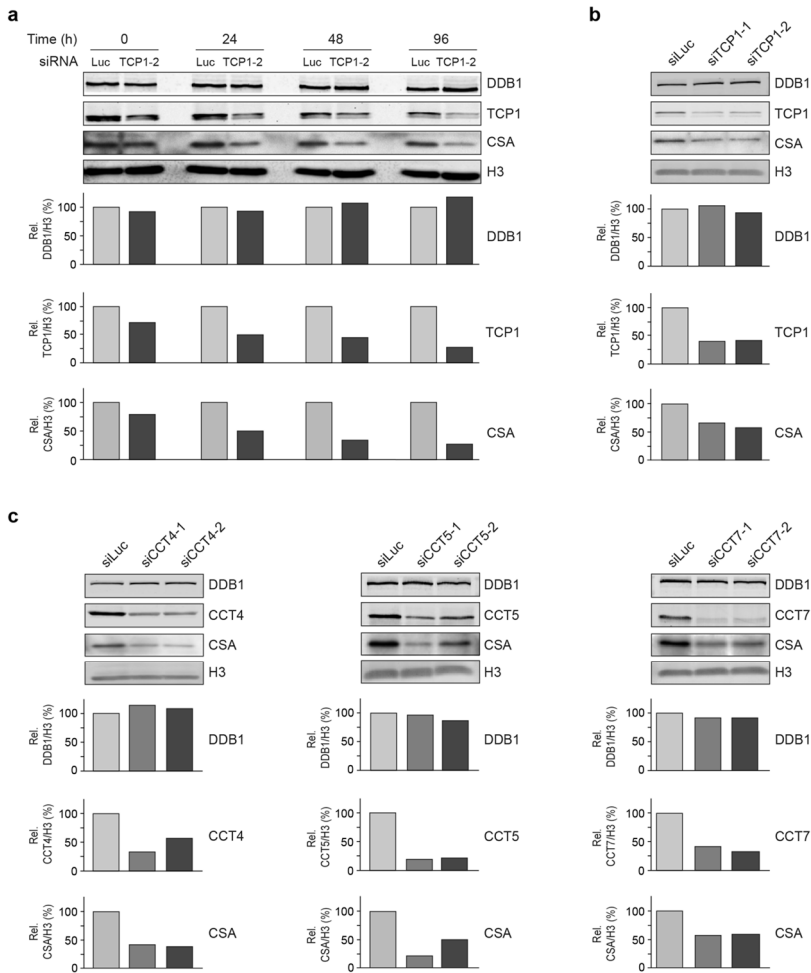
Supplementary Figure 1. Structural validation of xIP-MS data using a TRiC homology model

(a) A human TRiC homology model was produced using Phyre2 and pdb model 4V94 as a reference for subunit alignment. Mapped crosslinks are indicated as dark blue lines. (b) Distance analysis of mapped crosslinks indicates that all crosslinks are consistent with a maximal length constraint of 34 Å. We observe a typical log-normal distribution of crosslink lengths.



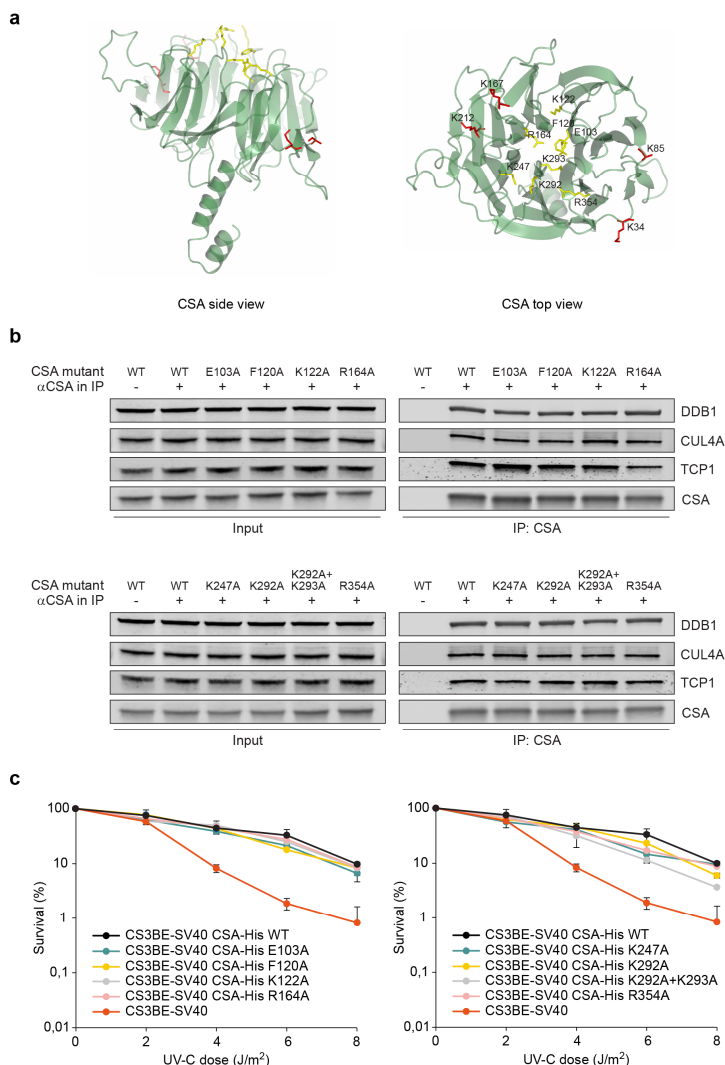
Supplementary Figure 2. Hand-over of CSA from TRiC to DDB1 occurs in the cytoplasm

(a) Cellular fractionation of U2OS cells expressing GFP or CSA-GFP. Cells were fractionated into cytoplasmic and nuclear fractions. (b) Cytoplasmic CSA interacts with both TRiC and DDB1 in GFP pulldowns using cytoplasmic cell extracts from a.



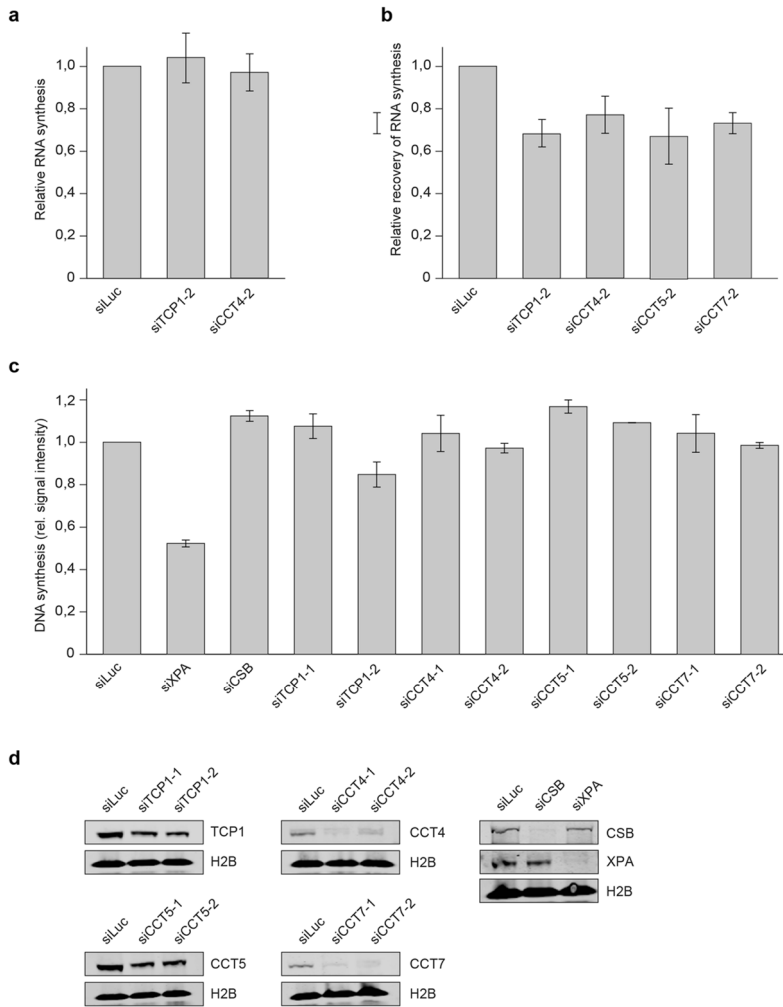
Supplementary Figure 3. Loss of TriC components causes reduced CSA stability

(a) Depletion of TCP1 decreases CSA protein abundance. VH10-hTert cells were transfected with the indicated siRNAs and whole cell extracts were prepared at the indicated time points after siRNA transfection. Protein levels were determined by Western blot analysis of the indicated proteins. H3 is a loading control. Graphs represent the ratio of protein signal intensities over H3 control signal intensities for siTCP1-treated cells relative to that for siLuc-treated control cells, which was set to 100%, at each time point. A repeat of the experiment is shown in Figure 3a. (b) Depletion of TCP1 decreases CSA protein abundance. As in a, except that two different siRNAs against TCP1 were used and that protein levels were determined 72 hours after siRNA transfection. A repeat of the experiment is shown in Figure 3b. (c) Depletion of CCT4, CCT5 or CCT7 decreases CSA protein abundance. As in a, except that CCT4, CCT5 or CCT7 siRNAs were used and that protein levels were determined 72 hours after siRNA transfection. A repeat of the experiment is shown in Figure 3c.



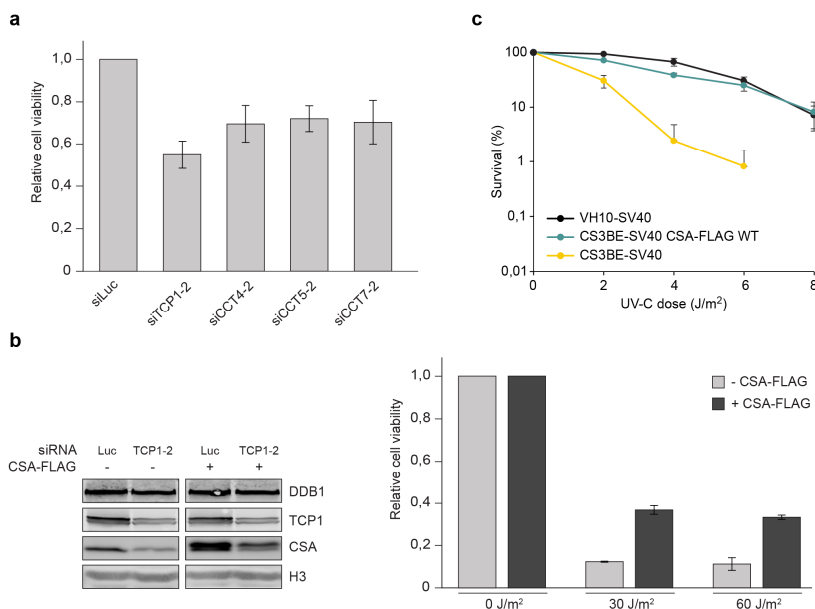
Supplementary Figure 4. Single amino acid substitutions in CSA's top platform do not affect TRiC binding or UV sensitivity

(a) Overview of CSA residues involved in TRiC binding. Side and top view of CSA. The amino acids Glu103, Phe120, Lys122, Arg164, Lys247, Lys292, Lys293 or Arg354 in the top platform were mutated to alanines and are shown in yellow. For comparison, the 4 residues Lys34, Lys85, Lys167, Lys212, which crosslinked to TRiC subunits as determined by xIP-MS, are shown in red. (b) Single amino acid substitutions in CSA do not cause altered DDB1 or TRiC binding. CSA harboring 1 of the substitutions mentioned in a, was immunoprecipitated from total extracts of CSA-deficient patient cells. Western blot analysis of the precipitated complexes shows DDB1, CUL4A and TCP1 binding comparable to WT CSA. (c) Expression of CSA harboring single amino acid substitutions rescues UV sensitivity of CSA-deficient patient cells. CS3BE-SV40 cells expressing the mutants described in a were UV-C-irradiated and assayed for clonogenic survival. Data represent mean \pm SEM of 2 independent experiments.



Supplementary Figure 5. Loss of TRiC components reduces RNA synthesis recovery, but not unscheduled DNA synthesis

(a) Basal transcription levels are not affected by TCP1 knockdown. VH10-hTert cells were transfected with the indicated siRNAs. RNA synthesis was measured by means of EU incorporation and normalized to that of siLuc-treated cells. Data represent mean \pm SEM of 4 independent experiments. (b) Loss of TRiC components reduces RNA synthesis recovery following UV-C irradiation. VH10-hTert cells were transfected with the indicated siRNAs and UV-C-irradiated (10 J/m^2). RNA synthesis was measured 24 hours after UV as in a. RNA synthesis levels were normalized to those in non-irradiated cells, which were set to 100%. Data represent the mean \pm SEM of 3 independent experiments. (c) Loss of TRiC components does not affect unscheduled DNA synthesis after UV-C irradiation. VH10-hTert cells were transfected with the indicated siRNAs, UV-C-irradiated at (20 J/m^2) and subjected to EdU incorporation, which served as a measure for unscheduled DNA synthesis during GG-NER. Data were normalized to EdU levels in siLuc-treated cells and represent the mean \pm SEM of 2 independent experiments. (d) Protein levels were determined by Western blot analysis of the indicated proteins using cells from c. H2B is a loading control.



Supplementary Figure 6. TRiC protects cells against UV damage

(a) Loss of TRiC components renders cells hypersensitive to UV damage. VH10-hTert cells were transfected with the indicated siRNAs, UV-C-irradiated (60 J/m²) and 72 hours later assayed for viability using alamarBlue®. Data represent mean ± SEM of 3 independent experiments. (b) Overexpression of CSA renders TCP1-depleted cells less sensitive to UV damage. VH10-hTert cells expressing wildtype CSA levels and those stably expressing additional CSA-FLAG were transfected with siLuc or siTCP1-2, UV-C-irradiated at the indicated doses and 72 hours later assayed for viability using alamarBlue®. Total cell extracts were prepared and protein levels were determined by Western blot analysis of the indicated proteins (left panel). Viability of siTCP1-2-treated cells normalized to that of siLuc-treated cells is shown relative to non-irradiated cells (right panel). Data represent mean ± SEM of 2 independent experiments. (c) Expression of CSA-FLAG in CSA-deficient patient cells complements their UV sensitivity. The indicated cells were UV-C-irradiated at different doses and clonogenic survival was measured. Data represent mean ± SEM of 2 independent experiments. VH10-SV cells served as wildtype control cells.

Supplementary Data

Supplementary Data 1. Mass spectrometry analysis of CSA-interacting proteins

Complete list of all proteins that were detected by mass spectrometry after pulldown of FLAG or CSA-FLAG from CS3BE-SV40 cells labeled using SILAC (Figure 1a).

Supplementary Data 2. xIP-MS analysis of crosslinked CSA-interacting proteins

Complete list of all crosslinks that were detected after xIP-MS of CSA-GFP from CS3BE-SV40 cells.

Supplementary data are available at <https://doi.org/10.1038/s41467-018-03484-6>.

Methods

Cell culture

Cells were cultured in DMEM (Invitrogen) supplemented with 10% fetal bovine serum (FBS; Bodinco BV) and penicillin/streptomycin (Sigma). The following cell lines were used: U2OS (ATCC), CS3BE-SV40 (GM01856; Coriell Institute), CS3BE-hTert (GM01856; Coriell Institute), VH10-hTert.

Generation of stable cell lines

Constructs encoding CSA-FLAG were established by cloning CSA cDNA (extended with a FLAG-tag by PCR) into pENTR4 (Invitrogen). GFP-tagged constructs were made by cloning CSA WT or CSA 8M, which was created by site-directed mutagenesis using the QuickChange site-directed mutagenesis kit (Agilent), into pENTR1A-GFP-N2 (Addgene). CSA constructs harboring single amino acid substitutions E103A, F120A, K122A, R164A, K247A, K292A, K292A+K293A and R354A and a C-terminal 10x-His-tag were created by PCR and cloned into pDONR221. Constructs were subsequently transferred to pLenti6.3 V5-DEST (pENTR4, pENTR1A-GFP) or pLenti4 V5-DEST (pDONR221) by Gateway LR Clonase II Enzyme Mix (Invitrogen). Lentivirus was produced using the pCMV-VSV-G, pMDLg-RRE and pRSV-REV plasmids (Addgene) and used to infect cells with Polybrene® (Sigma). Stable integrands were obtained after selection in medium containing blasticidin (ThermoFisher Scientific) (pLenti6.3) or zeocin (Invitrogen) (pLenti4).

U2OS Flp-In/T-Rex cells, which were generated by Prof. J. Parvin using the Flp-In™/T-Rex™ system (Thermo Fisher Scientific), were a gift of Dr. S. Pfister. These cells were cotransfected with pLV-U6g-PPB containing an antisense guide RNA targeting the CSA/ERCC8 gene (5-CCAGACTTCAAGTCACAAAGTTG-3) from the LUMC/Sigma-Aldrich sgRNA library together with an expression vector encoding Cas9-2A-GFP (pX458; Addgene #48138). Transfected U2OS Flp-In/T-Rex cells were selected on puromycin for 3 days, plated at low density, after which individual clones were isolated. Knockout of CSA and the absence of Cas9 integration/stable expression in the isolated clones was verified by Western blot analysis. The neomycin resistance gene in pcDNA5/FRT/TO-Neo (Addgene #41000) was replaced with a puromycin resistance gene to generate pcDNA5/FRT/TO-Puro. A fragment spanning GFP-NLS or GFP-N1 (Clontech) was inserted in this vector to create pcDNA5/FRT/TO-GFP-NLS-Puro and pcDNA5/FRT/TO-GFP-N1-Puro, respectively. CSA WT or CSA ΔN (lacking the first 21 amino acids) were amplified by PCR (primers: CSA WT 5-CACAATGCTAGCGCCACCATGCTGGGGTTTTGTCCG-3 and 5-GCATGGTGAACTACCGGTGCTCCTTCTTCATCACTGCTG-3, CSA ΔN 5-CTAGTAGAATTCATCGGACGCTAGCATGGAGTCAACACGGAGAGTTTGG-3 and 5-GCACCGACGACCTAGGCAGGATCCAGACTTCAAGTCACAAAG-3) and inserted into pcDNA5/FRT/TO/GFP-N1-Puro. One of the CSA knockout clones was subsequently used to stably express GFP-NLS, CSA-GFP WT or CSA-GFP ΔN by cotransfection of pcDNA5/FRT/TO-Puro plasmid encoding these CSA variants (2 μg), together with pOG44 plasmid encoding the Flp recombinase (0.5 μg). After selection on puromycin, single clones were isolated and expanded. Isolated U2OS CSA knockout clones stably expressing CSA-GFP WT or CSA-GFP ΔN were selected based on their equal and near-endogenous expression levels.

Generation and expression of CSA patient mutants

CSA cDNA was cloned into pEGFP-N2 (Addgene). Mutations A160T, A205P and D266G were created by site-directed mutagenesis using the QuickChange site-directed mutagenesis kit (Agilent). Plasmids were transfected using Lipofectamine® 2000 (Invitrogen) in Opti-MEM™ (Gibco) containing 10% FBS. 24 hours after transfection, cells were used for GFP-pulldown or fluorescence microscopy.

RNA interference

Proteins were depleted by two sequential transfections with 40 nM siRNA (Dharmacon, GE Healthcare) using Lipofectamine® RNAiMAX (Invitrogen) in Opti-MEM™ (Gibco) containing 10% FBS. The following siRNAs were used:

5'-CGUACGCGGAUACUUCGA-3' (luciferase);
5'-GCAAGGAAGCAGUGCGUUUU-3' (TCP1-1);
5'-GACCAAAUAGACAGAGAUU-3' (TPC1-2);
5'-GAACUGAGUGACAGAGAAUU-3' (CCT4-1);

5'-GUGUAAAUGCAGUGAUGAAUU-3' (CCT4-2);
 5'-GCAAAUACAAUGAGAACAUUU-3' (CCT5-1);
 5'-CAACACAAAUGGUUAGAAUUU-3' (CCT5-2);
 5'-CUGACAACUUUGAAGCUUUUU-3' (CCT7-1);
 5'-GGCAAUUGUUGAUGCUGAGUU-3' (CCT7-2);
 5'-UGAUAAUGGUGUUGUUUUUU-3' (DDB1-1);
 5'-AGAGAUUGCUCGAGACUUUUUU-3' (DDB1-2).

UV-C irradiation

UV damage was induced using a 254-nm TUV PL-S 9W lamp (Philips).

Treatment with TRiC inhibitor

Medium supplemented with 2.5 mM 2-[(4-chloro-2 λ^4 ,1,3-benzothiadiazol-5-yl)oxy]acetic acid (Vitas-M Laboratory Ltd., via MolPort-002-507-960) was added to attached cells in 6-wells plates every 24 hours during 72 hours.

Western blotting

Proteins were separated in 4-12% Bis-Tris NuPAGE® gels (Invitrogen) or Criterion™ gels (Bio-Rad) in MOPS (Life Technologies). For the detection of (endogenous) CSA by the Abcam rabbit CSA antibody, hand casted 10% or 13% acrylamide gels were used and electrophoresis was performed in a Tris-Glycine-SDS buffer. Separated proteins were blotted onto PVDF membranes (Millipore), which were incubated with the following primary antibodies: rabbit α -FLAG (Sigma, F7425; 1:2000); mouse α -Tubulin (Sigma, T6199; 1:5000); mouse α -GFP (Roche, #11814460001; 1:1000); mouse α -RNAPII α (Abcam, ab5408; 1:1000); goat α -DDB1 (Abcam, ab9194; 1:1000); rabbit α -CSA/ERCC8 (Abcam, ab137033; 1:1000); rabbit α -H3 (Abcam, ab1791; 1:5000); rabbit α -CSB/ERCC6 (Santa Cruz Biotechnology, sc-25370; 1:1000); goat α -CSB/ERCC6 (Santa Cruz Biotechnology, sc-10459; 1:1000); mouse α -CCT4 (Santa Cruz Biotechnology, sc-137092; 1:500); rabbit α -CUL4A (Bethyl Laboratories, A300-739A; 1:500); mouse α -TCP1 (Abnova, H00006950-M01; 1:1000); mouse α -CCT5 (Abnova, H00022948-M01; 1:500); mouse α -CCT7 (Abnova, H00010574-M01; 1:500). Protein bands were visualized using the Odyssey® Imaging System (LI-COR) after incubation with CF™ dye labelled secondary antibodies (Sigma; 1:10.000), or detected by the ECL™ Prime Western Blotting system (GE Healthcare) following incubation with Horseradish Peroxidase-conjugated secondary antibodies (Dako; 1:5000).

Immunoprecipitations and pulldowns

Cells were lysed in IP buffer (30 mM Tris pH 7.5, 150 mM NaCl, 2 mM MgCl₂, 0.5% Triton X-100, protease inhibitor cocktail (Roche)) during 1 hour at 4°C. The supernatant obtained by centrifugation is referred to as the soluble fraction, while the solubilized chromatin fraction was prepared by resuspension of the pellet followed by 1-2 hours of incubation in IP buffer containing 250 U/mL benzonase® nuclease (Novagen). Samples were subsequently incubated with the indicated antibody for immunoprecipitation during 2-4 hours.

For immunoprecipitation of proteins from total cell extracts, cells were directly lysed in IP buffer supplemented with 250 U/mL benzonase® nuclease and the desired antibody. Protein complexes were pulled down during 1-2 hours incubation with Protein A agarose beads (Millipore). GFP-tagged proteins were precipitated using GFP-Trap®_A beads (Chromotek), while FLAG-tagged proteins were precipitated using ANTI-FLAG® M2 Affinity Agarose Gel (Sigma). For tandem purification, proteins were eluted from the beads by addition of 3x FLAG peptide (Sigma). For subsequent analysis by Western blotting, proteins were eluted by boiling of the beads in Laemmli-SDS sample buffer.

Determination of overall protein levels by Western blotting

For detection of overall protein levels, whole cell extracts were prepared by lysis in 5 μ l IP buffer (30 mM Tris pH 7.5, 150 mM NaCl, 2 mM MgCl₂, 0.5% Triton X-100, protease inhibitor cocktail (Roche)) per 100.000 cells during 10 minutes at room temperature. Equal volumes of Laemmli-SDS sample buffer were added and the samples were heated at 95 °C for 10 minutes prior to Western blot analysis.

Fluorescence Microscopy

Cells were grown on glass coverslips and subjected to the indicated treatments. Cells were washed with PBS and fixed with 2% formaldehyde (Sigma) in PBS. For nuclear staining cells were permeabilized in 0.25% Triton X-100 (Sigma) and incubated with DAPI (Sigma). Images were acquired on a Zeiss AxioImager D2 widefield fluorescence microscope equipped with 40x, 63x and 100x PLAN APO (1.4 NA) oil-immersion objectives (Zeiss) and an HXP 120 metal-halide lamp used for excitation. Images were recorded using ZEN 2012 software and analyzed in ImageJ (<https://imagej.nih.gov/ij/>).

Identification of CSA-interacting proteins

For stable isotope labeling of amino acids in culture (SILAC) cells were grown in DMEM containing 10% dialyzed FBS (Gibco), 10% GlutaMAX (Life Technologies), penicillin/streptomycin (Life Technologies), unlabeled L-arginine-HCl and L-lysine-HCl or $^{13}\text{C}_6$, $^{15}\text{N}_4$ L-arginine-HCl and $^{13}\text{C}_6$, $^{15}\text{N}_2$ L-lysine-2HCl (Cambridge Isotope Laboratories), respectively. FLAG and CSA-FLAG complexes were pulled down from total cell extracts with ANTI-FLAG® M2 Affinity Gel (Sigma) and extensively washed. Bound proteins were eluted with FLAG peptide (0.2 mg/ml in PBS), separated in SDS-PAGE gels and visualized with Coomassie (SimplyBlue; Invitrogen). SDS-PAGE gel lanes were cut into 2-mm slices and subjected to in-gel reduction with dithiothreitol, alkylation with iodoacetamide (98%; D4, Cambridge Isotope Laboratories) and digestion with trypsin (sequencing grade; Promega). Nanoflow liquid chromatography tandem mass spectrometry (LC-MS/MS) was performed on an 1100 series capillary liquid chromatography system (Agilent Technologies) coupled to a Q-Exactive mass spectrometer (Thermo Scientific) operating in positive mode. Peptide mixtures were trapped on a ReproSil C18 reversed phase column (1.5 cm × 100 µm) at a rate of 8 µl/min, separated using a linear gradient of 0–80% acetonitrile (in 0.1% formic acid) during 60 min at a rate of 200 nl/min using a splitter. The eluate was directly sprayed into the electrospray ionization (ESI) source of the mass spectrometer. Spectra were acquired in continuum mode; fragmentation of the peptides was performed in data-dependent mode. Mass spectrometry data were analyzed with MaxQuant software (version 1.1.1.25).

LFQ and crosslinking mass spectrometry

Label-free quantification (LFQ), stoichiometry estimation, and crosslinking mass spectrometry were performed essentially as described previously^{20,21}. Briefly, GFP immunoprecipitations for LFQ and stoichiometry analysis were performed in triplicate using ChromoTek GFP-Trap beads or control non-GFP beads and 2 mg of whole cell lysate collected in a 1% NP-40 whole cell lysis buffer. After protein incubation, 2 washes were performed with 1M NaCl and 1% NP-40, followed by additional washes with PBS. Reduction and alkylation were performed in-solution, and samples were digested with trypsin overnight. Tryptic peptides were separated over a 120-minutes gradient from 7–32% acetonitrile with 0.1% formic acid and measured on a Thermo Q-Exactive mass spectrometer. Identification and quantification of peptides were performed using MaxQuant version 1.5.1.0⁴⁹. Relative stoichiometries were calculated by normalizing each protein by iBAQ value against the bait protein (CSA).

For crosslinking mass spectrometry, 2 independent experiments were conducted. Protein purifications and mass spectrometry analysis were essentially the same as stated above, with exceptions noted below. First, after washes, we crosslinked immunoprecipitated complexes on-bead for one hour at room temperature using 1 mM BS3 (bis(sulfosuccinimidyl)suberate) in 50 mM borate buffered saline. Crosslinking was quenched with 100 mM ammonium bicarbonate for 10 minutes and sample preparation for mass spectrometry was continued as previously, including reduction, alkylation, and digestion. Samples were measured on either a Thermo QExactive or a Thermo Fusion as above, but over a 4 hour 7–37% acetonitrile gradient with charge 2+ or lower masses excluded from fragmentation. Crosslinked peptides were identified using pLink with an FDR of 0.05²². Identified crosslinks were further filtered to remove matches where either peptide was not ≥5 or ≤40 amino acids in length and with an e-value for the spectral match of ≤0.0001. All identified crosslinks in any experiment meeting these criteria were combined for further analysis. Crosslinking data was structurally validated using a TRiC homology model where each subunit was produced using Phyre2 and aligned onto the eukaryotic TRiC in Chimera (PDB: 4V94^{50,51}). In cases where a crosslinked residue was not resolved in the structure, the nearest structurally resolved residue in the protein sequence was used for modeling. All structural images were

produced in UCSF Chimera, and crosslink distance analysis was performed using XlinkAnalyzer^{52,53}. Accessible interaction space was modeled using DisVis²³ and human CSA (PDB: 4A11⁴).

RNA synthesis recovery assay

Cells were seeded in 96-well plates, transfected with siRNAs (see above) and after 48 hours irradiated with UV-C (10 J/m²), and incubated for different time periods (0–30 hours) to allow RNA synthesis recovery. RNA was labeled for 1 hour in medium supplemented with 1 mM EU (Click-iT® RNA Alexa Fluor® 594 Imaging Kit, Life Technologies) according to the manufacturer's instructions. Imaging was performed on an Opera Phenix confocal High-Content Screening System (Perkin Elmer, Hamburg, Germany) equipped with solid state lasers. General nuclear staining (DAPI) and Alexa 594 were serially detected in 9 fields per well using a 20x air objective. 3 independent experiments were analyzed using a custom script in the Harmony 4.5 software (Perkin Elmer) in which nuclei were individually segmented based on the DAPI signal. RNA synthesis recovery was determined by measuring the mean Alexa 594 intensity of all nuclei per well.

DNA synthesis repair assay

Cells were seeded on coverslips and transfected with siRNA (see above). After 48 hours the cells were UV-C-irradiated (20 J/m²) and subsequently DNA was labeled for 3 hours in medium supplemented with 1 μM of EdU (Click-iT® DNA Alexa Fluor® 488 Imaging Kit, Life Technologies) according to the manufacturer's instructions. DNA synthesis repair was quantified by determining fluorescence intensities for >20 cells with ImageJ software of images obtained with a Zeiss LSM700.

UV and Illudin S survival assays

Cells were seeded at low density and UV-C-irradiated at different doses or treated with 300, 600 and 1000 pg/mL illudin S (Santa Cruz; sc-391575) for 72 hours. After 11–14 days of incubation, cells were washed with 0.9% NaCl and stained with methylene blue. Colonies of >20 cells were scored.

Cell viability (AlamarBlue) assay

Cells were seeded in 96-well plates, transfected with siRNAs (see above) and after 48 hours irradiated with UV-C (10 J/m²). AlamarBlue® (Life Technologies) was added and fluorescence was measured 72 hours later according to the manufacturer's instructions.

References

1. Hoeijmakers, J.H. DNA damage, aging, and cancer. *N Engl J Med* 361, 1475–85 (2009).
2. Marteijn, J.A., Lans, H., Vermeulen, W. & Hoeijmakers, J.H.J. Understanding nucleotide excision repair and its roles in cancer and ageing. *Nature Reviews Molecular Cell Biology* 15, 465–481 (2014).
3. Lagerwerf, S., Vrouwe, M.G., Overmeer, R.M., Fouteri, M.I. & Mullenders, L.H. DNA damage response and transcription. *DNA Repair (Amst)* 10, 743–50 (2011).
4. Hanawalt, P.C. & Spivak, G. Transcription-coupled DNA repair: two decades of progress and surprises. *Nat Rev Mol Cell Biol* 9, 958–70 (2008).
5. Dijk, M., Typas, D., Mullenders, L. & Pines, A. Insight in the multilevel regulation of NER. *Exp Cell Res* 329, 116–23 (2014).
6. Fischer, E.S. et al. The Molecular Basis of CRL4(DDB2/CSA) Ubiquitin Ligase Architecture, Targeting, and Activation. *Cell* 147, 1024–1039 (2011).
7. Groisman, R. et al. The ubiquitin ligase activity in the DDB2 and CSA complexes is differentially regulated by the COP9 signalosome in response to DNA damage. *Cell* 113, 357–367 (2003).
8. Groisman, R. et al. CSA-dependent degradation of CSB by the ubiquitin-proteasome pathway establishes a link between complementation factors of the Cockayne syndrome. *Genes & Development* 20, 1429–1434 (2006).
9. Schwertman, P. et al. UV-sensitive syndrome protein UVSSA recruits USP7 to regulate transcription-coupled repair. *Nature Genetics* 44, 598–+ (2012).

10. Nakazawa, Y. et al. Mutations in UVSSA cause UV-sensitive syndrome and impair RNA polymerase II processing in transcription-coupled nucleotide-excision repair. *Nature Genetics* 44, 586-+ (2012).
11. Zhang, X. et al. Mutations in UVSSA cause UV-sensitive syndrome and destabilize ERCC6 in transcription-coupled DNA repair. *Nature Genetics* 44, 593-+ (2012).
12. Cleaver, J.E., Lam, E.T. & Revet, I. Disorders of nucleotide excision repair: the genetic and molecular basis of heterogeneity. *Nature Reviews Genetics* 10, 756-768 (2009).
13. Hartl, F.U., Bracher, A. & Hayer-Hartl, M. Molecular chaperones in protein folding and proteostasis. *Nature* 475, 324-332 (2011).
14. Joachimiak, L.A., Walzthoeni, T., Liu, C.W., Aebersold, R. & Frydman, J. The Structural Basis of Substrate Recognition by the Eukaryotic Chaperonin TRiC/CCT. *Cell* 159, 1042-1055 (2014).
15. Fei, J. & Chen, J. KIAA1530 protein is recruited by Cockayne syndrome complementation group protein A (CSA) to participate in transcription-coupled repair (TCR). *J Biol Chem* 287, 35118-26 (2012).
16. Saijo, M. The role of Cockayne syndrome group A (CSA) protein in transcription-coupled nucleotide excision repair. *Mech Ageing Dev* 134, 196-201 (2013).
17. Cong, Y. et al. 4.0-A resolution cryo-EM structure of the mammalian chaperonin TRiC/CCT reveals its unique subunit arrangement. *Proc Natl Acad Sci U S A* 107, 4967-72 (2010).
18. Reissmann, S., Parnot, C., Booth, C.R., Chiu, W. & Frydman, J. Essential function of the built-in lid in the allosteric regulation of eukaryotic and archaeal chaperonins. *Nat Struct Mol Biol* 14, 432-40 (2007).
19. Russmann, F. et al. Folding of large multidomain proteins by partial encapsulation in the chaperonin TRiC/CCT. *Proceedings of the National Academy of Sciences of the United States of America* 109, 21208-21215 (2012).
20. Smits, A.H., Jansen, P.W., Poser, I., Hyman, A.A. & Vermeulen, M. Stoichiometry of chromatin-associated protein complexes revealed by label-free quantitative mass spectrometry-based proteomics. *Nucleic Acids Res* 41, e28 (2013).
21. Makowski, M.M., Willems, E., Jansen, P.W. & Vermeulen, M. Cross-linking immunoprecipitation-MS (xIP-MS): Topological Analysis of Chromatin-associated Protein Complexes Using Single Affinity Purification. *Mol Cell Proteomics* 15, 854-65 (2016).
22. Yang, B. et al. Identification of cross-linked peptides from complex samples. *Nat Methods* 9, 904-6 (2012).
23. van Zundert, G.C. & Bonvin, A.M. DisVis: quantifying and visualizing accessible interaction space of distance-restrained biomolecular complexes. *Bioinformatics* 31, 3222-4 (2015).
24. Yam, A.Y. et al. Defining the TRiC/CCT interactome links chaperonin function to stabilization of newly made proteins with complex topologies. *Nat Struct Mol Biol* 15, 1255-62 (2008).
25. Freund, A. et al. Proteostatic Control of Telomerase Function through TRiC-Mediated Folding of TCAB1. *Cell* 159, 1389-1403 (2014).
26. National Center for Biotechnology Information. PubChem BioAssay Database; AID=488991, <https://pubchem.ncbi.nlm.nih.gov/bioassay/488991>.
27. Jaspers, N.G. et al. Anti-tumour compounds illudin S and Irofulven induce DNA lesions ignored by global repair and exclusively processed by transcription- and replication-coupled repair pathways. *DNA Repair (Amst)* 1, 1027-38 (2002).
28. Laugel, V. et al. Mutation update for the CSB/ERCC6 and CSA/ERCC8 genes involved in Cockayne syndrome. *Hum Mutat* 31, 113-26 (2010).
29. Balchin, D., Hayer-Hartl, M. & Hartl, F.U. In vivo aspects of protein folding and quality control. *Science* 353, aac4354 (2016).
30. Hipp, M.S., Park, S.H. & Hartl, F.U. Proteostasis impairment in protein-misfolding and -aggregation diseases. *Trends Cell Biol* 24, 506-14 (2014).
31. Duan, Y. et al. HspA1A facilitates DNA repair in human bronchial epithelial cells exposed to Benzo[a]pyrene and interacts with casein kinase 2. *Cell Stress Chaperones* 19, 271-9 (2014).
32. Montesano Gesualdi, N. et al. Tumor necrosis factor-associated protein 1 (TRAP-1) protects cells from oxidative stress and apoptosis. *Stress* 10, 342-50 (2007).
33. Park, C., Suh, Y. & Cuervo, A.M. Regulated degradation of Chk1 by chaperone-mediated autophagy in response to DNA damage. *Nat Commun* 6, 6823 (2015).

34. Pennisi, R., Ascenzi, P. & di Masi, A. Hsp90: A New Player in DNA Repair? *Biomolecules* 5, 2589-618 (2015).
35. Munoz, I.G. et al. Crystal structure of the open conformation of the mammalian chaperonin CCT in complex with tubulin. *Nat Struct Mol Biol* 18, 14-9 (2011).
36. Camasses, A., Bogdanova, A., Shevchenko, A. & Zachariae, W. The CCT chaperonin promotes activation of the anaphase-promoting complex through the generation of functional Cdc20. *Molecular Cell* 12, 87-100 (2003).
37. Feldman, D.E., Thulasiraman, V., Ferreyra, R.G. & Frydman, J. Formation of the VHL-elongin BC tumor suppressor complex is mediated by the chaperonin TRiC. *Mol Cell* 4, 1051-61 (1999).
38. Kubota, S., Kubota, H. & Nagata, K. Cytosolic chaperonin protects folding intermediates of G ss from aggregation by recognizing hydrophobic ss-strands. *Proceedings of the National Academy of Sciences of the United States of America* 103, 8360-8365 (2006).
39. McLaughlin, J.N. et al. Regulatory interaction of phosducin-like protein with the cytosolic chaperonin complex. *Proceedings of the National Academy of Sciences of the United States of America* 99, 7962-7967 (2002).
40. Miyata, Y., Shibata, T., Aoshima, M., Tsubata, T. & Nishida, E. The Molecular Chaperone TRiC/CCT Binds to the Trp-Asp 40 (WD40) Repeat Protein WDR68 and Promotes Its Folding, Protein Kinase DYRK1A Binding, and Nuclear Accumulation. *Journal of Biological Chemistry* 289, 33320-33332 (2014).
41. Plimpton, R.L. et al. Structures of the G beta-CCT and PhLP1-G beta-CCT complexes reveal a mechanism for G-protein beta-subunit folding and G beta gamma dimer assembly. *Proceedings of the National Academy of Sciences of the United States of America* 112, 2413-2418 (2015).
42. Yi, C.L., Li, S.T., Wang, H., Wei, N. & Deng, X.W. Affinity purification reveals the association of WD40 protein constitutive photomorphogenic 1 with the hetero-oligomeric TCP-1 chaperonin complex in mammalian cells. *International Journal of Biochemistry & Cell Biology* 38, 1076-1083 (2006).
43. Zhong, F. et al. Disruption of telomerase trafficking by TCAB1 mutation causes dyskeratosis congenita. *Genes Dev* 25, 11-6 (2011).
44. Laugel, V. Cockayne syndrome: the expanding clinical and mutational spectrum. *Mech Ageing Dev* 134, 161-70 (2013).
45. Trinidad, A.G. et al. Interaction of p53 with the CCT complex promotes protein folding and wild-type p53 activity. *Mol Cell* 50, 805-17 (2013).
46. Kaisari, S., Sitry-Shevah, D., Miniowitz-Shemtov, S., Teichner, A. & Hershko, A. Role of CCT chaperonin in the disassembly of mitotic checkpoint complexes. *Proc Natl Acad Sci U S A* 114, 956-961 (2017).
47. Zhou, Z., He, M., Shah, A.A. & Wan, Y. Insights into APC/C: from cellular function to diseases and therapeutics. *Cell Div* 11, 9 (2016).
48. Roh, S.H., Kasembeli, M., Bakthavatsalam, D., Chiu, W. & Tweardy, D.J. Contribution of the Type II Chaperonin, TRiC/CCT, to Oncogenesis. *Int J Mol Sci* 16, 26706-20 (2015).
49. Cox, J. & Mann, M. MaxQuant enables high peptide identification rates, individualized p.p.b.-range mass accuracies and proteome-wide protein quantification. *Nat Biotechnol* 26, 1367-72 (2008).
50. Kelley, L.A., Mezulis, S., Yates, C.M., Wass, M.N. & Sternberg, M.J. The Phyre2 web portal for protein modeling, prediction and analysis. *Nat Protoc* 10, 845-58 (2015).
51. Leitner, A., Faini, M., Stengel, F. & Aebersold, R. Crosslinking and Mass Spectrometry: An Integrated Technology to Understand the Structure and Function of Molecular Machines. *Trends Biochem Sci* 41, 20-32 (2016).
52. Kosinski, J. et al. Xlink Analyzer: software for analysis and visualization of cross-linking data in the context of three-dimensional structures. *J Struct Biol* 189, 177-83 (2015).
53. Pettersen, E.F. et al. UCSF Chimera--a visualization system for exploratory research and analysis. *J Comput Chem* 25, 1605-12 (2004).

4

Regulation of the DNA damage response by the SUMO E3 ligase Zimp7

Madelon Dijk, Ekaterina Gracheva, Alex Pines, Anton J.L. de Groot, Alfred C.O. Vertegaal and Haico van Attikum

Abstract

The DNA damage response covers a network of signaling cascades and DNA repair pathways that serve to protect genome stability. Post-translational modifications of the involved proteins profoundly contribute to regulation of these processes. For example, protein SUMOylation has been described to be important in the response to different types of DNA lesions, including those caused by UV irradiation that are removed via nucleotide excision repair (NER). A focused siRNA screen that examines the effect of several proteins involved in (de)SUMOylation on RNA synthesis recovery upon exposure to UV, identified the PIAS-like protein Zimp7 as a potentially important factor in the transcription-coupled NER subpathway. While PIAS proteins are capable of catalyzing SUMOylation reactions by means of their highly conserved SP-RING domain, this function had not been demonstrated for Zimp7. We reveal that the SP-RING-like motif in Zimp7 confers true SUMOylating activity, uncovering Zimp7 as a new SUMO E3 ligase. Moreover, Zimp7 is recruited to laser-induced DNA damage and interacts with elongating RNA polymerase, as well as with PCNA. Together these findings suggest potential roles of Zimp7 in the DNA damage response, transcription and DNA replication.

Introduction

DNA lesions caused by endogenous processes or exogenous insults such as radiation and chemical agents, continuously pose a threat to genome stability and may lead to ageing-related diseases and cancer if left unattended. To maintain genome integrity, DNA damage occurrence triggers the activation of a variety of repair and signaling cascades, collectively referred to as the DNA damage response (DDR)^{1,2}.

Post-translational modifications of the involved proteins have been shown to significantly contribute to the regulation of these pathways, thereby facilitating accurate repair and cell cycle progression. For example, ubiquitination and SUMOylation have been described to be broadly implicated in the DDR³⁻⁵. These modifications involve the reversible covalent attachment of the structurally similar ubiquitin or small ubiquitin-like modifier (SUMO), respectively, to the target protein, altering protein functions and interactions.

Analogously to ubiquitination, SUMOylation is established in a cascade of enzymatic reactions executed by E1, E2 and E3 proteins, which yet differ from those responsible for ubiquitin conjugation. In short, a SUMO precursor protein is C-terminally cleaved by one of the sentrin-specific proteases (SENPs), which is followed by its activation by the dimeric E1 protein SUMO activating enzyme 1 and 2 (SAE1/2). Subsequently, the SUMO moiety is transferred to the E2 conjugating enzyme UBC9, which couples it to the acceptor lysine of the target protein. Importantly, although this is sufficient for the SUMOylation of several substrates, SUMO attachment to many targets requires coordination by one of the E3 SUMO ligase proteins that can catalyze the reaction and provide target specificity⁶.

The protein inhibitor of activated STAT (PIAS) proteins 1-4 comprise a class of SUMO E3 ligases that have been described to both enhance and negatively regulate transcription. This is not merely dependent on their SUMOylation activities but may also rely on their SUMO interacting motifs (SIMs) that modulate interactions with other proteins or DNA⁷⁻¹⁰. Their function as SUMOylation catalyzers depends on the highly conserved Siz/PIAS-RING (SP-RING) motif that resembles the RING domain in ubiquitin E3 ligase proteins^{7,11}. Particularly, their roles in the response to DNA damage have been extensively studied. For example, the accumulation of PIAS1 and PIAS4 at double-strand breaks induces SUMOylation and/or recruitment of numerous repair factors, including BRCA1, RAP80, 53BP1 and RNF168, and modulates repair complex disassembly by regulating RNF4 recruitment¹²⁻¹⁶. Moreover, overexpression of PIAS3 can enhance homologous recombination as well as non-homologous end-joining¹⁷. Apart from DSB repair, protein modification by SUMO conjugation is crucial in the response to several other types of DNA damage. During base excision repair (BER), SUMOylation of damage recognition factor TDG reduces its interaction with abasic sites and enables its turnover^{18,19}. Furthermore, in yeast the recruitment of the anti-recombinogenic helicase Srs2 to SUMOylated PCNA not only regulates replication events during uncompromised DNA synthesis, but also coordinates repair pathway choice upon stalling of replication forks by for instance MMS- or UV-induced DNA damage^{20,21}. Protein modification by SUMO hence comprises an important mechanism to control various aspects of the DNA damage response.

UV irradiation triggers the SUMOylation of PCNA, as well as that of factors that are essential for faithful nucleotide excision repair (NER). Removal of DNA helix-destabilizing lesions via NER is initiated by the recognition of damage either specifically in transcribed DNA, referred to as transcription-coupled repair (TC-NER), or throughout the whole genome during global genome repair (GG-NER)²². In both subpathways, DNA damage detection is followed by the excision of a lesion-containing single-stranded stretch of DNA, and subsequent DNA synthesis and gap sealing^{22,23}.

Whereas stalling of elongating RNA polymerase II at the lesion serves as a damage signal for the recruitment of CSA/CSB and activation of TC-NER, lesion recognition by GG-NER requires the damage sensor proteins XPC and DDB2. Notably, UV-induced SUMOylation of CSB appears to be critical for the repair of transcription-blocking lesions²⁴. Similarly, it has been demonstrated that SUMOylation of XPC upon UV irradiation triggers its recognition by the SUMO-targeted ubiquitin ligase (STUBL) RNF111 and the consequential K63-linked ubiquitination that regulates its recruitment to lesions^{25,26}. Although these findings underscore the importance of SUMOylation during both subpathways, the exact mechanisms by which SUMO ligases and proteases regulate NER remain to be established.

Here we study the contribution of (de)SUMOylation enzymes to TC-NER. We identify the PIAS-like protein Zimp7 (Zinc finger containing, Miz1, PIAS-like protein on chromosome 7) to be important for the recovery of RNA synthesis upon UV irradiation of VH10-hTert cells. Resembling the PIAS proteins, Zimp7 has been shown to regulate transcription in multiple ways. It has been described to augment transcription that is mediated by Wnt/ β -catenin, the androgen receptor and a number of other nuclear hormone receptors. Its function as a transcriptional regulator is further supported by the presence of a C-terminal transactivation domain (TAD)²⁷⁻²⁹. In addition, Zimp7 contains an SP-RING-like motif, which explains its classification as a PIAS-like protein²⁷. We show that this domain confers true SUMOylating activity, thereby revealing Zimp7 as a novel SUMO E3 ligase. Moreover, its *in vivo* SUMOylation and interaction with PIAS3 confirm Zimp7's involvement in the SUMO conjugation system. Finally, Zimp7 is recruited to laser-induced DNA damage and interacts with elongating RNA polymerase II and PCNA in the absence of DNA damage. These findings uncover Zimp7 as a promising SUMO E3 ligase in the context of the DNA damage response and DNA replication.

Results

Zimp7 may play a role in the DNA damage response

To identify factors involved in (de)SUMOylation that could play a role in transcription-coupled nucleotide excision repair (TC-NER), we performed a small screen in VH10-hTert cells that examined the effect of siRNA-mediated knockdown of candidate proteins on the recovery of RNA synthesis after UV irradiation (Supplementary Fig. 1a). Of the 27 proteins that were studied, knockdown of the PIAS-like protein Zimp7 led to the greatest impairment in RNA synthesis recovery when normalized to siGFP-treated control cells. Notably, the effect was comparable to that caused by depletion of CSB (Fig. 1a, Supplementary Fig. 1a).

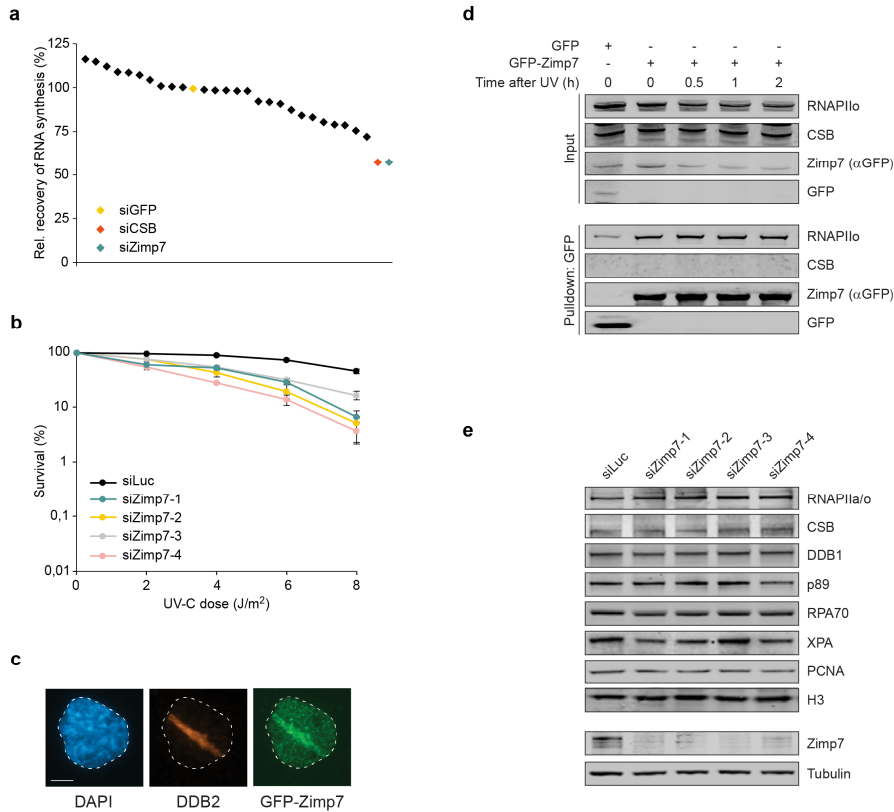


Figure 1. Zimp7 may play a role in the DNA damage response

(a) An siRNA-based screen targeting 27 different proteins potentially involved in (de)SUMOylation identified Zimp7 as a factor that is important for the recovery of RNA synthesis upon UV damage induction. VH10-hTert cells were transfected with siRNA, UV-C-irradiated at 10 J/m² and allowed to recover for 24 hours. RNA synthesis was determined by means of EU incorporation. Data represent the increase in RNA synthesis relative to non-irradiated cells between 2 and 24 hours after UV irradiation, normalized to that in siGFP-treated cells. (b) Loss of Zimp7 renders cells sensitive to UV irradiation. VH10-hT cells were transfected with the indicated siRNAs before UV irradiation at different doses. Clonogenic survival was determined after 2 weeks. Data represent mean \pm SEM of 2 independent experiments. (c) Zimp7 is recruited to DNA damage created by the multiphoton laser. DNA damage was inflicted in U2OS cells stably expressing GFP-Zimp7 by multiphoton laser micro-irradiation. Upon pre-extraction, cells were fixed and stained by DAPI and antibodies against the indicated proteins. Length of scale bar: 5 μ m. (d) Zimp7 interacts with RNAPII α . GFP or GFP-Zimp7 was pulled down from HAp1 Zimp7 KO cells stably expressing these proteins at the indicated times after UV-C irradiation at 20 J/m². (e) Zimp7 knockdown slightly affects XPA levels, but none of the other studied NER proteins. VH10-hTert cells were treated with the indicated siRNAs before preparation of whole cell extracts for determination of the presented protein levels.

Importantly, clonogenic survivals showed that knockdown of Zimp7 by 4 different siRNAs markedly increased UV sensitivity of VH10-hTert cells when compared to control cells (Fig. 1b). We therefore hypothesized that Zimp7 could be an important factor in the UV response. To study whether the contribution of Zimp7 would require the presence of the protein at the site of the damage, we stably expressed GFP-tagged Zimp7 in U2OS cells and created DNA damage locally by using a multiphoton laser (Fig. 1c). Interestingly, we could indeed detect recruitment of GFP-Zimp7 to sites of laser-induced DNA damage that were decorated with DDB2. Furthermore, pulldown of GFP-Zimp7 from HAP1 cells revealed that Zimp7 interacts with elongating RNA polymerase II (RNAPII_o), although this appeared to be independent of UV damage (Fig. 1d).

The observation that Zimp7 already interacts with RNAPII_o in the absence of damage, may be explained by a more general role of Zimp7 in transcription. For example, Zimp7 has been described to enhance androgen receptor-mediated transcription and augment Wnt/ β -catenin-mediated transcription^{27,28,29}. To determine whether regulation of TC-NER by Zimp7 could occur via controlling transcription of TC-NER genes, we studied the effect of Zimp7 depletion on the levels of several of the main NER factors (Fig. 1e). While most of the studied proteins remained unaffected by Zimp7 knockdown, we observed a substantial decrease in the levels of XPA upon treatment with siZimp7-1,-2 or -4. In contrast, siZimp7-3 did not negatively affect the abundance of XPA and only induced a minor increase in UV sensitivity when compared to the other siRNAs, while depleting Zimp7 with similar efficiency (Fig. 1b, Fig. 1e). These findings not only suggest that the loss of XPA was (at least partly) causative for the observed increase in UV sensitivity, but also indicate a possible off-target effect of siZimp7-1,-2 and -4 on XPA. Although our results may implicate a potential role for Zimp7 in the DNA damage response, siRNA-independent approaches are needed to further support this conclusion.

Knockout of Zimp7 does not increase UV sensitivity

To further study the effect of the absence of Zimp7 on XPA levels and NER, we generated Zimp7 knockout U2OS and RPE-1 cells. Analyzing 3 different clones in each cellular background, we were unable to verify the small decrease in XPA expression levels observed after siRNA-mediated Zimp7 depletion (Fig. 2a,c). We subsequently performed clonogenic survival assays following UV exposure of wildtype and Zimp7 knockout cells. Strikingly, we could not detect increased UV sensitivity in either U2OS (Fig. 2b) or RPE-1 (Fig. 2d) Zimp7 KO cells as compared to wildtype cells.

To circumvent the use of siRNAs and overcome the potential adaptation of Zimp7 knockout cells during their generation, we next studied the effect of 2 different shRNAs that target Zimp7 in U2OS cells. No reduction in XPA levels was detected upon shRNA-mediated Zimp7 depletion (Fig. 2e). Furthermore, neither of these shRNAs increased UV sensitivity as compared to control shRNA (Fig. 2f). Although several additional experiments are required to exclude other explanations for the observed data, these results suggest that the siRNAs used in VH10-hTert cells indeed caused an off-target effect on XPA, explaining the observed RNA synthesis recovery phenotype.

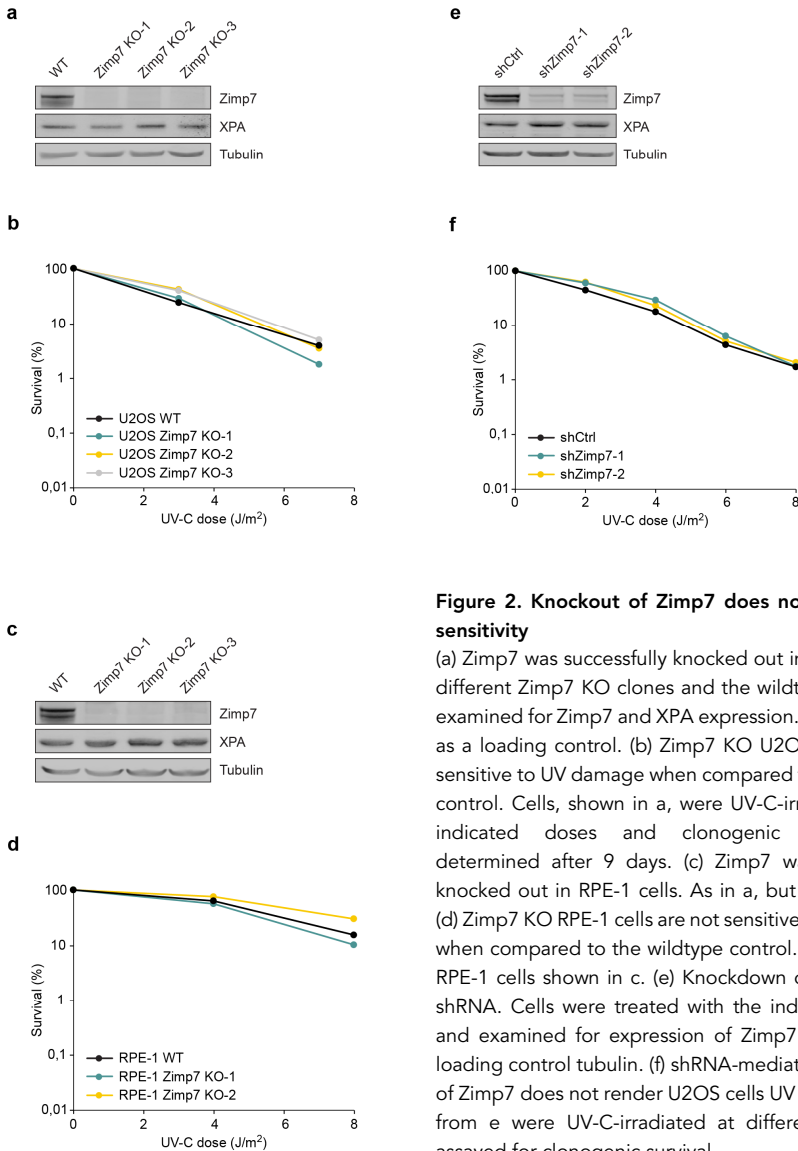


Figure 2. Knockout of Zimp7 does not increase UV sensitivity

(a) Zimp7 was successfully knocked out in U2OS cells. 3 different Zimp7 KO clones and the wildtype pool were examined for Zimp7 and XPA expression. Tubulin serves as a loading control. (b) Zimp7 KO U2OS cells are not sensitive to UV damage when compared to the wildtype control. Cells, shown in a, were UV-C-irradiated at the indicated doses and clonogenic survival was determined after 9 days. (c) Zimp7 was successfully knocked out in RPE-1 cells. As in a, but in RPE-1 cells. (d) Zimp7 KO RPE-1 cells are not sensitive to UV damage when compared to the wildtype control. As in b, but in RPE-1 cells shown in c. (e) Knockdown of Zimp7 using shRNA. Cells were treated with the indicated shRNAs and examined for expression of Zimp7, XPA and the loading control tubulin. (f) shRNA-mediated knockdown of Zimp7 does not render U2OS cells UV sensitive. Cells from e were UV-C-irradiated at different doses and assayed for clonogenic survival.

Zimp7 interacts with PCNA

Although we were not able to confirm a role for Zimp7 in the response to UV in U2OS cells, we had detected recruitment of GFP-Zimp7 to multiphoton laser-tracks in these cells (Fig. 1c). Since the laser that we used does not solely create DNA lesions that are normally induced by UV (6-4-PPs or CPDs), it is possible that GFP-Zimp7 is recruited to other types of DNA damage. These may for instance include DNA breaks or oxidative damage, raising the possibility that Zimp7 plays a role in DNA damage responses other than the UV damage response. To study this hypothesis, we first performed clonogenic survivals upon IR irradiation, which primarily inflicts DNA breaks (Fig. 3a-b). Knockout of Zimp7 did not increase the sensitivity of U2OS or RPE-1 cells to ionizing radiation-induced DNA damage. Similarly, proliferation assays on cells treated with the DNA alkylating agent MMS (Fig. 3c-d) did not reveal elevated drug sensitivity of Zimp7-depleted cells. Interestingly, several replication stress factors have been shown to accumulate in laser tracks³⁰⁻³⁴. Importantly, Zimp7 has been described to colocalize with PCNA at replication foci and was found to be enriched at hydroxyurea-stalled replication forks in an iPOND study^{11,27,28}. We therefore studied a potential role for Zimp7 in the replication stress response. Although knockout of Zimp7 did not render RPE-1 cells more sensitive to hydroxyurea, which causes replication stress by depleting the dNTP pool (Fig. 3e), we were able to observe a clear interaction between Zimp7 and PCNA³⁵. Pulldown of GFP-Zimp7 from HAP1 cells convincingly coprecipitated PCNA (Fig. 3f). Considering this interaction, in addition to the reported observation that Zimp7 depletion can cause severe defects in cell proliferation, we hypothesize that Zimp7 may play an important role in the response to replication stress as well as DNA replication in general²⁹.

Zimp7 is a true SUMO E3 ligase

To facilitate our study of the roles of Zimp7 in the DNA damage response and DNA replication, we decided to examine its molecular function as a PIAS-like protein. Originally identified as inhibitors of STAT transcription factors, PIAS proteins have been shown to broadly function as transcriptional coregulators and, by means of their highly conserved SP-RING-type domain, act as SUMO E3 ligases in different processes⁷. Next to a transactivation domain important in transcription, Zimp7 contains 2 SUMO interacting motifs and an SP-RING-like domain (Fig. 4a)²⁸. Indeed, alignment of Zimp7's SP-RING-like domain to that of PIAS1-4 showed a high degree of similarity (Fig. 4b). However, actual SUMOylating activity by Zimp7 has never been demonstrated. To study this potential activity, we expressed amino acids 419-920, containing the complete SP-RING-type domain, in *E. coli* and eased its purification by adding an N-terminal GST-tag. Next to the wildtype protein (GST-Zimp7 WT), we also purified the recombinant protein harboring a C616A mutation in the SP-RING domain (GST-Zimp7 CD) (Fig. 4a). As the respective cysteine in PIAS4 has been described to be required for its SUMO E3 ligase activity, this mutation would most likely render GST-Zimp7 CD catalytically dead^{36,37}.

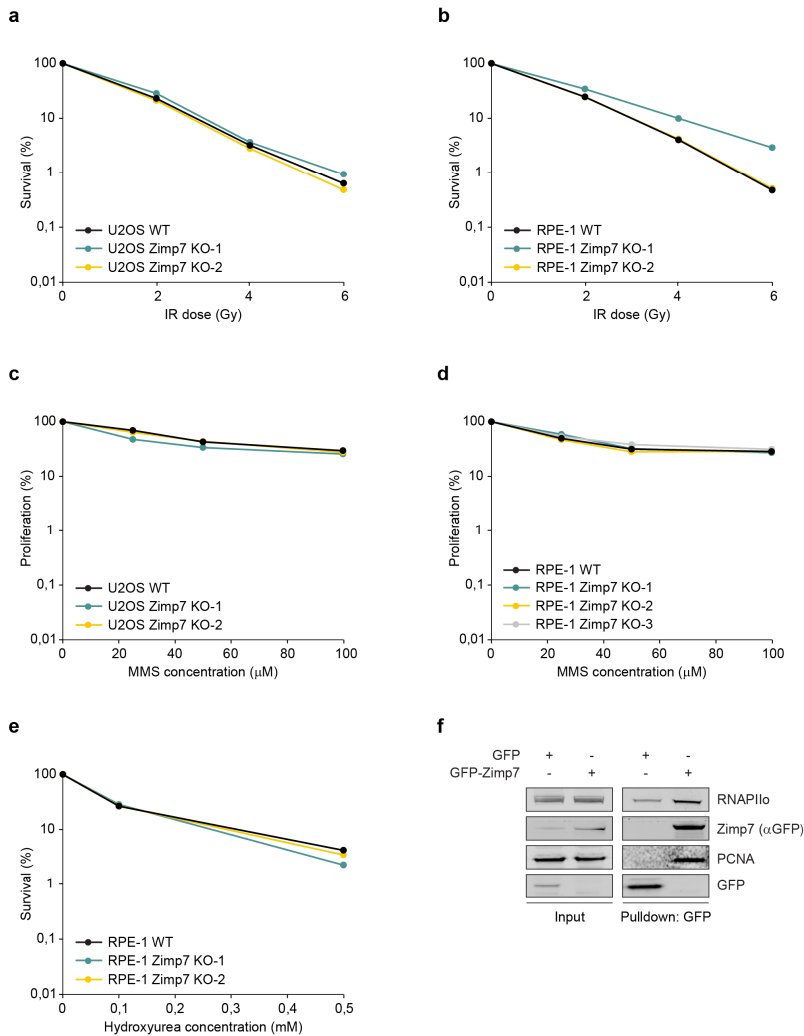


Figure 3. Zimp7 interacts with PCNA

(a) IR sensitivity of U2OS cells is not increased by Zimp7 knockout. Clonogenic survival of wildtype and Zimp7 KO U2OS cells was determined upon IR irradiation at the indicated doses. (b) IR sensitivity of RPE-1 cells is not increased by Zimp7 knockout. As in a, but using RPE-1 cells. (c) Zimp7 knockout does not negatively affect the proliferation of MMS-treated U2OS cells. Cells were incubated with the indicated concentrations of MMS during 24 hours. Proliferation was measured 48 hours after MMS removal. (d) Zimp7 knockout does not negatively affect the proliferation of MMS-treated RPE-1 cells. As in c, but using RPE-1 cells. (e) Zimp7 KO RPE-1 cells are not more sensitive to HU than the wildtype control pool. Cells were treated with different concentrations of hydroxyurea and clonogenic survival was determined. (f) Zimp7 interacts with PCNA. GFP-Zimp7 was pulled down from HAP1 Zimp7 KO cells. Among the coprecipitated proteins were RNAPII α and PCNA.

We next tested these proteins for their SUMOylating activity in an *in vitro* assay. SUMOylation of Zimp7 became apparent from a ladder of additional bands on top of wildtype Zimp7 as detected by Western blotting, upon addition of both the SAE1/2 and UBC9 proteins and either SUMO-1 or SUMO-2/3 to the reaction (Fig. 4c-d). Importantly, we did not observe this laddering pattern for GST-Zimp7 CD, suggesting that wildtype, but not CD ZIMP7 possesses (auto-)SUMOylating activity *in vitro*. To subsequently study (auto-)SUMOylation of Zimp7 *in vivo*, we pulled down GFP-Zimp7 WT and CD (Fig. 4a) from HAP1 cells under denaturing conditions. Probing the precipitated and Western blotted proteins with antibodies against GFP and SUMO-2/3, revealed that Zimp7 is SUMOylated *in vivo* as well (Fig. 4e). Strikingly however, we did not only detect SUMOylated GFP-Zimp7 WT, but also observed SUMOylation of GFP-Zimp7 CD. As we determined that the latter is not capable of auto-SUMOylation *in vitro* (Fig. 4c-d), this indicates that SUMOylation of Zimp7 *in vivo* may not (solely) result from its own SUMO E3 ligase activity. We then hypothesized that one of the PIAS proteins could be involved in Zimp7 SUMOylation, as interactions between Zimp7 and PIAS proteins have been described³⁸. In agreement, pulldown of GFP-Zimp7 WT from HAP1 cells showed a clear interaction between GFP-Zimp7 and PIAS3 (Fig. 4f). The relevance of this interaction remains elusive, although it has been suggested to contribute to Zimp7's stability and/or its transcriptional activity³⁸.

Together these data show that Zimp7 is a bona fide SUMO E3 ligase. Whether this function contributes to its role in the DNA damage response is yet to be determined. Furthermore, the fact that ZIMP7 interacts with PCNA (Fig. 3f, 4f) provides a promising foundation to investigate the involvement of Zimp7 as a SUMO E3 ligase in DNA replication.

Discussion

Zimp7 has mainly been studied as a transcriptional regulator. Initially identified as an enhancer of androgen receptor-mediated transcription, Zimp7 was found to also augment transcription that is moderated by a number of other nuclear hormone receptors and to act as a coactivator in the Wnt/ β -catenin signaling pathway^{28,29}. These roles are supported by physical interactions between Zimp7 and the hormone receptor or β -catenin, respectively, and most likely facilitated by Zimp7's C-terminal transactivation domain (TAD) that possesses intrinsic transcriptional activity²⁸. In contrast, much less is known about the contribution of the SP-RING- or Miz-like motif to Zimp7's cellular functions. Strikingly, despite the high sequence similarity to the SP-RING domains of the PIAS SUMO E3 ligases, the actual ability to catalyze SUMO conjugation had thus far never been demonstrated for Zimp7.

In this study, Zimp7 was revealed as a factor potentially implicated in the DNA damage response. Its classification as a PIAS-like protein made Zimp7 an attractive candidate in our screen, which examined the effects of knockdown of several (de)SUMOylating proteins on the recovery of RNA synthesis upon UV irradiation. This read-out specifically investigated a role for candidate proteins in transcription-coupled nucleotide excision repair and/or subsequent resumption of transcription.

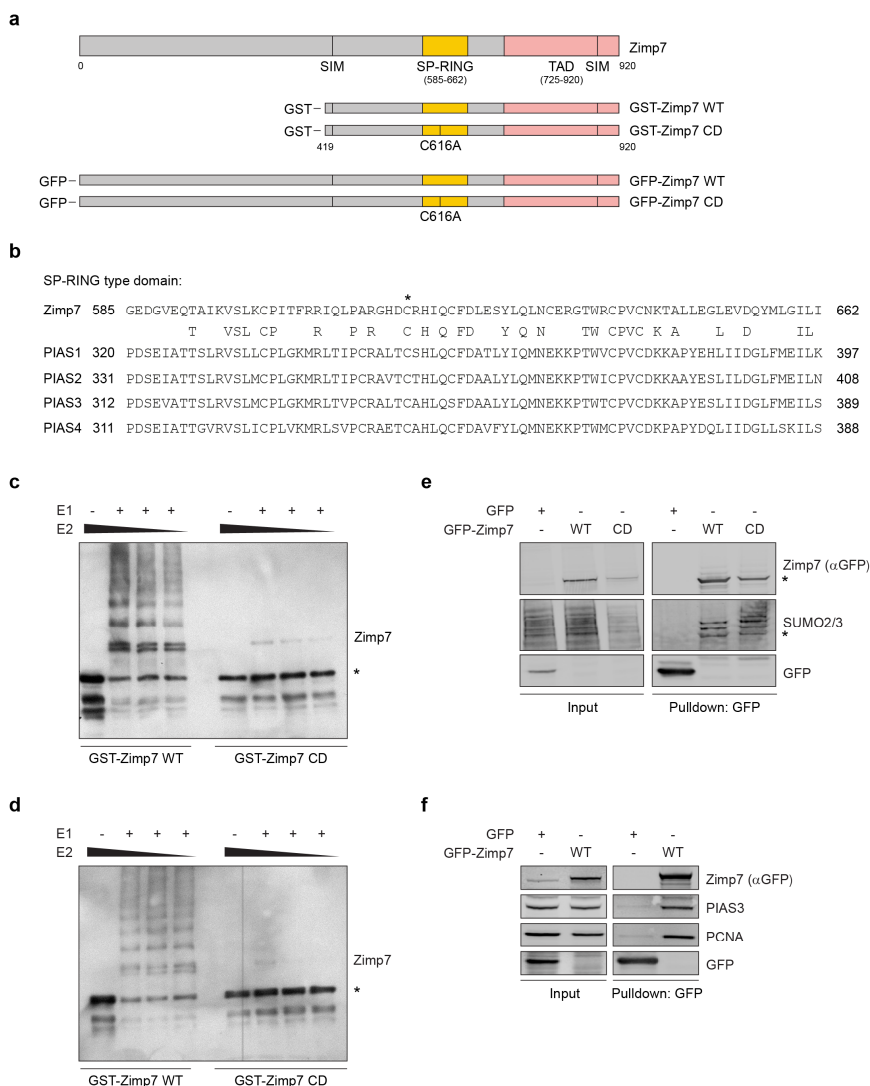


Figure 4. Zimp7 is a true SUMO E3 ligase

(a) Schematic overview of the Zimp7 protein, showing the SUMO interacting motifs (SIMs), the SP-RING-like domain important for SUMO E3 ligase activity and the transactivation domain (TAD) important for transcription. GST- and GFP-tagged Zimp7 constructs were created as shown, containing either the wildtype SP-RING domain (WT) or harboring mutation C616A (CD). (b) Alignment of Zimp7's SP-RING-type domain to that of PIAS1-4. The asterisk indicates residue C616 in Zimp7. (c) Zimp7 is capable of auto-SUMOylation using SUMO-1. Recombinantly produced GST-Zimp7 WT or CD, shown in a, was added to an in vitro reaction containing SUMO-1, the E1 enzyme and different amounts of the SUMO E2. After 3 hours, Zimp7 modifications were examined by Western blotting. The asterisk indicates non-modified GST-Zimp7. (d) Zimp7 is capable of auto-SUMOylation using SUMO-2/3. As in c, but using SUMO-2/3. (e) Zimp7 is SUMOylated in vivo. GFP-Zimp7 WT and CD were pulled down from HAP1 Zimp7 KO cells under denaturing conditions and examined for SUMOylation on a Western blot. The asterisk indicates the size of non-modified GFP-Zimp7. (f) Zimp7 interacts with PIAS3. GFP-Zimp7 WT was pulled down from HAP1 Zimp7 KO cells. Among the coprecipitated proteins were PCNA and PIAS3.

Our screen revealed Zimp7 as a promising factor that may regulate TC-NER. However, whereas the increased UV sensitivity of VH10-hTert cells upon siRNA-mediated depletion of Zimp7 confirmed a role for this protein in TC-NER, these observations could not be verified by knockout of Zimp7 in U2OS or RPE-1 cells, or by Zimp7 depletion using shRNAs in U2OS cells. The discrepancy between results that were obtained in different experimental set-ups did not warrant further mechanistic studies and demonstrates the need for additional validation experiments to determine which approach is most suitable to study Zimp7's cellular functions. The use of siRNAs seems questionable, as the observed effects of siZimp7-1,-2 and -4 on XPA levels and UV sensitivity were most likely caused by off-target effects. Ectopic expression of siRNA-resistant Zimp7 would therefore most likely not restore XPA levels nor rescue the UV sensitivity upon siRNA-mediated Zimp7 depletion, yet comprises a straightforward method that is required to affirm our interpretation of the data.

To circumvent the use of siRNAs, we generated Zimp7 knockout cell lines by CRISPR/Cas9-mediated targeting of the *Zimp7* gene. Although this is a frequently used approach to study phenotypes in the complete absence of a protein of interest, our observations indicate that it is critical to validate the obtained cell lines prior to their further use. Zimp7 depletion has been described to negatively affect proliferation and thus already leads to growth defects in unperturbed conditions²⁹. In contrast, major effects of Zimp7 knockout on cell growth were not evident in our experiments. This raises the possibility that the clones that were used had adapted to Zimp7 depletion, which potentially has also affected the outcomes of our experiments. Proliferation of the individual clones should therefore be evaluated more precisely, for example by cell count measurements or FAQS analyses. Similarly, the effect of Zimp7 depletion on transcriptional regulation of Wnt signaling genes could aid in the characterization of individual knockout clones²⁹. Considering the off-target effects of siRNAs and possible adaptation of Zimp7 knockout cells, the preferred approach to study Zimp7's cellular roles could involve the use of shRNAs, although it is recommended to first assess their application for example by performing complementation experiments.

Regardless of the need for additional validation experiments to establish the optimal experimental set-up, we have made several novel findings related to Zimp7's biological functions. The challenging question is whether these are related to its role as a transcriptional regulator, to its newly identified function as a SUMO E3 ligase or should even be ascribed to other, yet to be determined, activities. The first of these possible functions could be further studied by for instance RNA-seq experiments with control and Zimp7-depleted cells to examine which genes are regulated by Zimp7. Importantly, these will also indicate to what extent phenotypes that are observed in subsequent experiments are to be explained by an indirect role of Zimp7, that is via regulating levels of certain proteins, including those involved in the DDR. Evidently, the suggested experiments should be accompanied by studying the effects of DNA damage induction on the expression (and potential modification) of Zimp7 itself.

The recruitment of Zimp7 to multiphoton laser-inflicted damage, on the other hand, illustrates a potential direct role for Zimp7 at sites of DNA damage. Notably, Zimp7 was found to interact with the BAF57 and BRG1 components of the highly conserved SWI/SNF-like chromatin remodeling complexes²⁸. By destabilizing histone-DNA interactions and

thereby repositioning nucleosomes, these complexes allow binding of transcription factors to the DNA and facilitate transcription of the respective genes³⁹. Importantly, SWI/SNF-like factors have also been found implicated in the DDR, for example by promoting the repair of double-strand DNA breaks and UV-induced DNA damage⁴⁰⁻⁴³. We therefore speculate that Zimp7 could contribute to the chromatin remodeling that is required to increase accessibility of the lesion during DNA damage repair.

The emerging question concerning Zimp7's possible direct and indirect roles in the DDR, is whether these depend on its ability to catalyze SUMO conjugation. Future endeavors to unravel Zimp7's cellular functions, could therefore include pulldowns of SUMOylated proteins in the absence and presence of Zimp7. Analysis of the precipitated proteins by mass spectrometry could reveal Zimp7-specific SUMOylation targets that potentially shed light on the processes that Zimp7 participates in. Similarly, Zimp7 itself can be precipitated to examine (directly) interacting proteins.

Evidently, the sliding clamp PCNA and other DNA replication factors would be interesting proteins to look for in the hereby obtained data. Strengthening the observation that Zimp7 colocalizes with PCNA and newly synthesized DNA at replication foci in S-phase, we detected a clear interaction between these proteins in unperturbed conditions²⁸. This suggests that Zimp7 might play a role in DNA replication and/or the replication stress response. Notably, SUMOylation of PCNA, which is triggered by its loading onto DNA during uncompromised DNA replication, appears to play an important role in influencing pathway choice upon replication stress. In yeast, binding of the anti-recombinogenic protein Srs2 to PCNA, which is increased by its SUMOylation, prevents the formation of RAD51 filaments that could otherwise cause unwanted homologous recombination between the newly formed sister chromatids^{20,21,44}. Although levels of SUMOylated PCNA are much lower in mammalian cells, the human helicase PARI likewise interacts with modified PCNA via its PIP and SIM motifs and seems to function analogously to Srs2^{45,46}. The interaction between Zimp7 and PCNA and the reported colocalization at replication foci in S-phase, make it worthwhile to study whether Zimp7 contributes to regulation of DNA replication (stress pathways) and, if so, whether this can be ascribed to Zimp7-mediated SUMOylation of PCNA or other replication (stress) factors²⁸. An iPOND study, examining the presence of Zimp7 on nascent DNA in unperturbed conditions as well as under conditions of replication stress, could greatly improve our understanding of the spatiotemporal coordination of Zimp7 and its interaction with PCNA. Regulation of the SUMOylated PCNA status by Zimp7 in a DNA damage-dependent manner could suggest an important contribution of Zimp7 to the replication stress response and argue for investigating its role in modulating the PARI-PCNA interaction. Overall, studying Zimp7's biological functions might be difficult in case of redundancy between Zimp7 and for instance the PIAS proteins or its homolog Zimp10, which shares important domains such as the TAD and the SP-RING type motif²⁷. Despite their high sequence similarity and comparable nuclear localization, there are indications that Zimp7 and Zimp10 play different cellular roles. They have been described to have different expression profiles and possibly regulate different subsets of nuclear hormone receptors and other transcription factors. Furthermore, Zimp7 is not capable of fully compensating for loss of Zimp10 function in Zimp10 knockout mice, resulting in embryonic lethality^{27,28}. However,

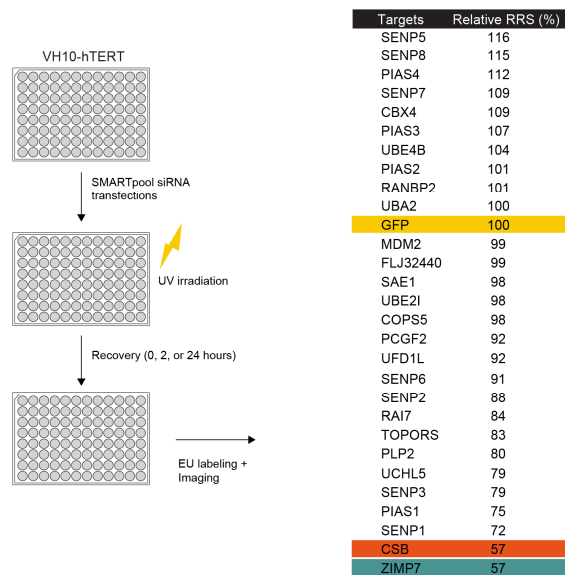
potentially overlapping or complementing functions in the DDR and/or DNA replication, for example by catalyzing SUMOylation of target proteins, have yet to be determined. In support of this, both Zimp7 and Zimp10 colocalize with SUMO-1 at replication foci in S-phase^{28,47}. Zimp10 would therefore be a promising factor to include in future studies.

Interestingly, Zimp10 interacts with the tumor suppressor and DDR protein p53, thereby altering its transcriptional activity⁴⁸. Although the relevance of p53-mediated transcription regulation by Zimp10 for the DDR remains to be established, it may explain how Zimp10 contributes to genome stability maintenance. Given their potential roles in the DDR and genome stability maintenance, Zimp7 and Zimp10 are both attractive proteins to study in the context of cancer development and ageing-related diseases.

Supplementary information

Supplementary figures

4



Supplementary Figure 1. Zimp7 is a promising hit in a screen for factors involved in RNA synthesis recovery upon UV irradiation

(a) An siRNA-based screen targeting 27 different proteins potentially involved in (de)SUMOylation identified Zimp7 as a factor that may be important for the recovery of RNA synthesis upon UV damage induction. VH10-hTert cells were transfected with siRNA, UV-C-irradiated at 10 J/m² and allowed to recover for 24 hours. RNA synthesis was determined by means of EU incorporation. Data represent the increase in RNA synthesis relative to non-irradiated cells between 2 and 24 hours after UV irradiation, normalized to that in siGFP-treated cells.

Methods

Cell culture

Cells were cultured in DMEM (Invitrogen) supplemented with 10% fetal bovine serum (FBS; Bodinco BV) and penicillin/streptomycin (Sigma). The following cell lines were used: VH10-hTert, U2OS, RPE-1 and HAP1.

Generation of stable cell lines

Stable expression of GFP-Zimp7 in U2OS cells was established by cloning Zimp7 cDNA into the multiple cloning site of pEGFP-C1, which is followed by an IRES and puromycin resistance gene that had previously been added to the plasmid. This construct was transfected using Lipofectamine® 2000 (Invitrogen) in Opti-MEM™ (Gibco) containing 10% FBS. Stable integrands were obtained by selection on puromycin (ThermoFisher Scientific). HAP1 Zimp7 KO cells were obtained from Horizon. For stable expression of GFP-tagged Zimp7, wildtype GFP-Zimp7 or that containing a C616A mutation (created by overlap PCR) was transferred from pEGFP-C1 into pLX304 (Addgene). Lentivirus was produced using the pCMV-VSV-G, pMDLg-RRE and pRSV-REV plasmids

(Addgene) and used to infect cells with Polybrene® (Sigma). Stable integrands were obtained after selection in medium containing blasticidin (ThermoFisher Scientific).

U2OS and RPE-1 Zimp7 KO cells were generated by CRISPR/Cas9-mediated targeting of the Zimp7 gene. Cells were transfected with pX458 (Addgene) into which the following guideRNA was cloned: GCTGAAGCGCGCGCAACAA. 48 hours after transfection, GFP-expressing cells were obtained by sorting using a BD FACSaria III Sorter (BD Biosciences) and seeded at low density. Single clones were examined for Zimp7 protein levels by Western blotting. Mutations in the Zimp7 gene were determined by Sanger sequencing of a PCR-amplified fragment of genomic DNA and analyzed by TIDE (NKI). The clones in this study all acquired premature stop codons, producing only 20% or less of the full-length Zimp7 protein.

Recovery of RNA synthesis screen

Transfections with SMARTpool siRNAs (Dharmacon) were performed in 96-well plates using Lipofectamine® RNAiMAX in Opti-MEMTM (Gibco) containing 10% FBS. siRNAs against the following targets were used: CBX4, COPS5, CSB, FLJ32440, GFP, MDM2, PCGF2, PIAS1, PIAS2, PIAS3, PIAS4, PLP2, RAI17, RANBP2, SAE1, SENP1, SENP2, SENP3, SENP5, SENP6, SENP7, SENP8, TOPORS, UBA1, UBE2I, UBE4B, UCHL5, UFD1L, ZIMP7. Cells were irradiated with UV-C (10 J/m²), and incubated for 0, 2 or 24 hours to allow RNA synthesis recovery. RNA was labeled for 1 hour in medium supplemented with 1 mM EU (Click-iT® RNA Alexa Fluor® 488 Imaging Kit, Life Technologies) according to the manufacturer's instructions. Nuclei were stained by DAPI (Sigma). Imaging was performed on a BD PathwayTM 855 Bioimager, using BD AttoVisionTM (BD Biosciences). RNA synthesis recovery was determined by measuring the mean Alexa 488 intensity of all nuclei per well and analyzed using Cell Profiler software.

RNA interference

For siRNA-mediated depletion of proteins using single siRNAs, two sequential transfections with 40 nM siRNA (Dharmacon) were performed using Lipofectamine® RNAiMAX (Invitrogen) in Opti-MEMTM (Gibco) containing 10% FBS. The following siRNAs were used:

5'-CGUACGCGGAUACUUGCA-3' (Luciferase);

5'-UCACCAAGAUAAAGCGGAUUU-3' (Zimp7-1);

5'-GCUUUGACCUGGAGUCGUUUU-3' (Zimp7-2);

5'-UCUACAAGACCCUGAUUUUUU-3' (Zimp7-3);

5'-ACUCUGACUAUGAGGAGAUUUU-3' (Zimp7-4).

To deplete Zimp7 by means of shRNA, lentivirus was produced from pLKO.1 plasmids that contained the shRNA of interest and the pMD2.G, pMDLg-RRE and pRSV-REV plasmids (Addgene). Cells were infected cells using Polybrene® (Sigma). The following shRNAs were used:

5'-ACCGGACACTCGAGCACTTTTGAATTC-3' (Control);

5'-CCGGCGGTGATGGTTCATTCGCATACTCGAGTATGCGAATGAACCATCACCGTTTTTG-3' (Zimp7-1);

5'-CCGGGACCTCCCTACGAACAACAATCTCGAATTGTTGTTCTAGGGAGGTCTTTTTG-3' (Zimp7-2).

Whole cell extract preparation

For detection of overall protein levels, whole cell extracts were prepared by lysis in 5 µl lysis buffer (30 mM Tris pH 7.5, 150 mM NaCl, 2 mM MgCl₂, 0.5 % Triton X-100, 500 U/mL Benzonase® nuclease, protease inhibitor cocktail (Roche)) per 100.000 cells during 10 min at room temperature. Equal volumes of Laemmli-SDS sample buffer were added and the samples were heated at 95 °C for 10 minutes prior to Western blot analysis.

GFP pulldowns

For isolation of protein complexes, cells were lysed in IP buffer (30 mM Tris pH 7.5, 150 mM NaCl, 2 mM MgCl₂, 0.5 % Triton X-100, 2.5 mM EGTA, 5 mM NaF, 5 mM β-glycerol phosphate, 5 mM NaPy, 10 mM NEM, 70 mM chloroacetamide, protease inhibitor cocktail (Roche)) supplemented with 250 U/mL benzonase® nuclease during 1-1.5 hours. Samples were centrifuged at 13.000 rpm.

For pulldown of proteins under denaturing conditions, cells were lysed in 200 µl denaturing IP buffer (20 mM Tris pH 7.5, 50 mM NaCl, 0.5% NP-40, 1% sodium deoxycholate (DOC), 1% SDS, 5 mM MgCl₂, 1 mM PMSF, protease inhibitor cocktail (Roche)) supplemented with 500 U/mL benzonase® nuclease during 30 minutes, with

forced resuspension of the pellet by pipetting every 10 min. 800 μ l wash buffer (20 mM Tris pH 7.5, 50 mM NaCl, 0.5% NP-40, 0.5% DOC, 1 mM EDTA, 1 mM PMSF, protease inhibitor cocktail (Roche)) was added before centrifugation of the samples at 13,000 rpm.

GFP-tagged proteins were precipitated from the supernatant using GFP-Trap®_A beads (Chromotek) and eluted by boiling of the beads in Laemmli-SDS sample buffer.

Western blotting

Proteins were separated in 4-12% Bis-Tris NuPAGE® gels (Invitrogen) or 4-12% Bis-Tris Criterion™ gels (BIO-RAD) in MOPS buffer (Life Technologies). Separated proteins were blotted onto PVDF membranes (Millipore), which were incubated with the following primary antibodies: mouse α -RNAPII α (Abcam, ab5408); rabbit α -RNAPII α (Abcam, ab5095); mouse α -RNAPII α /a (Santa Cruz Biotechnology, sc-17798); rabbit α -CSB (Santa Cruz Biotechnology, sc-25370); goat α -DDB1 (Abcam, ab9194); mouse α -Tubulin (Sigma, T6199); mouse α -GFP (Roche, #11814460001); rabbit α -GFP (Abcam, ab290); rabbit α -p89 (Santa Cruz Biotechnology, sc-19); mouse α -RPA70 (Calbiochem, NA13); mouse α -XPA (Invitrogen, MA5-13835); rabbit α -PCNA (Abcam, ab15497); rabbit α -H3 (Abcam, ab1791); rabbit α -PIAS3 (Cell Signaling, #9042); mouse α -SUMO-2/3 (Abcam, ab81371). Rabbit α -Zimp7 antibodies were kindly provided by Z.J. Sun. Protein bands were visualized using the Odyssey® Imaging System (LI-COR) after incubation with CFTM dye labelled secondary antibodies (Sigma) and analyzed using the Odyssey® Imaging System software (LI-COR).

UV-C irradiation

UV damage was induced using a 254-nm TUV PL-S 9W lamp (Philips).

Multiphoton laser micro-irradiation

Cells were grown on 18 mm coverslips, the medium was replaced by CO₂- independent Leibovitz's L15 medium supplemented with 10% FBS (Bodinco BV) and penicillin/streptomycin (Sigma), and coverslips were placed in a Chamlide CMB magnetic chamber in an environmental chamber set to 37 °C coupled to a Leica SP5 confocal microscope. UV-type laser damage was generated using a titanium-sapphire laser (λ = 800 nm, pulse length = 200 fs, repetition rate = 76 MHz). 1-15 minutes after damage induction, coverslips were incubated in CSK buffer (300 mM sucrose, 100 mM NaCl, 3 mM MgCl₂) containing 0.25% Triton X-100 (Sigma) during 2 minutes on ice and fixed in 2% formaldehyde during 20 minutes. Upon fixation, coverslips were incubated in 5% NP-40 (Sigma) during 5 minutes, washed with PBS, blocked in PBS containing 5 g/L BSA and 1.5 g/L glycine during 30 minutes and incubated overnight with mouse α -DDB2 (MyBioSource, MBS120183) primary antibody. Subsequently, coverslips were incubated goat α -mouse Alexa Fluor® 555 (Thermo Scientific) secondary antibody for visualization of DDB2 and DAPI (Sigma) for nuclear staining. Images were acquired on a Zeiss AxioImager D2 widefield fluorescence microscope equipped with 40x, 63x and 100x PLAN APO (1.4 NA) oil-immersion objectives (Zeiss) and an HXP 120 metal-halide lamp used for excitation. Images were recorded using ZEN 2012 software.

Treatment with hydroxyurea

Cells were seeded at low density. The next day, different concentrations of hydroxyurea (Sigma) were added and cells were incubated in HU-containing medium for 24 hours. Subsequently, plates were washed twice with PBS and fresh medium without HU was added. Clonogenic survival was determined after 8 days.

Proliferation assay upon treatment with MMS

Different concentrations of methyl methanesulfonate (MMS, Sigma) were added to attached cells in 6-well plates. 24 hours after addition of MMS, plates were washed twice with PBS and fresh medium without MMS was added. After 72 hours, cells were trypsinized and counted using a Coulter Counter (Beckman Coulter) to determine proliferation.

IR irradiation

Ionizing radiation (IR) damage was inflicted by a YXlon X-ray generator (YXlon International) at 200 kV, 12 mA and a dose rate of 4 Gy/min.

Clonogenic survivals

Cells were seeded at low density and UV or IR irradiated at different doses or treated with different concentrations of hydroxyurea. After 8-14 days of incubation, cells were washed with 0.9% NaCl and stained with methylene blue. Colonies of >20 cells were scored.

Production of recombinant proteins

DNA fragments encoding amino acids 419-920 of Zimp7 WT or CD were cloned into pGEX-6p-3. Upon transformation of Rosetta E.coli with these constructs, GST-Zimp7 WT or CD expression was induced by addition of 0.5 mM IPTG, 1 mM MgCl₂ and 0.05% glucose. After 5.5 hours cells were washed in cold PBS and lysates were prepared by resuspension in cold PBS containing 0.5 M NaCl, 1 mM PMSF and protease inhibitor cocktail (Roche) and sonification using a Misonix Sonicator 3000. Lysates were cleared by centrifugation and the soluble fraction was collected and incubated with GST-Sepharose beads (Amersham) during 2 hours at 4 °C. Beads were washed twice with cold PBS containing 0.5 mM NaCl, 1mM PMSF and protease inhibitors (without EDTA), followed by three washes with a washing buffer containing 50 mM Tris-HCl (pH 7.5) and 0.5 mM NaCl. Proteins were eluted once with 20 mM glutathione in washing buffer.

Purified SAE1 and UBC9 were obtained as previously described⁴⁹.

In vitro SUMOylation

In vitro SUMOylation reactions contained 0.3 µg SUMO E1 (except control samples), 0.05-0.2 µg SUMO E2 and 0.3 µg purified fragments of human ZIMP7 protein (see above). Each reaction contained 50 mM Tris-HCl (pH 7.5), 5 mM MgCl₂, 3.5 U/ml creatine kinase, 10 mM creatine phosphatase, 0.6 U/µl inorganic phosphatase and 0.5 µg either SUMO1 or SUMO2/3. Reactions were carried out for 3 hours at 37 °C before quenching with ¼ volume of 4x NuPAGE loading dye and flash-freezing in liquid nitrogen. SUMOylated proteins were detected by Western blotting.

References

1. Jackson, S.P. & Bartek, J. The DNA-damage response in human biology and disease. *Nature* 461, 1071-8 (2009).
2. Hoeijmakers, J.H. DNA damage, aging, and cancer. *N Engl J Med* 361, 1475-85 (2009).
3. Jackson, S.P. & Durocher, D. Regulation of DNA damage responses by ubiquitin and SUMO. *Mol Cell* 49, 795-807 (2013).
4. Bergink, S. & Jentsch, S. Principles of ubiquitin and SUMO modifications in DNA repair. *Nature* 458, 461-7 (2009).
5. Morris, J.R. SUMO in the mammalian response to DNA damage. *Biochem Soc Trans* 38, 92-7 (2010).
6. Hay, R.T. SUMO: a history of modification. *Mol Cell* 18, 1-12 (2005).
7. Rytinki, M.M., Kaikkonen, S., Pehkonen, P., Jaaskelainen, T. & Palvimo, J.J. PIAS proteins: pleiotropic interactors associated with SUMO. *Cell Mol Life Sci* 66, 3029-41 (2009).
8. Palvimo, J.J. PIAS proteins as regulators of small ubiquitin-related modifier (SUMO) modifications and transcription. *Biochem Soc Trans* 35, 1405-8 (2007).
9. Schmidt, D. & Muller, S. PIAS/SUMO: new partners in transcriptional regulation. *Cell Mol Life Sci* 60, 2561-74 (2003).
10. Sharrocks, A.D. PIAS proteins and transcriptional regulation--more than just SUMO E3 ligases? *Genes Dev* 20, 754-8 (2006).
11. Dugrawala, H. et al. The Replication Checkpoint Prevents Two Types of Fork Collapse without Regulating Replisome Stability. *Mol Cell* 59, 998-1010 (2015).
12. Galanty, Y. et al. Mammalian SUMO E3-ligases PIAS1 and PIAS4 promote responses to DNA double-strand breaks. *Nature* 462, 935-9 (2009).
13. Morris, J.R. et al. The SUMO modification pathway is involved in the BRCA1 response to genotoxic stress. *Nature* 462, 886-90 (2009).

14. Hu, X., Paul, A. & Wang, B. Rap80 protein recruitment to DNA double-strand breaks requires binding to both small ubiquitin-like modifier (SUMO) and ubiquitin conjugates. *J Biol Chem* 287, 25510-9 (2012).
15. Galanty, Y., Belotserkovskaya, R., Coates, J. & Jackson, S.P. RNF4, a SUMO-targeted ubiquitin E3 ligase, promotes DNA double-strand break repair. *Genes Dev* 26, 1179-95 (2012).
16. Bekker-Jensen, S. & Mailand, N. The ubiquitin- and SUMO-dependent signaling response to DNA double-strand breaks. *FEBS Lett* 585, 2914-9 (2011).
17. Liu, S. et al. PIAS3 promotes homology-directed repair and distal non-homologous end joining. *Oncol Lett* 6, 1045-1048 (2013).
18. Hardeland, U., Steinacher, R., Jiricny, J. & Schar, P. Modification of the human thymine-DNA glycosylase by ubiquitin-like proteins facilitates enzymatic turnover. *EMBO J* 21, 1456-64 (2002).
19. Steinacher, R. & Schar, P. Functionality of human thymine DNA glycosylase requires SUMO-regulated changes in protein conformation. *Curr Biol* 15, 616-23 (2005).
20. Papouli, E. et al. Crosstalk between SUMO and ubiquitin on PCNA is mediated by recruitment of the helicase Srs2p. *Mol Cell* 19, 123-33 (2005).
21. Pfander, B., Moldovan, G.L., Sacher, M., Hoege, C. & Jentsch, S. SUMO-modified PCNA recruits Srs2 to prevent recombination during S phase. *Nature* 436, 428-33 (2005).
22. Marteijn, J.A., Lans, H., Vermeulen, W. & Hoeijmakers, J.H. Understanding nucleotide excision repair and its roles in cancer and ageing. *Nat Rev Mol Cell Biol* 15, 465-81 (2014).
23. Spivak, G. Nucleotide excision repair in humans. *DNA Repair (Amst)* 36, 13-8 (2015).
24. Sin, Y., Tanaka, K. & Saijo, M. The C-terminal Region and SUMOylation of Cockayne Syndrome Group B Protein Play Critical Roles in Transcription-coupled Nucleotide Excision Repair. *J Biol Chem* 291, 1387-97 (2016).
25. Poulsen, S.L. et al. RNF111/Arkadia is a SUMO-targeted ubiquitin ligase that facilitates the DNA damage response. *J Cell Biol* 201, 797-807 (2013).
26. van Cuijk, L. et al. SUMO and ubiquitin-dependent XPC exchange drives nucleotide excision repair. *Nat Commun* 6, 7499 (2015).
27. Beliakoff, J. & Sun, Z. Zimp7 and Zimp10, two novel PIAS-like proteins, function as androgen receptor coregulators. *Nucl Recept Signal* 4, e017 (2006).
28. Huang, C.Y. et al. hZimp7, a novel PIAS-like protein, enhances androgen receptor-mediated transcription and interacts with SWI/SNF-like BAF complexes. *Mol Endocrinol* 19, 2915-29 (2005).
29. Lee, S.H. et al. Identification of a novel role of ZMIZ2 protein in regulating the activity of the Wnt/beta-catenin signaling pathway. *J Biol Chem* 288, 35913-24 (2013).
30. Haahr, P. et al. Activation of the ATR kinase by the RPA-binding protein ETAA1. *Nat Cell Biol* 18, 1196-1207 (2016).
31. Wilson, J.S. et al. Localization-dependent and -independent roles of SLX4 in regulating telomeres. *Cell Rep* 4, 853-60 (2013).
32. Gonzalez-Prieto, R., Cuijpers, S.A., Luijsterburg, M.S., van Attikum, H. & Vertegaal, A.C. SUMOylation and PARylation cooperate to recruit and stabilize SLX4 at DNA damage sites. *EMBO Rep* 16, 512-9 (2015).
33. Mosbech, A. et al. DVC1 (C1orf124) is a DNA damage-targeting p97 adaptor that promotes ubiquitin-dependent responses to replication blocks. *Nat Struct Mol Biol* 19, 1084-92 (2012).
34. Schubert, L. et al. RADX interacts with single-stranded DNA to promote replication fork stability. *EMBO Rep* 18, 1991-2003 (2017).
35. Alvino, G.M. et al. Replication in hydroxyurea: it's a matter of time. *Mol Cell Biol* 27, 6396-406 (2007).
36. Conn, K.L. et al. Novel Role for Protein Inhibitor of Activated STAT 4 (PIAS4) in the Restriction of Herpes Simplex Virus 1 by the Cellular Intrinsic Antiviral Immune Response. *J Virol* 90, 4807-26 (2016).
37. Sachdev, S. et al. PIASy, a nuclear matrix-associated SUMO E3 ligase, represses LEF1 activity by sequestration into nuclear bodies. *Genes Dev* 15, 3088-103 (2001).
38. Peng, Y., Lee, J., Zhu, C. & Sun, Z. A novel role for protein inhibitor of activated STAT (PIAS) proteins in modulating the activity of Zimp7, a novel PIAS-like protein, in androgen receptor-mediated transcription. *J Biol Chem* 285, 11465-75 (2010).

39. Tang, L., Nogales, E. & Ciferri, C. Structure and function of SWI/SNF chromatin remodeling complexes and mechanistic implications for transcription. *Prog Biophys Mol Biol* 102, 122-8 (2010).
40. Park, J.H. et al. Mammalian SWI/SNF complexes facilitate DNA double-strand break repair by promoting gamma-H2AX induction. *EMBO J* 25, 3986-97 (2006).
41. Hara, R. & Sancar, A. The SWI/SNF chromatin-remodeling factor stimulates repair by human excision nuclease in the mononucleosome core particle. *Mol Cell Biol* 22, 6779-87 (2002).
42. Ogiwara, H. et al. Histone acetylation by CBP and p300 at double-strand break sites facilitates SWI/SNF chromatin remodeling and the recruitment of non-homologous end joining factors. *Oncogene* 30, 2135-46 (2011).
43. Watanabe, R. et al. SWI/SNF factors required for cellular resistance to DNA damage include ARID1A and ARID1B and show interdependent protein stability. *Cancer Res* 74, 2465-75 (2014).
44. Watts, F.Z. Sumoylation of PCNA: Wrestling with recombination at stalled replication forks. *DNA Repair (Amst)* 5, 399-403 (2006).
45. Garcia-Rodriguez, N., Wong, R.P. & Ulrich, H.D. Functions of Ubiquitin and SUMO in DNA Replication and Replication Stress. *Front Genet* 7, 87 (2016).
46. Moldovan, G.L. et al. Inhibition of homologous recombination by the PCNA-interacting protein PARI. *Mol Cell* 45, 75-86 (2012).
47. Sharma, M. et al. hZimp10 is an androgen receptor co-activator and forms a complex with SUMO-1 at replication foci. *EMBO J* 22, 6101-14 (2003).
48. Lee, J., Beliakoff, J. & Sun, Z. The novel PIAS-like protein hZimp10 is a transcriptional co-activator of the p53 tumor suppressor. *Nucleic Acids Res* 35, 4523-34 (2007).
49. Tatham, M.H. et al. Polymeric chains of SUMO-2 and SUMO-3 are conjugated to protein substrates by SAE1/SAE2 and Ubc9. *J Biol Chem* 276, 35368-74 (2001).

How dextran sulfate affects C1-inhibitor activity: a model for polysaccharide potentiation

Madelon Dijk, Jolande Holkers, Patrick Voskamp, Bruno M. Giannetti,
Willem-Jan Waterreus, Harrie A. van Veen and Navraj S. Pannu

Published as:

How dextran sulfate affects C1-inhibitor activity: a model for polysaccharide potentiation
Structure 24, 2182-2189 (2016)

Abstract

C1-inhibitor is a key inhibitor of the complement and contact activation systems, and mutations in the protein can cause hereditary angioedema. Through an unknown mechanism, polysaccharides can increase C1-inhibitor activity against some of its target proteases. Here we present the crystal structures of the serine protease inhibitor (serpin) domain of active C1-inhibitor by itself and in complex with dextran sulfate. Unlike previously described interactions of serpins with polysaccharides, the structures and isothermal titration calorimetry experiments together reveal that dextran sulfate binds to C1-inhibitor's F1 helix with low affinity and does not invoke an allosteric change. Furthermore, one dextran sulfate molecule can bind multiple C1-inhibitor molecules. We propose that in a C1-inhibitor-protease-polysaccharide ternary complex, negatively charged polysaccharides link C1-inhibitor's positively charged F1 helix to positively charged autolysis loops of proteases. The described mechanism elegantly explains previous experiments, showing that polysaccharide potentiation is increased against proteases with a greater positive charge in the autolysis loop.

Introduction

C1-inhibitor replacement therapy is an established treatment for hereditary angioedema – a disease characterized by recurrent episodes of swelling of the skin or mucosa as a result of an acute, localized increase in vascular permeability¹. Additionally, C1-inhibitor therapy has been studied in sepsis, ischemia-reperfusion injury, and autoimmune diseases such as neuromyelitis optica^{2,3,4}.

C1-inhibitor is a plasma glycoprotein that belongs to the superfamily of serine protease inhibitors (serpins)⁵. Serpins are suicide inhibitors and in the active form, the reactive center loop protrudes from the bulk of the protein and presents the P1-P1' residues as a substrate for proteolytic attack. Upon binding of the target protease, the reactive center loop inserts into the serpin's central β -sheet while the attached protease moves to the opposite pole of the serpin, causing the disruption of the protease's active site⁶. Comparably, insertion of the reactive center loop into the central β -sheet can cause the spontaneous transition from a metastable active form to a more stable latent conformation.

C1-inhibitor is the only known plasma protein inhibitor of classical complement pathway serine proteases C1s and C1r. Furthermore, it inactivates MASP-1 and MASP-2 proteases from the mannose-binding lectin pathway, plasmin and tissue plasminogen activator from the fibrinolytic system, factor XIIa and plasma kallikrein from the contact activation system, and the coagulation system proteases factor XIa and thrombin¹. Given its wide range of biological activities, a potent therapy optimization would involve the fine-tuning and enhancement of C1-inhibitor activity against a particular protease⁷.

As observed for other serpins, glycosaminoglycans (GAGs) and negatively charged polysaccharides such as dextran sulfate have been shown to affect C1-inhibitor activity. For example, significant potentiation of C1-inhibitor by heparin against C1s was demonstrated by various techniques⁸⁻¹⁰. It was also shown that oversulfated chondroitin sulfate – a heparin contaminant that has been linked to severe clinical adverse events – potentiates C1-inhibitor activity on the complement pathway¹¹. Interestingly in view of therapy refinement, C1-inhibitor potentiation by GAGs has appeared to be different toward the various target proteases⁸.

The atomic mechanism behind the effect of polyanions on C1-inhibitor remains to be elucidated. Heparin binds to antithrombin and heparin cofactor II at helix D and causes an allosteric change in these serpins^{12,13}. Unraveling the mechanism behind the enhancement of C1-inhibitor activity by polysaccharides may contribute to the development of molecules that improve C1-inhibitor's efficiency and specificity.

Here we present the crystal structures of the serpin domain of C1-inhibitor in its active form by itself and in complex with dextran sulfate. These structures and our isothermal titration calorimetry studies show that dextran sulfate binds to multiple C1-inhibitor molecules with low affinity at C1-inhibitor's F1 helix and does not invoke an allosteric change.

Results and discussion

To elucidate how polysaccharides interact with C1-inhibitor we purified the recombinant protein, lacking the first 96 residues of C1-inhibitor's heavily glycosylated N-terminus, from the milk of transgenic rabbits. The remaining serpin domain of C1-inhibitor has previously been shown to have full inhibitory activity¹⁴. Subsequently, C1-inhibitor was crystallized by itself, as well as co-crystallized with dextran sulfate. Crystals of recombinant human C1-inhibitor diffracted to 2.1 Å whereas crystals of the protein in complex with dextran sulfate diffracted to 2.9 Å (Table 1).

Table 1: Data collection and refinement statistics

	C1-inhibitor	C1-inhibitor with dextran sulfate
Data collection		
Space group	P 2 ₁ 2 ₁ 2 ₁	C2
Cell dimensions		
a, b, c (Å)	57.40, 75.48, 203.89	112.10, 197.42, 56.78
α, β, γ (°)	90.00, 90.00, 90.00	90.00, 103.31, 90.00
Resolution (Å)	2.1	2.9
Wilson plot B-factor	32.9	77.7
R _{pim}	0.057 (0.570)*	0.089 (1.987)*
CC(1/2)	0.998 (0.790)	0.996 (0.117)
<I/σI>	13.9 (1.6)	7.2 (0.4)
Completeness (%)	99.93	98.68
Multiplicity	4.7	3.0
Refinement		
No. of unique reflections	43663	24919
Molecules in ASU	2	2
R _{work} / R _{free}	0.197/0.257	0.239/0.281
RMSD		
Bond lengths (Å)	0.025	0.011
Bond angles (°)	2.19	1.57

* Numbers in brackets are values for the highest resolution shell. For the uncomplexed structure, the highest resolution shell is 2.10 to 2.16 Å. For the complex structure, the highest resolution shell is 2.90 to 3.08 Å.

Structure of active C1-inhibitor

We first solved the overall structure of uncomplexed C1-inhibitor (Fig. 1a). The full exposure of the relatively short reactive center loop (shown in red and pink) characterizes inhibitory serpins in their active form. Clear electron density is seen for the reactive center loop residues Arg444 to Val448 (shown in red). These residues stack with the same reactive center loop residues but in the opposite direction to the other C1-inhibitor molecule present in the asymmetric unit. Both C1-inhibitor molecules lack electron density for reactive center loop residues Ala443 to Ser441 (shown in pink). Residues Arg444 and Thr445 within the reactive

center loop are the substrate P1 and P1' residues that are responsible for trapping the target protease. In the latent and cleaved conformation of C1-inhibitor, the reactive center loop inserts between strand s3A and s5A of the central β -sheet, rendering the inhibitor inactive.

The model contains two disulfide bridges at Cys101-Cys406 and Cys108-Cys183 that stabilize the structure.

Lys307, previously predicted to be involved in GAG binding, specifically stabilizes the reactive center loop in its active conformation by hydrogen bonding to the carboxyl group of Ala436¹⁵. Notably, an A436T mutation causes type II hereditary angioedema and results in a non-cleavable reactive center loop¹⁶. Our structure shows that the threonine residue likely increases the interaction with Lys307 or Lys306 to prevent cleavage, leading to insertion of the exposed reactive center loop into strand A of another C1-inhibitor molecule. Importantly, these results also explain why heparin interacts more strongly with the latent form of C1-inhibitor, as in its active conformation the reactive center loop hinders exposure of the positive charge of Lys306 and Lys307¹⁵.

Comparing the latent and active C1-inhibitor structures not only shows the expected shifts in β -sheet A required for loop insertion, but also displays a conformational change in strand s3C and s4C, a region that is expected to shift during latent transition as well¹⁷. The strands follow the C-terminal end of the reactive center loop as it is inserted into the β -sheet A and are shifted down and outward in the latent C1-inhibitor molecule.

Structure of active C1-inhibitor bound to dextran sulfate

We next analyzed the crystal structure of C1-inhibitor co-crystallized with dextran sulfate. The crystallographic asymmetric unit again contains two C1-inhibitor molecules with their reactive center loops fully exposed and in close proximity to each other (displayed as a ribbon and electrostatic representation in two different orientations in Fig. 1b; a single C1-inhibitor molecule is shown in Fig. 1c). The negatively charged dextran sulfate neutralizes the positive charge around the F1 helix of the C1-inhibitor molecules. Supporting our model, mutating the F1 helix residue Lys284 has been shown to affect the binding of C1-inhibitor to glycosaminoglycans¹⁸. Arg287 is another nearby residue that was predicted to be important for glycosaminoglycan binding, but its positive charge is stabilized by hydrogen bonding to the amino group of Lys284 of the other C1-inhibitor molecule¹⁸.

The overall structures of C1-inhibitor by itself and in complex with dextran sulfate are very similar: the root mean square deviation is 0.486 Å for C- α positions of all residues apart from Ala437-Phe449 of the reactive center loop. Thus, in contrast to what has been described for other serpins, binding of dextran sulfate does not invoke an allosteric change. The similarity of the structures is consistent with the results obtained by circular dichroism showing no allosteric change upon polysaccharide binding¹⁰. A saccharide electrostatically interacts with Lys284 of one C1-inhibitor molecule and Lys299 of the other C1-inhibitor molecule at the edge of the protein (Fig. 1d, showing the $2F_o - F_c$ electron density for the modelled dextran sulfate saccharides). This novel interaction is the first time a charge neutralization mechanism with low affinity binding has been observed for a serpin and a polysaccharide.

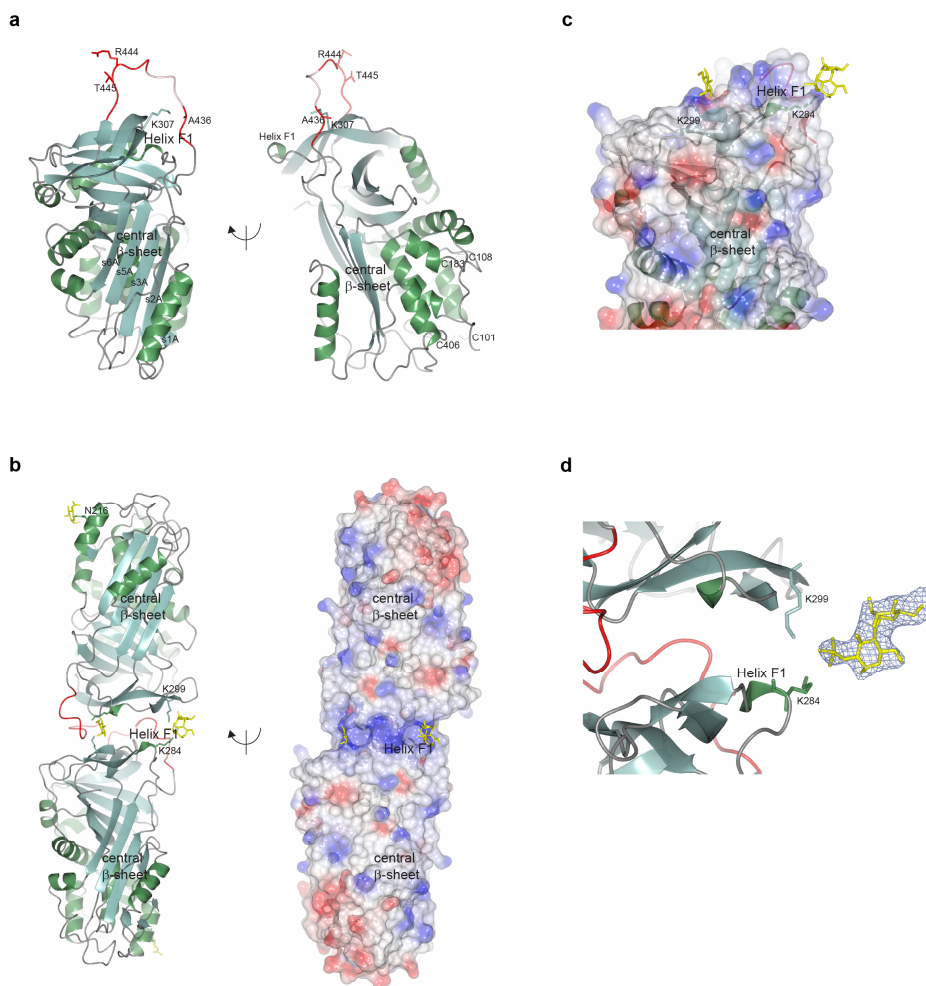


Figure 1. Structure of active C1-inhibitor by itself and bound to dextran sulfate

(a) The overall structure of active C1-inhibitor in two different orientations. The fully exposed reactive center loop is shown in red where the loop has clear electron density and light pink where the loop is disordered. The P1 Arg444 residue and P1' Thr445 residue are displayed, along with residue Lys307 that stabilizes the reactive center loop by hydrogen bonding to the carboxyl oxygen of Ala436. Helix F1 is the polyanion binding site. The central β -sheet A and the disulfide bridges at Cys101-Cys406 and Cys108-Cys183 are also labeled. (b) The overall structure of active C1-inhibitor bound to dextran sulfate in two different orientations, showing a ribbon diagram and an electrostatic surface of C1-inhibitor with positively charged regions in blue and negatively charged regions in red. C1-inhibitor is positively charged at the dextran sulfate (in yellow) binding site. Three dextran sulfate saccharides were built in the crystal structure and link Lys284 from helix F1 of one C1-inhibitor molecule to Lys299 on the other C1-inhibitor molecule. The glycosylation at Asn216 was also modeled in the complex crystal structure. (c) Electrostatic surface of the top of one C1-inhibitor molecule with dextran sulfate (in yellow). The reactive center loop is shown in red. The side chains for Lys284 and Lys299 (the residues interacting with the saccharide molecules) are also shown. (d) 2Fo-Fc electron density map (blue mesh) of a disaccharide of dextran sulfate contoured at 1.1σ . All figures were produced by ccp4mg²³.

The modelled polysaccharide molecules are in a large channel between symmetry-related C1-inhibitor molecules: the channel has sufficient space for a dextran sulfate molecule of 5 kDa. However, only 3 saccharide molecules could be modelled while the density of the other polysaccharides is too weak for modelling, probably due to the random linkage and sulfation pattern of dextran sulfate. The monosaccharide molecules interacting with Lys284 to Lys299 from the same C1-inhibitor molecule are about 20 Å apart.

Importantly, although negatively charged polysaccharides can enhance C1-inhibitor activity against proteases, its inhibiting activity could be impeded if the polysaccharide would induce C1-inhibitor multimerization over protease binding.

Stoichiometry and binding affinity of dextran sulfate binding to C1-inhibitor

To assess the binding of dextran sulfate to C1-inhibitor, we performed isothermal titration calorimetry (ITC) experiments, for which 5, 10 or 20 kDa dextran sulfate was added to full-length C1-inhibitor (Fig. 2a-c). Supporting our crystal structure, the ITC results show 1 low-affinity binding site on C1-inhibitor for the polysaccharide independent of its size. Multiple C1-inhibitor molecules can bind to 1 molecule of dextran sulfate: the stoichiometry of the C1-inhibitor-dextran sulfate complex is 1:1 for 5 kDa, 2:1 for 10 kDa and 3:1 for 20 kDa dextran sulfate. Based on the model curves from the ITC data, representing the best fit obtained for the data (Fig. 2a-c), we calculated the stoichiometries and binding constants for complex formation in this experimental set-up (Table 2). The low-affinity electrostatic binding is in agreement with previously determined values by several groups^{9,10,19}.

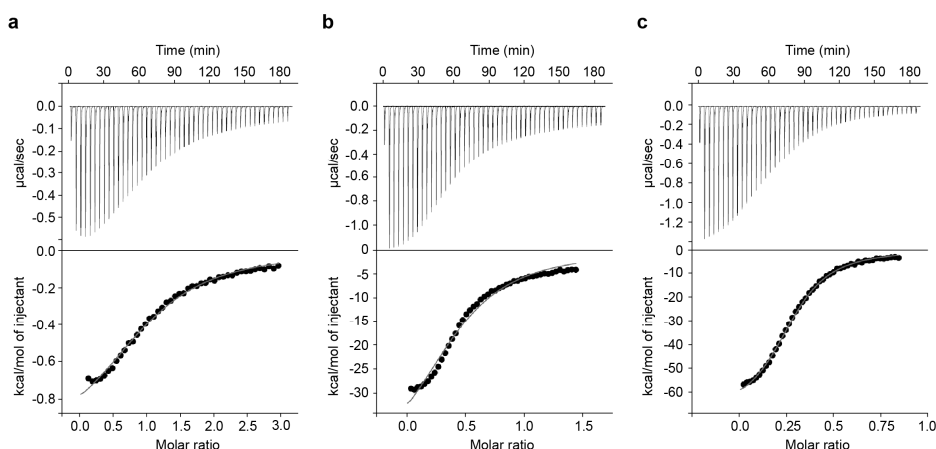


Figure 2. Stoichiometry and binding affinity of dextran sulfate binding to C1-inhibitor

Isothermal titration calorimetry experiments showing the titration of dextran sulfate of different sizes to C1-inhibitor in the sample cell. (a) Titration of 5 kDa dextran sulfate. (b) Titration of 10 kDa dextran sulfate. (c) Titration of 20 kDa dextran sulfate.

Table 2: Binding constants and stoichiometry for the binding of C1-inhibitor to dextran sulfate

Dextran sulfate (kDa)	Binding constant ($\times 10^5 \text{ M}^{-1}$)	Stoichiometry
5	1.16 ± 0.12	1.16 ± 0.03
10	1.80 ± 0.21	0.479 ± 0.021
20	8.34 ± 0.28	0.294 ± 0.002

C1s-C1-inhibitor and kallikrein-C1-inhibitor Michaelis complex models

GAG binding to C1-inhibitor can greatly enhance its activity against C1s, while the effect on kallikrein inactivation is minimal. We created models of the Michaelis complex of C1s-C1-inhibitor by superimposing the protease and C1-inhibitor on several previously solved Michaelis serpin-protease complexes, available in the Protein Data Bank (PDB) as 1k9o²⁰, 1jmo¹³, 1oph²¹, and 4dy7²². Despite the different relative orientation between the serpin and the protease in the different Michaelis complexes published, all of the resulting complexes show C1-inhibitor's helix F1 residues Lys284 and/or Arg287 neighboring autolysis loop residues Lys560 and Arg561. The Michaelis complexes based on PDB entries 1k9o, 1oph, and 4dy7 show C1-inhibitor residue Lys284 in close proximity to C1s residue Lys560 and C1-inhibitor residue Arg287 near C1s residue Arg561 (Fig. 3a, created with 1k9o). Docking the C1-inhibitor and C1s structures using PDB entry 1jmo shows C1-inhibitor residues Arg287 and Lys299 in the close vicinity of C1s residues Lys560 and Arg561, respectively (Fig. 3b). The crystal structure of C1-inhibitor-dextran sulfate revealed that residue Lys299 interacts with saccharide molecules. Notably, both models indicate that a negatively charged polysaccharide molecule would neutralize the repulsive forces between indicated basic side chains, thereby enhancing C1-inhibitor activity. Interestingly, a model for the Michaelis complex of kallikrein and C1-inhibitor based on the Michaelis complex from PDB entry 1k9o (Fig. 3c), shows again that residues Lys284 and Arg287 of C1-inhibitor are in close proximity to the autolysis loop residues Lys147 and Glu150. However, in contrast to C1s, an attractive electrostatic force already exists between C1-inhibitor residue Arg287 and residue Glu150 of kallikrein, so a polyanion would not further promote activity by neutralizing charges. Unlike in the case of C1s described above, all created kallikrein-C1-inhibitor models display a similar interaction between the indicated residues of C1-inhibitor and kallikrein.

Taking together the structures of C1-inhibitor, the proteases C1s and kallikrein, and the Michaelis serpin-protease complexes, negatively charged polysaccharides likely increase the activity of C1-inhibitor by neutralizing at least the positive charges of C1-inhibitor residues in or near the F1 helix, namely Lys284 and Arg287, and possibly C1-inhibitor residue Lys299 and positive residues of the autolysis loop of target proteases. In this mechanism, the saccharide is not in between the protease and inhibitor and thus does not form a 'sandwich' as previously predicted, but instead binds on the outer edge of both the protease and the inhibitor¹⁵. The positive patches near Lys306 are sterically hindered by the relatively short reactive center loop from forming charge neutralization interactions. Our model provides important insight into how C1-inhibitor activity toward its different targets is sensitive to

potentiation by GAG binding to different extents, depending on the nature of the protease's autolysis loop.

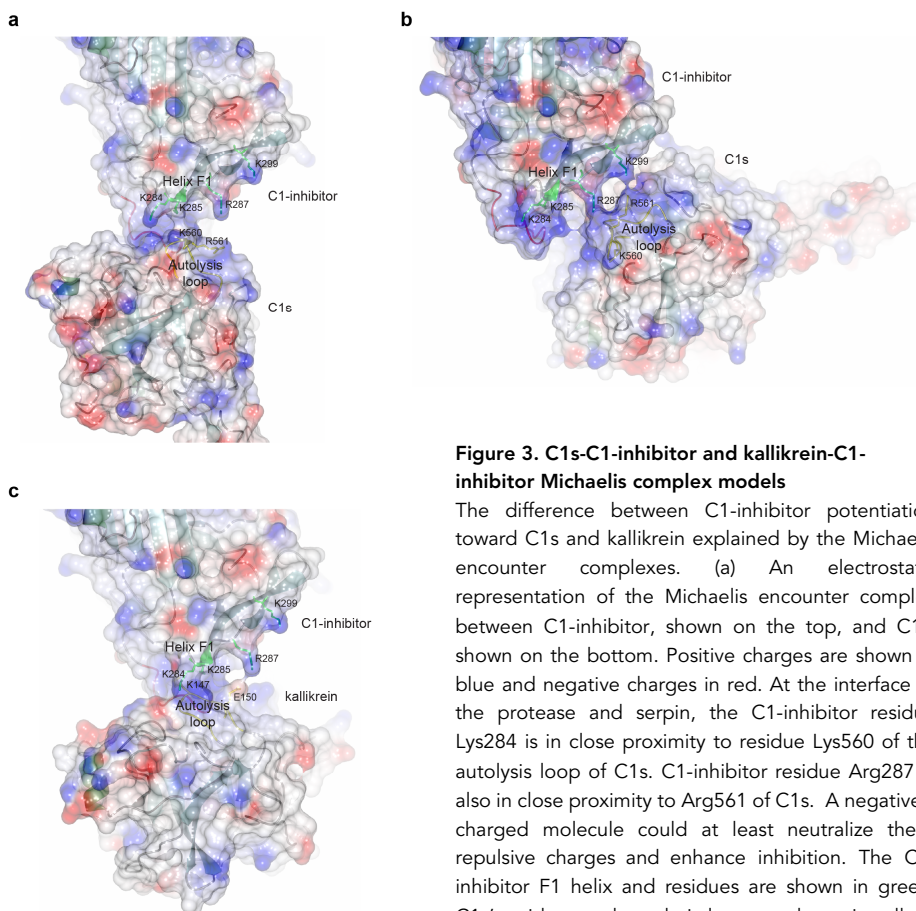


Figure 3. C1s-C1-inhibitor and kallikrein-C1-inhibitor Michaelis complex models

The difference between C1-inhibitor potentiation toward C1s and kallikrein explained by the Michaelis encounter complexes. (a) An electrostatic representation of the Michaelis encounter complex between C1-inhibitor, shown on the top, and C1s, shown on the bottom. Positive charges are shown in blue and negative charges in red. At the interface of the protease and serpin, the C1-inhibitor residue Lys284 is in close proximity to residue Lys560 of the autolysis loop of C1s. C1-inhibitor residue Arg287 is also in close proximity to Arg561 of C1s. A negatively charged molecule could at least neutralize these repulsive charges and enhance inhibition. The C1-inhibitor F1 helix and residues are shown in green, C1s' residues and autolysis loop are shown in yellow. This model is based on the serpin-protease complex

from PDB entry 1k9o. (b) An electrostatic representation of the Michaelis encounter complex between C1-inhibitor, shown on the top, and C1s, shown on the bottom. Positive charges are shown in blue and negative charges in red. At the interface of the protease and serpin, the C1-inhibitor residue Arg287 is in close proximity to residue Lys560 of the autolysis loop of C1s. C1-inhibitor residue Lys299 is also in close proximity to Arg561 of C1s. A negatively charged molecule could at least neutralize these repulsive charges and enhance inhibition. The C1-inhibitor residues are shown in green, while C1s' residues and autolysis loop are shown in yellow. This model is based on the serpin-protease complex from PDB entry 1jmo. (c) An electrostatic representation of the Michaelis encounter complex between C1-inhibitor, shown on the top, and kallikrein, shown on the bottom. Positive charges are shown in blue and negative charges in red. At the interface of the protease and serpin, the C1-inhibitor residue Lys284 is in close proximity to residue Lys147 of the autolysis loop of kallikrein, but C1-inhibitor residue Arg287 forms an electrostatic interaction with Glu150 of kallikrein. The C1-inhibitor residues are shown in green, while kallikrein's residues and autolysis loop are shown in yellow. This model is based on the serpin-protease complex from PDB entry 1k9o. All figures were produced by ccp4mg²³.

Supplementary information

Methods

Protein expression, purification and crystallization

Production of recombinant human C1-inhibitor secreted in the milk of transgenic rabbits was performed as previously described¹⁴. Functionally active C1-inhibitor lacking the first 96 residues, present in negligible amounts in purified C1-inhibitor¹⁴, were separated from intact molecules by a sequence of cation exchange chromatography on SP Sepharose High Performance (GE Healthcare) and affinity chromatography on Jacalin Agarose (Vector Labs). Fractions obtained from the Jacalin Agarose column containing C1-inhibitor lacking the first 96 residues were concentrated to about 10 mg/ml in 20 mM sodium citrate pH 7.0 + 0.15 M NaCl and stored at -70 °C until use. Diffraction quality crystals of active C1-inhibitor were obtained after about 7 days in 20% PEG3350 w/v and 200 mM KF with a crystallization drop size of 1 µl and a protein content of 70% w/v using the sitting-drop vapour diffusion method. These conditions were optimized from initial hits found in both JCSG+ and PACT (Qiagen) screens. For co-crystallization, 11 mg/ml of C1-inhibitor was mixed with 5 kDa dextran sulfate (Sigma-Aldrich) in a 1:2 molar ratio and incubated on ice for an hour. Again, crystallization trials were set up with JCSG+ and PACT screens and initial hits were optimized to obtain the final conditions of 0.1 M SPG (pH 9), 25% w/v PEG 1500 0.1 M MgCl hexahydrate, with crystals appearing after 10 days.

Data collection

Crystals were caught with SPINE sample loops and put in cryoprotectant solution (precipitant solution with 10-15% glycerol) and flash-frozen. Data for the native, active C1-inhibitor were collected at beam line BM14 at the European Synchrotron Radiation Facility (Grenoble, France)²⁴. 120 images were collected with an oscillation angle of 1.0 degree and exposure time of 20 s per frame at 100 K. For the C1-inhibitor/dextran sulfate complex crystal, 1074 images were collected with a 0.15 degree oscillation angle and an exposure time of 0.037 s per frame at 100 K on beamline ID23-1²⁵. The images were processed with *XDS*²⁶. Scaling and merging were done with *AIMLESS* (Evans, 2006) from the *CCP4* suite²⁷. The complex crystal diffracted anisotropically as clearly shown in the half set correlations, $CC(1/2)$ ²⁸ for different axes: along the k-axis the $CC(1/2)$ was 0.515 at 2.9 Å, but the $CC(1/2)$ was 0.3 at 3.55 Å along the h-axis and 3.14 Å along the l-axis. Data collection statistics are shown in Table 1.

Structure solution and refinement

The structure of uncomplexed C1-inhibitor was solved by molecular replacement using the latent structure of C1-inhibitor (PDB entry 2OAY) as a search model¹⁵. A vast majority of the model was automatically rebuilt using *Arp/Warp*²⁹ and refined with *Refmac*³⁰, coupled with manual fitting using *Coot*³¹. For the C1-inhibitor-dextran sulfate complex, the phase problem was solved by molecular replacement using the native C1-inhibitor structure as a search model. Clear difference density was visible for the dextran sulfate as well as glycosylation sites. The saccharides of dextran sulfate were automatically built with *Coot* using the 'Find ligand' function. The carbohydrate configuration and density were validated with the program *Privateer*²²; the real space correlation coefficient for the three saccharides built were 0.83, 0.78 and 0.75. The model was refined with *Refmac* and further manual fitting was also performed using *Coot*. For the C1-inhibitor-dextran sulfate model, refinement using different resolution cutoffs and data truncated by the anisotropic diffraction data server was attempted, but no major effect on electron density quality or R-factor statistics was observed: the anisotropic scaling in *Refmac* appeared to appropriately weight down the reflections in the weakly diffracting directions. The final R-factor and R_{free} for uncomplexed C1-inhibitor were 0.197 and 0.257 respectively and 0.239 and 0.281 for C1-inhibitor in complex with dextran sulfate. Refinement statistics are shown in Table 1.

Isothermal titration calorimetry

Measurements were performed on a MicroCal VP-ITC instrument (Malvern Instruments). Recombinant full-length C1-inhibitor was used and prepared as previously described and buffer exchanged into dialysis buffer (20 mM NaCitrate, 10 mM NaCl, pH 7.0) using a Slide-A-Lyzer dialysis cassette (Thermo Scientific). Protein

concentrations were determined by the A_{280} as measured by a Nanodrop2000 (Thermo Scientific), using $\epsilon = 26880 \text{ M}^{-1} \text{ cm}^{-1}$. Dextran sulfate with a mean molecular weight of 5 kDa, 10 kDa or 20 kDa and high sulfation levels (16-20% sulfur) (TdB Consultancy) was dissolved into dialysis buffer. Titrations of 0.15-0.35 mM dextran sulfate into the sample cell containing 25 μM C1-inhibitor were performed at 25 °C. Data was analyzed using the MicroCal ITC-Origin analysis software and for the analysis, the first titration has been removed for 10 kDa and 20 kDa dextran sulfate, while the first two titrations have been removed for 5 kDa. The results are shown in Table 2.

Models of the Michaelis complex of C1s:C1-inhibitor and kallikrein:C1-inhibitor

Using the previously determined structures of the Michaelis serpin-protease complex of alaserpin and trypsin²⁰ (pdb code 1k9o), heparin cofactor II and thrombin¹³ (pdb code 1jmo), alpha-1-antitrypsin and trypsin²¹ (pdb code 1oph) and protease nexin-1 and thrombin²² (pdb code 4dy7) as templates, as well as the structure of C1-inhibitor in complex with dextran sulfate presented here and the previously determined structures of C1s³³ and the catalytic domain of human plasma kallikrein³⁴, models of the C1s-C1-inhibitor and kallikrein-C1-inhibitor Michaelis complexes were created using the SSM superposition function in the program *Coot*. For the protease nexin-1-thrombin structure, two Michaelis complexes were present in the asymmetric unit; our analysis used the complex that would permit proteolytic cleavage.

Protein data bank accession codes

5DU3 (native structure), 5DUQ (complex with dextran sulfate)

References

1. Davis, A.E., III, Lu, F. & Mejia, P. C1 inhibitor, a multi-functional serine protease inhibitor. *Thromb. Haemost* 104, 886-893 (2010).
2. Caliezi, C. et al. C1-inhibitor in patients with severe sepsis and septic shock: beneficial effect on renal dysfunction. *Crit Care Med* 30, 1722-1728 (2002).
3. Lu, F., Fernandes, S.M. & Davis, A.E., III. The effect of C1 inhibitor on myocardial ischemia and reperfusion injury. *Cardiovasc. Pathol* 22, 75-80 (2013).
4. Levy, M. & Mealy, M.A. Purified human C1-esterase inhibitor is safe in acute relapses of neuromyelitis optica. *Neurol. Neuroimmunol. Neuroinflamm* 1, e5 (2014).
5. Irving, J.A., Pike, R.N., Lesk, A.M. & Whisstock, J.C. Phylogeny of the serpin superfamily: implications of patterns of amino acid conservation for structure and function. *Genome Res* 10, 1845-64 (2000).
6. Huntington, J.A., Read, R.J. & Carrell, R.W. Structure of a serpin-protease complex shows inhibition by deformation. *Nature* 407, 923-926 (2000).
7. Karnaukhova, E. C1-Esterase inhibitor: biological activities and therapeutic applications. *J Hematol Thromb Dis* 1(2013).
8. Wuillemin, W.A. et al. Potentiation of C1 inhibitor by glycosaminoglycans: dextran sulfate species are effective inhibitors of in vitro complement activation in plasma. *J. Immunol* 159, 1953-1960 (1997).
9. Caldwell, E.E. et al. Heparin binding and augmentation of C1 inhibitor activity. *Arch. Biochem. Biophys* 361, 215-222 (1999).
10. Rajabi, M., Struble, E., Zhou, Z. & Karnaukhova, E. Potentiation of C1-esterase inhibitor by heparin and interactions with C1s protease as assessed by surface plasmon resonance. *Biochim. Biophys. Acta* 1820, 56-63 (2012).
11. Zhou, Z.H., Rajabi, M., Chen, T., Karnaukhova, E. & Kozlowski, S. Oversulfated chondroitin sulfate inhibits the complement classical pathway by potentiating C1 inhibitor. *PLoS. One* 7, e47296 (2012).
12. Jin, L. et al. The anticoagulant activation of antithrombin by heparin. *Proc. Natl. Acad. Sci. U. S. A* 94, 14683-14688 (1997).
13. Baglin, T.P., Carrell, R.W., Church, F.C., Esmon, C.T. & Huntington, J.A. Crystal structures of native and thrombin-complexed heparin cofactor II reveal a multistep allosteric mechanism. *Proc. Natl. Acad. Sci. U. S. A* 99, 11079-11084 (2002).

14. van Veen, H.A. et al. Characterization of recombinant human C1 inhibitor secreted in milk of transgenic rabbits. *J. Biotechnol* 162, 319-326 (2012).
15. Beinrohr, L. et al. C1 inhibitor serpin domain structure reveals the likely mechanism of heparin potentiation and conformational disease. *J. Biol. Chem* 282, 21100-21109 (2007).
16. Aulak, K.S. et al. A hinge region mutation in C1-inhibitor (Ala436-->Thr) results in nonsubstrate-like behavior and in polymerization of the molecule. *J Biol. Chem* 268, 18088-18094 (1993).
17. Mottonen, J. et al. Structural basis of latency in plasminogen activator inhibitor-1. *Nature* 355, 270-3 (1992).
18. Bos, G.A.C. C-inhibitor potentiation by glycosaminoglycans. PhD thesis (University of Amsterdam) (2003).
19. Rossi, V. et al. Functional characterization of the recombinant human C1 inhibitor serpin domain: insights into heparin binding. *J. Immunol* 184, 4982-4989 (2010).
20. Ye, S. et al. The structure of a Michaelis serpin-protease complex. *Nat. Struct. Biol* 8, 979-983 (2001).
21. Dementiev, A., Simonovic, M., Volz, K. & Gettins, P.G. Canonical inhibitor-like interactions explain reactivity of alpha1-proteinase inhibitor Pittsburgh and antithrombin with proteinases. *J Biol Chem* 278, 37881-7 (2003).
22. Li, W. & Huntington, J.A. Crystal structures of protease nexin-1 in complex with heparin and thrombin suggest a 2-step recognition mechanism. *Blood* 120, 459-67 (2012).
23. Potterton, L. et al. Developments in the CCP4 molecular-graphics project. *Acta Crystallogr. D. Biol. Crystallogr* 60, 2288-2294 (2004).
24. Grenoble, E. http://www.embl.fr/services/synchrotron_access/bm14/. (2015).
25. Nurizzo, D. et al. The ID23-1 structural biology beamline at the ESRF. *J. Synchrotron. Radiat* 13, 227-238 (2006).
26. Kabsch, W. XDS. *Acta Crystallogr. D. Biol. Crystallogr* 66, 125-132 (2010).
27. Winn, M.D. et al. Overview of the CCP4 suite and current developments. *Acta Crystallogr. D. Biol. Crystallogr* 67, 235-242 (2011).
28. Karplus, P.A. & Diederichs, K. Linking crystallographic model and data quality. *Science* 336, 1030-1033 (2012).
29. Perrakis, A., Morris, R. & Lamzin, V.S. Automated protein model building combined with iterative structure refinement. *Nat. Struct. Biol* 6, 458-463 (1999).
30. Murshudov, G.N. et al. REFMAC5 for the refinement of macromolecular crystal structures. *Acta Crystallogr. D. Biol. Crystallogr* 67, 355-367 (2011).
31. Emsley, P., Lohkamp, B., Scott, W.G. & Cowtan, K. Features and development of Coot. *Acta Crystallogr. D. Biol. Crystallogr* 66, 486-501 (2010).
32. Agirre, J., Davies, G., Wilson, K. & Cowtan, K. Carbohydrate anomalies in the PDB. *Nat. Chem. Biol* 11, 303 (2015).
33. Gaboriaud, C., Rossi, V., Bally, I., Arlaud, G.J. & Fontecilla-Camps, J.C. Crystal structure of the catalytic domain of human complement c1s: a serine protease with a handle. *EMBO J* 19, 1755-1765 (2000).
34. Tang, J. et al. Expression, crystallization, and three-dimensional structure of the catalytic domain of human plasma kallikrein. *J Biol Chem* 280, 41077-89 (2005).

6

Perspectives

The genomic DNA provides all the instructions for correct development and functioning of organisms. Damage to this DNA may interfere with critical cellular processes such as transcription and replication, and has the potential to drive mutagenesis, which in turn may underlie inherited disorders and accelerate progression of cancer and ageing-related diseases^{1,2}. The protection of cells and organisms against these potentially devastating effects of DNA damage largely relies on the DNA damage response (DDR), which comprises a network of signaling and repair pathways that coordinate lesion removal and accommodate suitable adjustments in for instance transcription and cell cycle status³.

Although essential in the protection against DNA damage, the DDR is not sufficient to protect us against all conceivably life-threatening hazards. For example, a first line of defense against pathogens, which upon host invasion can cause serious diseases, is provided by the immune system. Activation of the immune response encompasses multiple mechanisms, including physical barriers and biochemical cascades that are specialized in the neutralization of potentially harmful germs^{4,5}. Importantly, by recognizing and facilitating the clearance of non-self cells or molecules, the immune system also contributes to the prevention of cancer⁶.

Evidently, it is crucial that all proteins that are involved in the pathways that protect our cells, be it via the DDR, the immune system or other defense mechanisms, function correctly. Plain (upregulation of) transcription to produce the required proteins is not sufficient to guarantee their performances in the respective stress responses. Additionally, it is essential that protein functionality is tweaked by post-translational modifications (PTMs) that fine-tune activity, localization and interactions. Such modifications range from the stabilization of a protein by creating disulfide bonds, to its activation by cleavage of a small peptide or the reversible introduction of a functional group to spatiotemporally coordinate the different steps of a pathway. Clearly, extension of our knowledge regarding these post-translational control mechanisms could significantly contribute to our understanding of the development, and potentially the treatment, of the numerous disorders that are associated with loss of protein regulation in protective responses. The research described in this thesis has already improved our insights into how the availability of functional proteins is maintained, as well as how their activities are further modulated by PTMs, yet has raised some additional questions that provide a base for further research and discussion.

The importance of chaperonins in the prevention of disease

Upon translation, folding of a nascent polypeptide into a stable and potentially active protein can be considered the first critical step in guaranteeing its subsequent functioning. Protein homeostasis is maintained by a network of chaperones and protein degradation machineries, collectively referred to as the proteostasis network (PN)⁷. Assistance in the folding of fast-folding proteins is usually provided by the heat shock protein families, which mainly act as monomers or homodimers that stabilize hydrophobic regions of nascent polypeptides until the desired conformation has been established. Proteins that are more difficult to fold are transferred to specialized chaperone systems that apply a method of non-native protein encapsulation in a central cavity, as displayed by the chaperonin TRiC⁸⁻¹⁰. We uncovered a crucial role for TRiC in ensuring the stability of the CSA protein that is essential in DNA damage recognition and subsequent DNA damage repair via transcription-coupled

nucleotide excision repair (TC-NER) (described in Chapter 3). When not folded or stabilized correctly, CSA is degraded instead of being incorporated into the cullin-RING E3 ubiquitin ligase complex CRL^{CSA}, leading to a deficiency in functional CSA/CRL^{CSA}. Importantly, we discovered that patient mutations in CSA's WD40 domain cause increased binding of CSA to TRiC, indicating the protein's instability and/or folding complications¹¹. While the mechanism behind the cause of Cockayne syndrome by these mutations had thus far remained elusive, this finding may provide an important explanation for how they affect the functioning of CSA and could ultimately underlie disease. Most likely, the examined mutations inhibit proper folding and thereby the release of CSA by TRiC. Alternatively, CSA harboring these mutations is incapable of adopting the correct conformation, even despite the assistance of TRiC, making incorporation into CRL^{CSA} impossible and resulting in re-binding of the unstable CSA protein by TRiC.

By regulating the functioning of CSA, TRiC likely contributes to preserving genome stability in response to transcription-stalling DNA damage. Given that TRiC's interactome has been estimated to comprise at least 5-10% of all cytoplasmic proteins, it is conceivable that it facilitates the folding and/or stabilization of additional, yet to be identified DDR factors, and thus protects genome stability in an even broader manner than currently anticipated¹². The frequently applied method of protein precipitation followed by mass spectrometry to analyze coprecipitated factors could be a first step in identifying TRiC-bound proteins. However, if aiming to tag the TRiC complex to ease its purification, the subunit should be carefully chosen to prevent interference with complex build-up, as well as masking of the tag inside the chaperonin complex. Furthermore, tagging of the endogenous protein via CRISPR-Cas9-mediated gene editing is preferred over ectopic (over)expression of a tagged subunit to minimize overshadowing of TRiC by tagged protein that has not been incorporated into the complex.

Ultimately, TRiC's involvement in the DDR may also imply a role for this chaperonin in suppressing cancer development. Accordingly, TRiC was shown to stabilize several proteins that are implicated in genome stability maintenance and cancer progression, including the tumor suppressors VHL and p53 and oncoproteins cyclin B and cyclin E, which have all been shown to function in the DDR as well¹³⁻²¹.

Evidently, given its role as a chaperonin, TRiC may also be crucial in the prevention of (ageing-related) neurodegenerative diseases that are hallmarked by protein aggregation. In agreement, TRiC-interacting proteins were shown to be enriched for aggregation-prone polypeptides. Importantly, its substrates include the Huntingtin protein, which in its aggregated form has been linked to Huntington's disease^{12,22,23}. A possible association between the chaperone system and abnormal protein deposits in the brain is furthermore supported by a decline in the expression of heat shock proteins in Alzheimer's disease patients²⁴. In contrast, cancer cells display upregulated levels of TRiC, as well as other molecular chaperones, resulting from de novo protein synthesis^{19,24}. Thus, regulation of the levels of PN components seems to be crucial in the prevention of disease. Interestingly, however, elevated chaperone protein levels do not necessarily correlate with increased activity, as this is likely modulated by the functional interplay with other chaperones. For example, overall TRiC folding activity was shown to be reduced when levels of co-chaperones

Hsc/p70 and prefoldin are high and vice versa¹⁹. Potentially this implies the precise fine-tuning of specific chaperone activities, and consequently protein homeostasis, by modulating co-chaperone as well as substrate protein availabilities. Likewise, we speculate that disease-causing mutations that lead to high levels of protein persistently bound to TRiC could also have an impact on pathways in which the mutated protein is not (in)directly involved. By lowering the amount of free chaperone that is available to facilitate the folding/stabilization of other proteins, even seemingly unrelated cellular processes may be negatively affected.

The contribution of Zimp7 to cellular functioning

Further expanding our knowledge on protein-modifying enzymes, we uncovered the PIAS-like protein Zimp7 as a conceivable new SUMO E3 ligase. Its Siz/PIAS-RING (SP-RING) domain, which resembles that in PIAS ligases, appeared to confer bona fide SUMO-conjugating activity. Evidently, the ligase activity of full-length Zimp7, which may adopt a conformation that differs from the truncated protein that we studied, remains to be established. Furthermore, its actual behavior *in vivo* may be precisely regulated and needs to be examined as well. Mass spectrometry using cells that express either wildtype or SP-RING-mutated Zimp7 would be a straightforward first approach to reveal its contribution to overall SUMOylation under various conditions. In addition, this may expose specific potential targets, which subsequently could be validated in an *in vitro* set-up. Although the catalytic activity of Zimp7's SP-RING domain already is a valuable finding in terms of our general understanding of the repertoire of PTM-catalyzing factors, the true challenge lies in elucidating Zimp7's specific biological functions. Our observations, which are supported by those described in literature, indicate potential roles for Zimp7 in normal DNA replication and transcription, as well as in the DDR (described in Chapter 4).

In agreement with the colocalization of Zimp7 with newly synthesized DNA and PCNA at replication foci in S-phase, we established a clear interaction between Zimp7 and PCNA in unperturbed conditions, strengthening its possible involvement in DNA replication²⁵. Furthermore, the described enrichment of Zimp7 at hydroxyurea-stalled replication forks, as detected in an iPOND study, argues for an additional role in the response to replication stress²⁶. In yeast, adjustment of the PCNA SUMOylation status comprises an important mechanism to coordinate normal DNA replication as well as pathway choice upon replication stress. SUMOylation of PCNA influences its interaction with the anti-recombinogenic protein Srs2 that prevents (undesired) RAD51 filament formations that could facilitate homologous recombination between the newly formed sister chromatids²⁷⁻²⁹. Likewise, the human helicase PARI interacts with PCNA and may function analogously to Srs2^{30,31}. Investigating potential functions of Zimp7 in regulating the SUMOylation of PCNA and other replication (stress) factors and/or the spatiotemporal modulation of the PARI-PCNA interaction could shed significant light on Zimp7's contribution to DNA replication and associated stress response pathways.

In addition, Zimp7's function may extend to (other pathways of) the DDR, which is demonstrated by its recruitment to sites of laser-induced DNA damage. The importance of the SUMO conjugation system for various aspects of the DDR is underscored by for example roles of PIAS1 and PIAS4 in the SUMOylation and/or recruitment of numerous factors in

response to double-strand DNA breaks (such as BRCA1, RAP80, 53BP1, RNF168 and RNF4), the enhancement of both homologous recombination and non-homologous end-joining by PIAS3, and the SUMOylation of proteins during BER (for instance TDG) or NER (including GG-NER factors XPC and DDB2, and TC-NER factor CSB)³²⁻⁴¹. Exploring Zimp7's interaction partners and SUMOylation targets will gain more insight into the DNA damage response(s) that Zimp7 is involved in. Given that Zimp7 interacts with the BRG1 and BAF57 components of the SWI/SNF-like chromatin remodeling complexes, which have been implicated in several DDR pathways, it is interesting to speculate that Zimp7 assists in making structural adjustments in the chromatin that contribute to lesion accessibility during repair^{25,42-44}. Furthermore, this may constitute a mechanism by which Zimp7 modulates regular transcription, during which chromatin remodeling is essential as well. Since Zimp7 was originally identified as an enhancer of androgen receptor-mediated transcription, studies related to its function have consequently focused on its transcription-regulating capacities^{25,45,46}. Accordingly, augmentation of transcription that is controlled by a number of other nuclear hormone receptors, as well as the coactivation of the Wnt/ β -catenin signaling pathway have been functionally ascribed to Zimp7^{25,47}. RNA-seq experiments that examine the varying transcriptome in the presence or absence of Zimp7 would comprise a meaningful extension to this research, which has solely been based on reporter assays, and could enlighten a role in regular transcription. Importantly, the ability to regulate transcription would further justify Zimp7's classification as a PIAS-like protein, as numerous cases of either transcriptional activation or repression by the PIAS proteins have been reported⁴⁸. Interestingly, whereas most of these were shown to depend on the SUMO-conjugating function of the involved PIAS protein, implying a functional link between its SUMOylating and transcription-regulating activities, this catalytic activity appeared to be dispensable for other cases of PIAS-dependent transcriptional regulation. For example, gene activation that is mediated by the DNA-binding protein SATB2 was shown to be decreased by PIAS1-induced SUMOylation⁴⁹. On the contrary, although PIAS1 and PIAS4 were shown to SUMOylate the transcription factors Msx1 and LEF1, respectively, their effects on transcription via modulating the subnuclear localization of these proteins may occur through SUMO-independent mechanisms^{48,50,51}. Regulation of hormone receptor-mediated transcription by Zimp7 is most likely at least in part facilitated by the intrinsic transcriptional activity that is provided by a C-terminal transactivation domain (TAD)²⁵. The identification of a specific mutation that renders Zimp7 incapable of promoting SUMO conjugation, that is C616A, will significantly aid in determining to what extent Zimp7's functions, including those in transcription, can (additionally) be explained by its SUMOylating activity. Given Zimp7's potential implications in the correct functioning of several crucial cellular processes such as transcription and DNA replication, as well as the protection against the hazardous effects of DNA damage, resolving its specific functions may also prove Zimp7's importance in the prevention of ageing-related diseases and cancer development. For example, Zimp7 was shown to be highly expressed in prostate cells, which require correct functioning of the androgen receptor (AR) for normal development as well as the prevention of tumorigenesis^{45,52}. In addition to Zimp7, all the PIAS proteins have been shown to affect AR-mediated transcription in prostate cancer cells and presumably play important roles in

tumor initiation and progression⁵³⁻⁵⁷. Interestingly, again both coactivating and co-repressing effects on AR-controlled genes have been reported. Regulation of AR target genes by the PIAS proteins has consequentially been suggested to be target specific^{54,57}. Furthermore, a delicate interplay between the AR, transcription factors and the PIAS proteins seems to regulate transcriptional activity⁵⁸. Since we detected a clear interaction between Zimp7 and PIAS3, and interactions with other PIAS proteins have been described as well, it is tempting to hypothesize that Zimp7 may contribute to (physical) protein-protein interaction competitions and thereby provide an additional regulatory layer to AR-mediated transcription⁵⁹. As the TAD in Zimp7 is (partly) responsible for Zimp7-induced stimulation of transcription that is controlled by the AR, the engagement of this domain in the involved interactions would be interesting to investigate²⁵. Evidently, the requirement of Zimp7's SUMOylating catalytic activity for such mechanisms and regulation of AR-coordinated transcription in general should be assessed as well.

Most likely, future studies will not only give insight into Zimp7's role in the protection against tumorigenesis of prostate cells, but instead reveal general mechanisms that extend to the prevention of other types of cancer and ageing-related diseases. Although we are just at the beginning of unraveling its exact biological functions, Zimp7's broad implications in the processes that ensure correct cellular development and functioning, including genome stability maintenance, already seem to predict its significance in health and disease.

The association between NER defects and varying human disorders

The biological relevance of accurate spatiotemporal coordination of TC-NER stages and signaling cascades is illustrated by the broadly varying clinical consequences that are associated with inherited NER defects. The observation that not only different mutations in the same gene/protein, but even identical genetic alterations can have multiple clinical outcomes adds even more complexity to explaining the multifaceted disease manifestations^{3,60}. Overall, defects in one of the XP (xeroderma pigmentosum) proteins that function in GG-NER seem to predominantly render patients hypersensitive to sunlight and increase cancer susceptibility⁶¹. This may be explained by the accumulation of DNA lesions throughout the genome, leading to mutagenesis in case of impaired GG-NER and bypass by translesion DNA polymerases during DNA replication⁶². Mutations in genes encoding the TC-NER proteins CSA or CSB primarily cause neurodevelopmental problems and accelerated ageing, while not augmenting cancer predisposition^{63,64}. These clinical hallmarks of Cockayne syndrome may at least in part be accounted for by the accelerated cell death that is induced by persistently stalled transcription complexes². This simplified explanation of the clinical consequences of defective NER also elegantly provides an interpretation of the combined XP/CS phenotypes that can be observed for (certain) mutations in proteins that function in the core NER machinery, that is XPA, XPB, XPD, XPF or XPG^{61,65-67}.

The hypothesis that the ability of cells to degrade lesion-stalled RNA polymerase and repair complexes when NER is compromised may contribute to the clinical outcome of NER gene mutations has remained an important matter of debate. The rationale behind this theory is not only that avoidance of persistently stalled RNA polymerase is crucial in the prevention of a p53-mediated signaling response that leads to premature cell death, but also involves the

accessibility of lesions to other repair pathways that could be generated by displacement of incompetent repair complexes^{62,68-70}. If valid, this would imply that the more severe (neurological) phenotypes are to be expected when DNA damage-induced RNAPII degradation is disabled. Interestingly, while wildtype fibroblasts showed an overall decrease in the levels of the serine 5-phosphorylated RPB1 subunit of RNAPII (p-S5-RPB1) upon UV irradiation, we indeed observed that CS-A and CS-B patient cells were incapable of degrading p-S5-RPB1 after DNA damage induction. In contrast, cells derived from UVsS patients displayed slightly faster UV-induced p-S5-RPB1 degradation as compared to wildtype, which is in agreement with the relatively mild clinical phenotype of photosensitivity³. Furthermore, cells derived from an XP patient with a defect in XPA, for whom no neurological problems have been described, displayed a decrease in p-S5-RPB1 levels upon UV irradiation as well. Surprisingly, however, when we examined cells that were derived from two different patients that both harbored a mutation in the *XPB* gene, yet suffered from either XP or combined XP/CS, UV-induced p-S5-RPB1 degradation was detectable in (and comparable between) both cell lines. Thus, although seemingly a valid explanation for the difference between CS and UVsS, the ability to remove stalled RNAPII or repair complexes does not necessarily preclude the development of neurological problems. Evidently, the impact of a single cellular event, in this case the removal of stalled RNA polymerase, on the clinical outcome of a genetic defect is difficult to evaluate. In our efforts to explain patient phenotypes, potential implications of the associated defective protein in cellular processes other than NER, or even outside the DDR, should be taken into account as well. This is illustrated by mutations in *XPB* or *XPD* that not only cause CS features, but owing to their functions as subunits of the transcription factor TFIIH, additionally result in brittle hair and nails – a disorder known as trichothiodystrophy⁷². Similarly, roles for the CS proteins in transcription, maintenance of mitochondrial DNA stability and oxidative damage repair have been described⁷³⁻⁷⁸. For example, CSB may contribute to BER by facilitating the recruitment of XRCC1 to transcription-stalled RNAPII that is trapped at repair intermediates⁷⁹. Removal of oxidative damage may be of particular importance in the brain, where the relatively high metabolic activity generates high levels of reactive oxygen species. Accordingly, defective oxidative damage repair in neurons has been linked to neurodegenerative disorders such as Alzheimer's disease and Parkinson's disease^{80,81}. Defects in CS proteins that, next to TC-NER impairment, cause additional defects in oxidative damage repair, could therefore (theoretically) lead to even more severe neurological problems.

Altogether, the complexity of NER-associated diseases and the clinical heterogeneity between patients, argue for research that not only studies the changes in cellular responses in the complete absence of a NER factor, but also examines the effect of specific patient mutations. As described previously, such an approach has already provided us with some important insights regarding the TRiC-mediated stability of CSA, by explaining how specific missense mutations can cause an overall decrease in protein availability¹¹. Notably, the absolute absence of a protein may in some cases even be less detrimental than the presence of a defective one, as has been demonstrated for a case of UVsS that is associated with a mutation in the *CSB* gene causing a complete deficiency in CSB protein⁸². Although studying

individual patient mutations may at first complicate disease explanations even further, this will eventually improve our understanding of (the heterogeneity in) NER-related disorders.

Potential of C1-inhibitor activity by polysaccharides

The consequences of protein defects that negatively interfere with pathway progression and restrict its proper and complete execution have been described extensively. Yet, inappropriate or uncontrolled activation of protective responses may be equally harmful. Good examples are provided by the numerous autoimmune disorders that are characterized by abnormal activation of self-reactive immune responses, resulting in the attack of healthy body tissue. As a part of the immune system, cascades of proteolytic cleavages in short time can amplify a signal to evoke a massive response⁸³. The serine protease inhibitor (serpin) C1-inhibitor regulates several of these pathways by trapping the initiating proteases into a conformation with a disrupted active site, thereby preventing their spontaneous activations⁸⁴. Fundamental to C1-inhibitor's function is its reactive center loop (RCL), which contains the P1-P1' residues that appear as a substrate to the target protease. Attempts of the protease to process this bond result in an irreversible conformational change that transfers the protease to the other side of the serpin⁸⁵⁻⁸⁷. Importantly, deficiency of C1-inhibitor has been shown to underlie hereditary angioedema (HAE), which is hallmarked by recurrent attacks of swellings that are potentially life-threatening when occurring in the upper airways^{88,89}. Disproportional activation of the kallikrein-kinin cascade of the contact system, which is under control of C1-inhibitor, results in the release of bradykinin that increases vascular permeability. Since its development in the 1970s, replacement therapy using C1-inhibitor isolated from human blood plasma has been used as a treatment for HAE^{90,91}. Despite its proven effectiveness in the treatment of acute attacks, the use of plasma-derived protein has its downsides, including its availability and the risk of contamination. A significant step towards improving the therapy was made by the production of recombinant human C1-inhibitor secreted in the milk of transgenic rabbits, which for instance eliminates the risk of contamination with blood-borne viruses, but has its own limitations⁹². We suggest that further optimization can be sought in increasing the activity and/or effectiveness of the medicated serpin. The reported potentiation by glycosaminoglycans (GAGs), of which heparin and the synthetic dextran sulfate have been studied the most in this context, therefore seems a promising observation⁹³⁻⁹⁵. It would be interesting to explore the possibility to administer a pre-incubated GAG-C1-inhibitor complex or a combination of C1-inhibitor and a specifically designed molecule that enhances its activity. Evidently, a good understanding of how this potentiation is established is a prerequisite for such design. Our model, which is based on the structure of active serpin crystallized in the presence of dextran sulfate, provides some essential insights into the binding of the ligand to C1-inhibitor. Dextran sulfate binds to C1-inhibitor's F1 helix without inducing a conformational change.

Importantly, our docking studies also explain why potentiation of C1-inhibitor's activity is different towards its various target proteins – a finding that can be relevant in developing a molecule that specifically enhances the inhibition of a certain protease. Most likely, negatively charged polysaccharides neutralize the repulsive forces between the serpin's positively charged F1 helix and the protease's autolysis loop⁹⁶. To validate these models (described in

Chapter 5), we propose that crystallization and structure solving of C1-inhibitor and dextran sulfate together with the studied proteases are performed.

Clearly, in view of therapy optimization, formation of single C1-inhibitor-GAG-protease complexes is preferred over the binding of either multiple C1-inhibitor or protease molecules. Although binding of GAGs can potentiate the activity of C1-inhibitor against some of its target proteases, the molecule to be used should therefore be carefully designed to prevent polymerization. Accordingly, we observed that multiple C1-inhibitor molecules bind to increasing sizes of dextran sulfate⁹⁶. Isothermal calorimetry (ITC) experiments in the presence of a protease could show whether this would interfere with serpin-protease complex formation and which relative concentrations would be a suitable starting point for further research. Complex formation and stoichiometries could additionally be studied by native PAGE or (another method of) size exclusion chromatography, followed by immunoblotting.

Overall, exploring the possibilities for implementation of C1-inhibitor potentiation in disease treatment involves multiple complicated considerations that should guarantee therapy improvement as opposed to for example inducing multimerization or affecting other cellular processes. Furthermore, the desired specific promotion of kallikrein inhibition by a GAG(-like molecule) seems challenging, as our models indicate that the introduction of dextran sulfate mainly affects the inactivation of proteases with a positively charged autolysis loop. Nevertheless, we consider dextran sulfate a good foundation for further research, as it does not seem to interfere with antithrombin functioning (in contrast to heparin) and doses required for potentiation might be non-toxic, as suggested by some of our valuable insights into its binding and potentiating behavior^{96,97}.

References

1. Bartek, J., Bartkova, J. & Lukas, J. DNA damage signalling guards against activated oncogenes and tumour progression. *Oncogene* 26, 7773-9 (2007).
2. Hoeijmakers, J.H. DNA damage, aging, and cancer. *N Engl J Med* 361, 1475-85 (2009).
3. Dijk, M., Typas, D., Mullenders, L. & Pines, A. Insight in the multilevel regulation of NER. *Exp Cell Res* 329, 116-23 (2014).
4. Parkin, J. & Cohen, B. An overview of the immune system. *Lancet* 357, 1777-89 (2001).
5. Marshall, J.S., Warrington, R., Watson, W. & Kim, H.L. An introduction to immunology and immunopathology. *Allergy Asthma Clin Immunol* 14, 49 (2018).
6. Candeias, S.M. & Gaip, U.S. The Immune System in Cancer Prevention, Development and Therapy. *Anticancer Agents Med Chem* 16, 101-7 (2016).
7. Balchin, D., Hayer-Hartl, M. & Hartl, F.U. In vivo aspects of protein folding and quality control. *Science* 353, aac4354 (2016).
8. Freund, A. et al. Proteostatic Control of Telomerase Function through TRiC-Mediated Folding of TCAB1. *Cell* 159, 1389-1403 (2014).
9. Horwich, A.L., Fenton, W.A., Chapman, E. & Farr, G.W. Two families of chaperonin: physiology and mechanism. *Annu Rev Cell Dev Biol* 23, 115-45 (2007).
10. Leitner, A. et al. The molecular architecture of the eukaryotic chaperonin TRiC/CCT. *Structure* 20, 814-25 (2012).
11. Pines, A. et al. TRiC controls transcription resumption after UV damage by regulating Cockayne syndrome protein A. *Nat Commun* 9, 1040 (2018).
12. Yam, A.Y. et al. Defining the TRiC/CCT interactome links chaperonin function to stabilization of newly made proteins with complex topologies. *Nat Struct Mol Biol* 15, 1255-62 (2008).
13. Espana-Agusti, J., Warren, A., Chew, S.K., Adams, D.J. & Matakidou, A. Loss of PBRM1 rescues VHL dependent replication stress to promote renal carcinogenesis. *Nat Commun* 8, 2026 (2017).
14. Feldman, D.E., Spiess, C., Howard, D.E. & Frydman, J. Tumorigenic mutations in VHL disrupt folding in vivo by interfering with chaperonin binding. *Mol Cell* 12, 1213-24 (2003).
15. Melville, M.W., McClellan, A.J., Meyer, A.S., Darveau, A. & Frydman, J. The Hsp70 and TRiC/CCT chaperone systems cooperate in vivo to assemble the von Hippel-Lindau tumor suppressor complex. *Mol Cell Biol* 23, 3141-51 (2003).
16. Metcalf, J.L. et al. K63-ubiquitylation of VHL by SOCS1 mediates DNA double-strand break repair. *Oncogene* 33, 1055-65 (2014).
17. Trinidad, A.G. et al. Interaction of p53 with the CCT complex promotes protein folding and wild-type p53 activity. *Mol Cell* 50, 805-17 (2013).
18. Reinhardt, H.C. & Schumacher, B. The p53 network: cellular and systemic DNA damage responses in aging and cancer. *Trends Genet* 28, 128-36 (2012).
19. Boudiaf-Benmamar, C., Cresteil, T. & Melki, R. The cytosolic chaperonin CCT/TRiC and cancer cell proliferation. *PLoS One* 8, e60895 (2013).
20. Won, K.A., Schumacher, R.J., Farr, G.W., Horwich, A.L. & Reed, S.I. Maturation of human cyclin E requires the function of eukaryotic chaperonin CCT. *Mol Cell Biol* 18, 7584-9 (1998).
21. Nakayama, Y. & Yamaguchi, N. Role of cyclin B1 levels in DNA damage and DNA damage-induced senescence. *Int Rev Cell Mol Biol* 305, 303-37 (2013).
22. Shahmoradian, S.H. et al. TRiC's tricks inhibit huntingtin aggregation. *Elife* 2, e00710 (2013).
23. Tam, S. et al. The chaperonin TRiC blocks a huntingtin sequence element that promotes the conformational switch to aggregation. *Nat Struct Mol Biol* 16, 1279-85 (2009).
24. Calderwood, S.K. & Murshid, A. Molecular Chaperone Accumulation in Cancer and Decrease in Alzheimer's Disease: The Potential Roles of HSF1. *Front Neurosci* 11, 192 (2017).
25. Huang, C.Y. et al. hZimp7, a novel PIAS-like protein, enhances androgen receptor-mediated transcription and interacts with SWI/SNF-like BAF complexes. *Mol Endocrinol* 19, 2915-29 (2005).
26. Dugrawala, H. et al. The Replication Checkpoint Prevents Two Types of Fork Collapse without Regulating Replisome Stability. *Mol Cell* 59, 998-1010 (2015).

27. Papouli, E. et al. Crosstalk between SUMO and ubiquitin on PCNA is mediated by recruitment of the helicase Srs2p. *Mol Cell* 19, 123-33 (2005).
28. Pfander, B., Moldovan, G.L., Sacher, M., Hoege, C. & Jentsch, S. SUMO-modified PCNA recruits Srs2 to prevent recombination during S phase. *Nature* 436, 428-33 (2005).
29. Watts, F.Z. Sumoylation of PCNA: Wrestling with recombination at stalled replication forks. *DNA Repair (Amst)* 5, 399-403 (2006).
30. Garcia-Rodriguez, N., Wong, R.P. & Ulrich, H.D. Functions of Ubiquitin and SUMO in DNA Replication and Replication Stress. *Front Genet* 7, 87 (2016).
31. Moldovan, G.L. et al. Inhibition of homologous recombination by the PCNA-interacting protein PARI. *Mol Cell* 45, 75-86 (2012).
32. Morris, J.R. et al. The SUMO modification pathway is involved in the BRCA1 response to genotoxic stress. *Nature* 462, 886-90 (2009).
33. Hu, X., Paul, A. & Wang, B. Rap80 protein recruitment to DNA double-strand breaks requires binding to both small ubiquitin-like modifier (SUMO) and ubiquitin conjugates. *J Biol Chem* 287, 25510-9 (2012).
34. Galanty, Y., Belotserkovskaya, R., Coates, J. & Jackson, S.P. RNF4, a SUMO-targeted ubiquitin E3 ligase, promotes DNA double-strand break repair. *Genes Dev* 26, 1179-95 (2012).
35. Bekker-Jensen, S. & Mailand, N. The ubiquitin- and SUMO-dependent signaling response to DNA double-strand breaks. *FEBS Lett* 585, 2914-9 (2011).
36. Liu, S. et al. PIAS3 promotes homology-directed repair and distal non-homologous end joining. *Oncol Lett* 6, 1045-1048 (2013).
37. Hardeland, U., Steinacher, R., Jiricny, J. & Schar, P. Modification of the human thymine-DNA glycosylase by ubiquitin-like proteins facilitates enzymatic turnover. *EMBO J* 21, 1456-64 (2002).
38. Steinacher, R. & Schar, P. Functionality of human thymine DNA glycosylase requires SUMO-regulated changes in protein conformation. *Curr Biol* 15, 616-23 (2005).
39. Poulsen, S.L. et al. RNF111/Arkadia is a SUMO-targeted ubiquitin ligase that facilitates the DNA damage response. *J Cell Biol* 201, 797-807 (2013).
40. van Cuijk, L. et al. SUMO and ubiquitin-dependent XPC exchange drives nucleotide excision repair. *Nat Commun* 6, 7499 (2015).
41. Sin, Y., Tanaka, K. & Saijo, M. The C-terminal Region and SUMOylation of Cockayne Syndrome Group B Protein Play Critical Roles in Transcription-coupled Nucleotide Excision Repair. *J Biol Chem* 291, 1387-97 (2016).
42. Hara, R. & Sancar, A. The SWI/SNF chromatin-remodeling factor stimulates repair by human excision nuclease in the mononucleosome core particle. *Mol Cell Biol* 22, 6779-87 (2002).
43. Ogiwara, H. et al. Histone acetylation by CBP and p300 at double-strand break sites facilitates SWI/SNF chromatin remodeling and the recruitment of non-homologous end joining factors. *Oncogene* 30, 2135-46 (2011).
44. Park, J.H. et al. Mammalian SWI/SNF complexes facilitate DNA double-strand break repair by promoting gamma-H2AX induction. *EMBO J* 25, 3986-97 (2006).
45. Beliakoff, J. & Sun, Z. Zimp7 and Zimp10, two novel PIAS-like proteins, function as androgen receptor coregulators. *Nucl Recept Signal* 4, e017 (2006).
46. Li, X. et al. ZMIZ1 preferably enhances the transcriptional activity of androgen receptor with short polyglutamine tract. *PLoS One* 6, e25040 (2011).
47. Lee, S.H. et al. Identification of a novel role of ZMIZ2 protein in regulating the activity of the Wnt/beta-catenin signaling pathway. *J Biol Chem* 288, 35913-24 (2013).
48. Sharrocks, A.D. PIAS proteins and transcriptional regulation--more than just SUMO E3 ligases? *Genes Dev* 20, 754-8 (2006).
49. Dobрева, G., Dambacher, J. & Grosschedl, R. SUMO modification of a novel MAR-binding protein, SATB2, modulates immunoglobulin mu gene expression. *Genes Dev* 17, 3048-61 (2003).
50. Lee, H. et al. PIAS1 confers DNA-binding specificity on the Msx1 homeoprotein. *Genes Dev* 20, 784-94 (2006).
51. Sachdev, S. et al. PIASy, a nuclear matrix-associated SUMO E3 ligase, represses LEF1 activity by sequestration into nuclear bodies. *Genes Dev* 15, 3088-103 (2001).

52. Leach, D.A. & Buchanan, G. Stromal Androgen Receptor in Prostate Cancer Development and Progression. *Cancers (Basel)* 9(2017).
53. Gross, M., Yang, R., Top, I., Gasper, C. & Shuai, K. PIASy-mediated repression of the androgen receptor is independent of sumoylation. *Oncogene* 23, 3059-66 (2004).
54. Toropainen, S. et al. SUMO ligase PIAS1 functions as a target gene selective androgen receptor coregulator on prostate cancer cell chromatin. *Nucleic Acids Res* 43, 848-61 (2015).
55. Junicho, A. et al. Protein inhibitor of activated STAT3 regulates androgen receptor signaling in prostate carcinoma cells. *Biochem Biophys Res Commun* 278, 9-13 (2000).
56. Rabellino, A., Andreani, C. & Scaglioni, P.P. The Role of PIAS SUMO E3-Ligases in Cancer. *Cancer Res* 77, 1542-1547 (2017).
57. Kotaja, N., Aittomaki, S., Silvennoinen, O., Palvimo, J.J. & Janne, O.A. ARIP3 (androgen receptor-interacting protein 3) and other PIAS (protein inhibitor of activated STAT) proteins differ in their ability to modulate steroid receptor-dependent transcriptional activation. *Mol Endocrinol* 14, 1986-2000 (2000).
58. Yamamoto, T. et al. Molecular interactions between STAT3 and protein inhibitor of activated STAT3, and androgen receptor. *Biochem Biophys Res Commun* 306, 610-5 (2003).
59. Peng, Y., Lee, J., Zhu, C. & Sun, Z. A novel role for protein inhibitor of activated STAT (PIAS) proteins in modulating the activity of Zimp7, a novel PIAS-like protein, in androgen receptor-mediated transcription. *J Biol Chem* 285, 11465-75 (2010).
60. Colella, S., Nardo, T., Botta, E., Lehmann, A.R. & Stefanini, M. Identical mutations in the CSB gene associated with either Cockayne syndrome or the DeSanctis-cacchione variant of xeroderma pigmentosum. *Hum Mol Genet* 9, 1171-5 (2000).
61. DiGiovanna, J.J. & Kraemer, K.H. Shining a light on xeroderma pigmentosum. *J Invest Dermatol* 132, 785-96 (2012).
62. Marteijn, J.A., Lans, H., Vermeulen, W. & Hoeijmakers, J.H. Understanding nucleotide excision repair and its roles in cancer and ageing. *Nat Rev Mol Cell Biol* 15, 465-81 (2014).
63. Laugel, V. et al. Mutation update for the CSB/ERCC6 and CSA/ERCC8 genes involved in Cockayne syndrome. *Hum Mutat* 31, 113-26 (2010).
64. Laugel, V. Cockayne syndrome: the expanding clinical and mutational spectrum. *Mech Ageing Dev* 134, 161-70 (2013).
65. Bradford, P.T. et al. Cancer and neurologic degeneration in xeroderma pigmentosum: long term follow-up characterises the role of DNA repair. *J Med Genet* 48, 168-76 (2011).
66. Barnes, D.E. & Lindahl, T. Repair and genetic consequences of endogenous DNA base damage in mammalian cells. *Annu Rev Genet* 38, 445-76 (2004).
67. Rahbar, Z. & Naraghi, M. De Sanctis-Cacchione syndrome: A case report and literature review. *Int J Womens Dermatol* 1, 136-139 (2015).
68. Ljungman, M. & Zhang, F. Blockage of RNA polymerase as a possible trigger for u.v. light-induced apoptosis. *Oncogene* 13, 823-31 (1996).
69. Vrouwe, M.G., Pines, A., Overmeer, R.M., Hanada, K. & Mullenders, L.H. UV-induced photolesions elicit ATR-kinase-dependent signaling in non-cycling cells through nucleotide excision repair-dependent and -independent pathways. *J Cell Sci* 124, 435-46 (2011).
70. Ljungman, M. & Lane, D.P. Transcription - guarding the genome by sensing DNA damage. *Nat Rev Cancer* 4, 727-37 (2004).
71. Brooks, P.J. Blinded by the UV light: how the focus on transcription-coupled NER has distracted from understanding the mechanisms of Cockayne syndrome neurologic disease. *DNA Repair (Amst)* 12, 656-71 (2013).
72. Kraemer, K.H. et al. Xeroderma pigmentosum, trichothiodystrophy and Cockayne syndrome: a complex genotype-phenotype relationship. *Neuroscience* 145, 1388-96 (2007).
73. Balajee, A.S., May, A., Dianov, G.L., Friedberg, E.C. & Bohr, V.A. Reduced RNA polymerase II transcription in intact and permeabilized Cockayne syndrome group B cells. *Proc Natl Acad Sci U S A* 94, 4306-11 (1997).
74. Selby, C.P. & Sancar, A. Cockayne syndrome group B protein enhances elongation by RNA polymerase II. *Proc Natl Acad Sci U S A* 94, 11205-9 (1997).

75. van Gool, A.J. et al. The Cockayne syndrome B protein, involved in transcription-coupled DNA repair, resides in an RNA polymerase II-containing complex. *EMBO J* 16, 5955-65 (1997).
76. Menoni, H., Hoeijmakers, J.H. & Vermeulen, W. Nucleotide excision repair-initiating proteins bind to oxidative DNA lesions in vivo. *J Cell Biol* 199, 1037-46 (2012).
77. Aamann, M.D. et al. Cockayne syndrome group B protein promotes mitochondrial DNA stability by supporting the DNA repair association with the mitochondrial membrane. *FASEB J* 24, 2334-46 (2010).
78. Scheibye-Knudsen, M., Croteau, D.L. & Bohr, V.A. Mitochondrial deficiency in Cockayne syndrome. *Mech Ageing Dev* 134, 275-83 (2013).
79. Menoni, H. et al. The transcription-coupled DNA repair-initiating protein CSB promotes XRCC1 recruitment to oxidative DNA damage. *Nucleic Acids Res* 46, 7747-7756 (2018).
80. Canugovi, C., Misiak, M., Ferrarelli, L.K., Croteau, D.L. & Bohr, V.A. The role of DNA repair in brain related disease pathology. *DNA Repair (Amst)* 12, 578-87 (2013).
81. Narciso, L. et al. The Response to Oxidative DNA Damage in Neurons: Mechanisms and Disease. *Neural Plast* 2016, 3619274 (2016).
82. Horibata, K. et al. Complete absence of Cockayne syndrome group B gene product gives rise to UV-sensitive syndrome but not Cockayne syndrome. *Proc Natl Acad Sci U S A* 101, 15410-5 (2004).
83. Giang, J. et al. Complement Activation in Inflammatory Skin Diseases. *Front Immunol* 9, 639 (2018).
84. Davis, A.E., III, Lu, F. & Mejia, P. C1 inhibitor, a multi-functional serine protease inhibitor. *Thromb. Haemost* 104, 886-893 (2010).
85. Gettins, P.G. & Olson, S.T. Inhibitory serpins. New insights into their folding, polymerization, regulation and clearance. *Biochem J* 473, 2273-93 (2016).
86. Huntington, J.A. Serpin structure, function and dysfunction. *J. Thromb. Haemost* 9 Suppl 1, 26-34 (2011).
87. Huntington, J.A., Read, R.J. & Carrell, R.W. Structure of a serpin-protease complex shows inhibition by deformation. *Nature* 407, 923-926 (2000).
88. Cugno, M., Zanichelli, A., Foeni, F., Caccia, S. & Cicardi, M. C1-inhibitor deficiency and angioedema: molecular mechanisms and clinical progress. *Trends Mol. Med* 15, 69-78 (2009).
89. Carugati, A., Pappalardo, E., Zingale, L.C. & Cicardi, M. C1-inhibitor deficiency and angioedema. *Mol. Immunol* 38, 161-173 (2001).
90. Prematta, M.J., Prematta, T. & Craig, T.J. Treatment of hereditary angioedema with plasma-derived C1 inhibitor. *Ther Clin Risk Manag* 4, 975-82 (2008).
91. Henry Li, H., Riedl, M. & Kashkin, J. Update on the Use of C1-Esterase Inhibitor Replacement Therapy in the Acute and Prophylactic Treatment of Hereditary Angioedema. *Clin Rev Allergy Immunol* 56, 207-218 (2019).
92. van Veen, H.A. et al. Characterization of recombinant human C1 inhibitor secreted in milk of transgenic rabbits. *J. Biotechnol* 162, 319-326 (2012).
93. Caldwell, E.E. et al. Heparin binding and augmentation of C1 inhibitor activity. *Arch. Biochem. Biophys* 361, 215-222 (1999).
94. Willemin, W.A. et al. Potentiation of C1 inhibitor by glycosaminoglycans: dextran sulfate species are effective inhibitors of in vitro complement activation in plasma. *J. Immunol* 159, 1953-1960 (1997).
95. Zhou, Z.H., Rajabi, M., Chen, T., Karnaukhova, E. & Kozlowski, S. Oversulfated chondroitin sulfate inhibits the complement classical pathway by potentiating C1 inhibitor. *PLoS. One* 7, e47296 (2012).
96. Dijk, M. et al. How Dextran Sulfate Affects C1-inhibitor Activity: A Model for Polysaccharide Potentiation. *Structure* 24, 2182-2189 (2016).
97. Bos, I.G. et al. The potentiation of human C1-inhibitor by dextran sulphate is transient in vivo: studies in a rat model. *Int. Immunopharmacol* 1, 1583-1595 (2001).



Summary

Samenvatting

Curriculum vitae

Publications

Acknowledgements

Summary

Our cells are continuously challenged by numerous external as well as internal hazards that, if not dealt with in an appropriate manner, may interfere with critical processes and underlie disease. Therefore, they heavily rely on essential protective mechanisms that recognize and counteract potential risks. For example, the physical barriers and biochemical cascades of the immune system provide a first line of defense against pathogens, which attempt to invade host cells and could cause serious illness. In addition, the well-coordinated networks of the DNA damage response (DDR) detect and remove damaged nucleotides that could drive mutagenesis and thereby provoke inherited disorders or ageing-related diseases. Evidently, the correct activation, execution and completion of the implicated pathways, as well as their crosstalk, is of key importance. This necessitates the well-timed and -positioned presence of proteins with the desired functionality. Apart from regulation of the overall availability of such proteins by adjusting transcription or translation, this is to a great extent established by post-translational modifications (PTMs). A variety of chemical alterations is able to fine-tune protein activity, localization and interactions. The research described in this thesis addresses the role and importance of PTMs in the mechanisms that safeguard our cells. The background for this study is provided by Chapter 1.

An important strategy to coordinate the proteins of the DDR involves the reversible, covalent addition of functional groups. As combining multiple (types of) PTMs can work either supportive or antagonistically, their introduction is perfectly balanced to guarantee optimal protein and pathway functioning.

A frequently applied modification is the attachment of a small regulatory protein called ubiquitin. This reaction, referred to as ubiquitination, is in many cases catalyzed by a protein complex from the family of cullin-RING ligases (CRLs). Two of such CRLs play important roles during nucleotide excision repair (NER) – a mechanism that protects our cells against certain types of DNA damage and, in humans, is the only pathway capable of removing the covalent linkages between adjacent pyrimidines in the DNA that are inflicted by sunlight. In the subpathway of NER that acts on the DNA damage throughout the entire genome, the CRL that is built with DDB2 (CRL^{DDB2}) significantly contributes to DNA damage detection. Fascinatingly, the activity of CRLs is in turn regulated through another PTM, that is the attachment of the ubiquitin-like protein NEDD8, known as NEDDylation. When not required, the ligase functionality of CRL^{DDB2} is indeed kept inactivated through the removal of NEDD8. However, in response to DNA damage CRL^{DDB2} activation leads to the ubiquitination of many target proteins, thereby altering their performances in a manner that contributes to efficient DNA damage repair. Interestingly, the architecturally similar CRL^{CSA}, which is built with CSA instead of DDB2, is indispensable for the NER subpathway that specifically removes damage from active genes. When RNA polymerase II (RNAPII) gets stalled at such damage during transcription, CRL^{CSA} is one of the first complexes that is recruited. As described in Chapter 2, NEDDylation not only regulates the activation of the CRL, but also appears to modulate the interaction with RNAPII. Inhibition of NEDD8 activation leads to increased association of CRL^{CSA} with RNAPII. Furthermore, both NEDDylation in general and the specific presence of

CSA appear to be important for the UV-dependent degradation of RNAPII that can result from UV irradiation. This method to remove stalled RNAPII presumably avoids cell death when NER is compromised. Possibly, this last resort mechanism plays a role in the prevention of the neurodevelopmental problems that characterize Cockayne syndrome, which can be caused by *CSA* gene mutations that result in CSA deficiency.

To warrant sufficient levels of functional CSA, and thus CRL^{CSA}, not only gene integrity but also protein stability is essential. In Chapter 3, we uncover a crucial role for the TRiC chaperonin in regulating CSA stability and localization, as well as the assembly of CRL^{CSA}. As a part of the proteostasis network that serves to maintain protein homeostasis, TRiC facilitates the folding of many proteins. Accordingly, TRiC also appears to stabilize CSA. This seems critical for the correct functioning of CRL^{CSA} in transcription-coupled NER and possibly other protective responses. Importantly, disease-associated missense mutations in the *CSA* gene lead to increased binding of the mutated protein to TRiC, which at least in part may explain the consequences of such mutations for the development of Cockayne syndrome.

&

In addition to protein modification by ubiquitination or NEDDylation, also the conjugation of the ubiquitin-like protein SUMO (SUMOylation) plays an important role in the detection and repair of DNA damage and during the required signaling responses. The PIAS proteins, through their highly conserved catalytic SP-RING domains, act as SUMO ligases in many different (DDR) pathways. In Chapter 4, we demonstrate that the SP-RING-like domain of Zimp7, which resembles the catalytic domain of the PIAS proteins, confers true SUMOylating activity as well. Since Zimp7 appears to be recruited to sites of DNA damage, this newly identified SUMO ligase may be an important DDR factor. Furthermore, Zimp7 might play a role in DNA replication, as indicated by its interaction with the sliding clamp PCNA. Its exact biological functions are yet to be determined and seem to not only depend on its SUMOylating activity but also on its intrinsic transcriptional activity. However, current knowledge suggests a broad implication of Zimp7 in securing proper cellular functioning.

Whereas the connection and disconnection of functional groups is a leading example of pathway regulation in the DDR, PTM-mediated regulation of many immune response pathways involves the activation of proteins through peptide cleavage. Sequential cleavage of a protease that in turn catalyzes the activation of the next enzyme can quickly amplify a signal and evoke a massive response. Although this enables rapid pathogen elimination, these cascades should be tightly controlled as both defective as well as disproportional activation may have devastating effects. C1-inhibitor regulates several pathways of the immune system by trapping the initiating proteases into a conformation with a disrupted active site, thereby preventing their spontaneous activations. Interestingly, the activity of this inhibitor itself can be potentiated by the interaction with long linear polysaccharides, called glycosaminoglycans (GAGs). Our model, shown in Chapter 5, explains why this potentiation can only be observed towards specific target proteases. Since most likely the polysaccharide neutralizes the repulsive forces between C1-inhibitor and the protease's autolysis loop, GAG binding is only helpful in case this loop is positively charged. Fine-tuning C1-inhibitor's activity against its different targets may be a good strategy to optimize replacement therapy

in the treatment of hereditary angioedema – a disorder that is characterized by recurrent attacks of potentially life-threatening swelling. This uncontrolled immune response results from C1-inhibitor deficiency, showing once more the importance of a regulatory protein in health and disease.

The methods of protein regulation described in this thesis are just a fine selection of the broad repertoire of modifications that can be applied by our cells. Nevertheless, they one by one are indispensable to the resilience against internal and external threats. Chapter 6 outlines how our research provides valuable insights in this area, as well as a base for further research and discussion. Together, these findings improve our understanding, and ultimately contribute to the treatment or prevention, of the numerous disorders that are associated with loss of protein regulation in the implicated cell-protecting pathways.



Samenvatting

De cellen in ons lichaam worden continu uitgedaagd door allerlei interne bedreigingen en schadelijke invloeden van buitenaf. Als hier niet op een goede manier mee wordt omgegaan, worden mogelijk kritieke processen verstoord en kan dit zelfs tot ziekte leiden. Onze cellen zijn daarom sterk afhankelijk van een aantal mechanismen die ze beschermen tegen mogelijke gevaren. De fysieke barrières en biochemische signaleringsroutes van het immuunsysteem vormen bijvoorbeeld een belangrijke eerste verdediging tegen pathogenen, die gastheercellen proberen binnen te dringen en zo ernstige aandoeningen kunnen veroorzaken. Het uitgebreide netwerk van de DNA-schaderespons draagt anderzijds de verantwoordelijkheid voor het opsporen en repareren van beschadigde nucleotiden in het DNA, die het ontstaan van mutaties kunnen bevorderen en bijdragen aan de ontwikkeling van erfelijke of ouderdom-gerelateerde ziektes. Het is natuurlijk cruciaal dat de processen die onderdeel uitmaken van dergelijke mechanismen correct worden geactiveerd en uitgevoerd. Hiertoe is het belangrijk dat eiwitten met de gewenste functionaliteit op het juiste moment op de juiste plaats zijn. Bovendien moet er onderling goed gecommuniceerd worden. Afgezien van het reguleren van de productie van de benodigde eiwitten, wordt dit grotendeels mogelijk gemaakt door zogenaamde post-translationele modificaties (PTM's): een verscheidenheid aan chemische aanpassingen die de activiteit, lokalisatie en interacties van bestaande eiwitten verder verfijnen. Het onderzoek beschreven in dit proefschrift is gericht op de rol en het belang van PTM's in de mechanismen die onze cellen beschermen. De achtergrond van deze studie wordt uitgebreid beschreven in hoofdstuk 1.

Een belangrijke strategie om het gedrag van eiwitten tijdens de DNA-schaderespons te coördineren is het koppelen en ontkoppelen van functionele groepen. Wanneer meerdere van zulke (typen) PTM's gecombineerd worden, kunnen ze elkaars effect versterken of juist tegenwerken. Alleen door ze perfect op elkaar af te stemmen, wordt dus gezorgd voor het optimaal functioneren van eiwitten en processen.

Zo'n veelgebruikte modificatie is het koppelen van een klein regulerend eiwit genaamd ubiquitine. Deze koppelingsreactie wordt vaak gestimuleerd door een eiwitcomplex uit de familie van cullin-RING ligases (CRL's). Voor twee van zulke CRL's is een belangrijke rol weggelegd tijdens nucleotide-excisieherstel (nucleotide excision repair, NER) – een uiterst belangrijk mechanisme dat ons tegen bepaalde vormen van DNA-schade beschermt. In de mens is dit zelfs het enige proces waarmee de gevaarlijke verbindingen tussen aangrenzende pyrimidines in het DNA, die door zonlicht kunnen worden toegebracht, verwijderd kunnen worden. In de subroute van NER die werkzaam is op al ons DNA, speelt de CRL die is opgebouwd met het eiwit DDB2 (CRL^{DDB2}) een grote rol in het opsporen van beschadigingen. Zolang niet nodig wordt de ubiquitine-koppelingsfunctionaliteit van dit complex inactief gehouden. Echter, in reactie op DNA-schade leidt de activering van CRL^{DDB2} ertoe dat verschillende doeleiwitten worden gemodificeerd met ubiquitine. Dit draagt bij aan het afstemmen van het gedrag van deze eiwitten op een efficiënte reparatie van de schade. Een CRL met een vergelijkbare structuur, maar opgebouwd met CSA in plaats van DDB2 (CRL^{CSA}), is onmisbaar in de andere subroute van NER, die specifiek beschadigingen herstelt in DNA

dat actief wordt uitgelezen door RNA-polymerase. Wanneer RNA-polymerase bezig is het DNA te vertalen naar RNA, maar tijdens dit proces (de transcriptie) vastloopt bij schade, wordt CRL^{CSA} als een van de eerste complexen aangetrokken. Een interessant gegeven is dat de ubiquitine-koppelingsactiviteit van CRL's op haar beurt afhankelijk is van een andere modificatie, namelijk de koppeling van het ubiquitine-achtige eiwit NEDD8. Zoals beschreven in hoofdstuk 2, blijkt deze NEDD8-modificatie niet alleen de CRL te activeren, maar ook invloed uit te oefenen op de interactie tussen CRL^{CSA} en RNA-polymerase. Het verhinderen van de NEDD8-koppeling zorgt namelijk voor een verhoogde binding van de CRL^{CSA}-eiwitten aan de polymerase. Daarnaast blijkt zowel deze NEDD8-modificatie in het algemeen als de aanwezigheid van CSA belangrijk te zijn voor de afbraak van RNA-polymerase, die kan optreden onder invloed van UV-straling. Deze manier om vastgelopen RNA-polymerase te verwijderen lijkt een laatste redmiddel om geprogrammeerde celdood tegen te gaan wanneer NER niet goed uitgevoerd kan worden en RNA-polymerase te lang blijft stilstaan. Mogelijk speelt dit mechanisme een rol in het voorkomen van de neurologische ontwikkelingsproblemen die kenmerkend zijn voor Cockayne syndroom, dat onder andere veroorzaakt kan worden door een CSA-tekort als gevolg van mutaties in het CSA-gen.

Om voldoende functioneel CSA, en dus CRL^{CSA}, te garanderen, is niet alleen de integriteit van het CSA-gen, maar ook de stabiliteit van het eiwit essentieel. In hoofdstuk 3 onthullen we een cruciale rol voor het chaperonne-complex genaamd TRiC in het reguleren van de CSA-stabiliteit en -lokalisatie, alsook in de opbouw van CRL^{CSA}. TRiC maakt deel uit van het netwerk dat de totale eiwitbalans waarborgt en faciliteert hiertoe de vouwing van vele eiwitten. TRiC blijkt ook CSA te stabiliseren en daarmee onmisbaar te zijn voor het goed functioneren van CRL^{CSA} in transcriptie-gekoppeld NER en wellicht ook voor andere processen (van de DNA-schaderespons). Een aantal zogeheten missense-mutaties in het CSA-gen, die in verband zijn gebracht met Cockayne syndroom, leiden bovendien tot een verhoogde binding van het gemuteerde eiwit aan TRiC. Mogelijk verklaart dit (deels) hoe zulke mutaties bijdragen aan de ontwikkeling van deze ziekte.

Naast de modificaties door ubiquitine en NEDD8, speelt ook de koppeling van het ubiquitine-achtige eiwit SUMO een belangrijke rol in de detectie en reparatie van DNA-schade, evenals in de signaaluitwisseling met andere processen. Dankzij een goed-geconserveerd katalytisch domein, treden de PIAS-eiwitten op als SUMO-koppelaars in vele verschillende (DNA-schaderespons)routes. In hoofdstuk 4 tonen we aan dat het SP-RING-achtige domein van Zimp7, dat erg op dit katalytische domein in de PIAS-eiwitten lijkt, eveneens ware SUMO-koppelingsactiviteit kan bieden. Aangezien Zimp7 ook blijkt te worden aangetrokken naar plaatsen van DNA-schade is deze SUMO-koppelaar wellicht een belangrijke factor in de DNA-schaderespons. Daarnaast wijst de interactie met PCNA, dat als het ware een bindingsplatform voor DNA polymerase en andere eiwitten op het DNA vormt, op een mogelijke rol voor Zimp7 in het proces waarin DNA gekopieerd wordt (de replicatie). De precieze biologische functies van Zimp7 moeten nog verder ontrafeld worden. Deze kunnen afhankelijk zijn van de ontdekte SUMO-koppelingsactiviteit, maar ook gebaseerd zijn op de eigenschap DNA-transcriptie te kunnen stimuleren. De huidige kennis doet

vermoeden dat Zimp7 breed verweekeld is in de processen die het juist functioneren van cellen moeten veiligstellen.

Waar de DNA-schaderespons vooral gebruik maakt van het koppelen en ontkoppelen van functionele groepen, worden de routes en eiwitten van het immuunsysteem vaak gereguleerd door middel van het (af)knippen van kleine stukjes eiwit. Deze PTM wordt veelal ingezet om de zogenaamde protease-functionaliteit van een eiwit te activeren, zodat dit weer een volgend eiwit kan knippen. Zo'n aaneenschakeling van protease-activeringen zorgt ervoor dat een signaal in korte tijd opgeschaald kan worden tot een enorme reactie. Hoewel dit een snelle eliminatie van ziekteverwekkers mogelijk maakt, kan zowel het gebrekkig als het onevenredig vaak starten van een dergelijk proces ernstige gevolgen hebben. C1-inhibitor (C1-esteraseremmer) reguleert verschillende routes van het immuunsysteem door de vouwing van de eiwitten die zo'n kettingreactie initiëren dusdanig te veranderen dat de protease-activiteit niet spontaan geactiveerd kan worden. De activiteit van deze remmer zelf kan worden verhoogd door de interactie met lange ketens van disacchariden, beter bekend als glycosaminoglycanen (GAG's). Ons model, getoond in hoofdstuk 5, verklaart waarom zo'n GAG de remmende werking van C1-inhibitor op specifieke, maar niet alle proteasen, kan bevorderen. Waarschijnlijk neutraliseert een negatief geladen GAG de afstotende krachten tussen C1-inhibitor en een bepaalde lus in de protease. Tussenkoms van zo'n saccharideketen lijkt dan ook alleen een stimulerend effect te hebben op C1-inhibitor's activiteit wanneer deze gericht is tegen een protease met een positief geladen lus. Het optimaliseren van de remmende werking van C1-inhibitor op de verschillende proteasen, lijkt een goede manier om de huidige behandeling van hereditair angio-oedeem door het toedienen van gezuiverd C1-inhibitor te verbeteren. Deze aandoening wordt gekenmerkt door terugkerende aanvallen van mogelijk levensbedreigende zwellingen die in het hele lichaam kunnen ontstaan. De onderliggende ongecontroleerde reactie van het immuunsysteem wordt veroorzaakt door een tekort aan functioneel C1-inhibitor, wat nogmaals het belang van een regulerend eiwit in ziekte en gezondheid benadrukt.

De in dit proefschrift beschreven manieren van eiwitregulatie zijn slechts een kleine selectie uit het brede repertoire van modificaties die door onze cellen worden ingezet. Stuk voor stuk leveren ze echter een onmisbare bijdrage aan de weerbaarheid tegen interne en externe dreigingen. In hoofdstuk 6 wordt uiteengezet hoe ons onderzoek de kennis op dit gebied vergroot en aanknopingspunten biedt voor vervolgstudies. Samen ondersteunen de bevindingen ons begrip, en uiteindelijk ook de behandeling of de preventie, van de vele aandoeningen die in verband staan met het verlies van eiwitregulatie in de processen die onze cellen beschermen.

Curriculum vitae

Madelon Dijk was born on June 3, 1988 in Rotterdam, The Netherlands. In 2006 she successfully completed grammar school at Johan de Witt Gymnasium in Dordrecht and started the study of Life Science and Technology at Leiden University (UL) and Delft University of Technology (TU Delft). After studying the behavior of *S. cerevisiae* at near-zero growth rates during an internship at the department of Industrial Microbiology at TU Delft, she obtained her bachelor's degree cum laude (with honors) in 2009. During her master's education, she investigated catalytic intermediates of cytochrome bd-I oxidases at the former department of Enzymology at TU Delft. Furthermore, she intended to optimize the immobilization of lipases for industrial purposes during an internship at ChiralVision in Leiden. In 2011, the master's degree was obtained cum laude. Subsequently, she joined the former department of Toxicogenetics at Leiden University Medical Center (LUMC) as a PhD student to investigate the regulation of the nucleotide excision DNA repair pathway under the supervision of Prof. dr. Leon H. Mullenders. In addition, she worked with Dr. Navraj S. Pannu at the department of Biophysical Structural Chemistry at UL on a project on C1-inhibitor. From 2014 on, the research on protein regulation during DNA damage repair was continued at the department of Human Genetics at the LUMC under the supervision of Prof. dr. Haico van Attikum. After finishing the practical part of the PhD project, she started working in the field of data analysis at the National Office for Identity Data (Rijksdienst voor Identiteitsgegevens) in Den Haag.



Publications

- 2018 **TRiC controls transcription resumption after UV damage by regulating Cockayne syndrome protein A**
Alex Pines*, Madelon Dijk*, Matthew Makowski, Elisabeth M. Meulenbroek, Mischa G. Vrouwe, Yana van der Weegen, Marijke Baltissen, Pim J. French, Martin E. van Royen, Martijn S. Luijsterburg, Leon H. Mullenders, Michiel Vermeulen, Wim Vermeulen*, Navraj S. Pannu* and Haico van Attikum*
*co-first authors, *co-corresponding authors
Nature Communications; 9(1): 1040
- 2016 **How dextran sulfate affects C1-inhibitor activity: a model for polysaccharide potentiation**
Madelon Dijk, Jolande Holkers, Patrick Voskamp, Bruno M. Giannetti, Willem-Jan Waterreus, Harrie A. van Veen and Navraj S. Pannu
Structure; 24(12): 2182-2189
- 2014 **Insight in the multilevel regulation of NER**
Madelon Dijk, Dimitris Typas, Leon H. Mullenders and Alex Pines
Experimental Cell Research; 329(1): 116-123
- 2012 **Oxoferryl-porphyrin radical catalytic intermediate in cytochrome bd oxidases protects cells from formation of reactive oxygen species**
Angela Paulus, Sebastiaan G.H. Rossius, Madelon Dijk and Simon de Vries
Journal of Biological Chemistry; 287(12): 8830-8838
- 2011 **Extreme calorie restriction and energy source starvation in *Saccharomyces cerevisiae* represents distinct physiological states**
Léonie G.M. Boender, Marinka J.H. Almering, Madelon Dijk, Antonius J.A. van Maris, Johannes H. de Winde, Jack T. Pronk and Pascale Daran-Lapujade
Biochimica et Biophysica Acta - Molecular Cell Research; 1813(12): 2133-2144

Acknowledgements

In this thesis I have addressed the importance of regulatory proteins. Without them, pathways would never be properly activated, correctly executed and timely completed. In fact, they may stall halfway or totally derail. I found that the same holds true for a PhD track. Although to the PhD student it may sometimes feel like a solitary expedition, there are some indispensable cofactors that safeguard both the trajectory and the student. On the road to this thesis, I experienced the significance of such factors, embodied by colleagues, friends and family.

Leon, thank you for initiating the pathway and always believing in its successful completion. I appreciate both your scientific enthusiasm and your interest in my personal well-being. Raj, coactivator, I also value your guidance along the way.

As illustrated by many aspects of the DNA damage response, alternative pathways are crucial. Haico, thank you for welcoming me in your lab, providing such routes and being willing to coordinate them as my promotor. Silvère, the adjustment to the friendly, inspiring working environment of your department was easy.

One should also not underestimate the significance of crosstalk with other proteins, even when pathways separate. Alex, I enjoyed collaborating with you and I think we did great at complementing and strengthening each other's work. Romy, Juliette, Leonie and Jenny, thanks for sharing frustrations and breakthroughs while being challenged by comparable internal and external hazards. A warm thanks also goes to my two paronyms. Hanneke, I was lucky to have you as a constant and close factor in my ever-changing environment. Chantal, although you joined later on, it feels like you have always been there for scientific and emotional support.

Finally, I can't stress enough the importance of the chaperones that are fundamental to a protein's stability. Papa, thank you for being the proud, concerned, encouraging dad I can always depend on. Mama, your love and support will always be remembered. Lianne, Justin, I feel so fortunate to form this stable, inseparable complex with the two of you. Chris, thanks for knowing me so well, recognizing exactly when I need protection, distraction, motivation or, sometimes, inhibition. I couldn't have done this without you.

While this thesis only describes a fine selection of regulatory mechanisms, it is the combination of all modulating factors that directs successful protein and pathway functioning. Likewise, I owe a big thanks to all colleagues, lab mates, students, staff members, roommates, friends and family that either crossed my path occasionally or supported me for longer. Together, you contributed significantly to this accomplishment.

